Experimental Investigation of Well Cement Integrity in Abandoned Oil and Gas Wells

by

Muhammad Abdurrahman Thaika

A thesis submitted in partial fulfillment of the requirements for the degree of

Master of Science

in

Petroleum Engineering

Department of Civil and Environmental Engineering
University of Alberta

Abstract

When a well reaches the end of its life cycle, it needs to be abandoned. Leakage issues are being reported in legacy wells and the literature blames cement shrinkage as the main culprit for these leakage issue. Instead of blaming the cement, the isolation capabilities of the entire system need to be evaluated as there is a lack of cement integrity testing at relevant wellbore conditions. In this study, we evaluated the integrity of the cement plug under relevant wellbore conditions. We used 4 methods to investigate the integrity of cement plugs used in abandonment operations, including: 1) Testing the isolation capabilities of small-scale samples; 2) testing the isolation capabilities of optimally placed cement using the wellbore simulator; 3) investigating the effects of cement contamination; and 4) the remediation capabilities of various cement blends.

In the first test, the permeability of small-scale cement samples was tested. From the testing results, we determined that the permeability of the bulk cement was very low, but with the addition of an interface around the cement plug (metal casing), the permeability of the system increased.

In the second test, the permeability of two different cement blends was tested using a physical wellbore simulator, which allowed cement curing and subsequent permeability testing under elevated pressure and temperature conditions. The two blends were Neat G cement without any additives and a Class G cement with additives that had been engineered to enhance its sealing performance. The wellbore simulator experiments showed that the Class G cement blend with additives outperformed Neat G cement blend in every testing scenario. The class G cement with additives also resisted the formation of a micro annulus better than the Neat G cement. These results formed the baseline guidance towards how to ideally place cement plugs during abandonment operations.

In the third test, we tested the effect of contaminants on the integrity of the cement plugs. Water contamination was first investigated. For the neat G cement, it was observed that as the water contamination increased, the zonal isolation capabilities of the cement decreased. The dominant fluid pathways were located at cement-casing interface. For Class G cement with additives, contaminated with water, the isolation capabilities of the cements were reduced drastically. The dominant fluid pathways were through the center of the cement matrix. The fluid loss additives used in this slurry prevented the cement from expelling excess water out of the slurry. This excess water would have been trapped in the cement matrix, forming larger pores; increasing the permeability. The effect of oil contamination was also investigated. Neat G cement was contaminated with 2.5% light crude oil. This had little to no effect on the isolation capabilities of the cement as long as the entire sealing system was left undisturbed (i.e., without stress changes). Changes to the effective stresses acting on the cement caused the sealing capabilities of the cement plug to reduce drastically (i.e., water permeability increased). Isolation capabilities against nitrogen remained almost unchanged when the effective stress changed. Class G cement with additives was then contaminated with 2.5% light cured oil; a similar trend was observed. As long as the effective stresses acting on the cement were unchanged, the isolation capabilities against the flow of water was unchanged. Changes to the effective stress reduced the isolation capabilities against water drastically. The isolation capabilities against nitrogen, however, was reduced greatly. Gas breakthrough was immediately observed for the contaminated sample.

Lastly, since the micro annulus was the dominant flow pathway for the majority of the experiments, remediation experiments were carried out in the fourth test in an attempt to improve cement's sealing performance. Three cements with varying grain sizes were used for the remediation experiments: the standard class G cement with the largest grain size, Portland limestone cement

(PLC) with the medium grain size, and microfine cement with the smallest grainsize. It was observed that the microfine cement could penetrate fracture widths as low as 35 microns and reduce the fracture conductivity by 5 orders of magnitude. The PLC could penetrate fractures as small as 65 microns, but bridging was observed at fracture widths of 50 microns. Class G cement bridged at a fracture width of 200 microns.

Preface

This thesis is an original work by Muhammad Abdurrahman Thaika. The research was carried out under the supervision of Dr. Ergun Kuru and Dr. Huazhou Li at the University of Alberta and Dr. Simon Iremonger at Sanjel Energy Services, Calgary.

Chapter 2 was published in the 43rd International Conference on Ocean, Offshore & Arctic Engineering as “Thaika, MA., Hu, K., Kuru, E., Li, H., Iremonger, S., Lin, Z., and DeBruijn, G. Experimental Investigation of Well Cement Integrity In Abandoned Oil and Gas Wells, In International Conference on Offshore Mechanics and Arctic Engineering, American Society of Mechanical Engineers, Singapore, 2024”.

Publication of Chapters 3 and 4 in refereed journals will be attempted at a future date.

Acknowledgements

Words cannot express my gratitude to my professor, Dr. Ergun Kuru for first of all accepting my application to study the MSc in Petroleum Engineering program at the University of Alberta. I would like to express my deepest appreciation to both Dr. Ergun Kuru and Dr. Huazhou Li for their priceless guidance throughout my research projects. Their patience, encouragement and constructive feedback guided me to complete my research. It was a great honour to work under the supervision of both Drs. Kuru and Li and the lessons that I learnt during my time at the University of Alberta will stay with me forever.

I also could not have completed this journey without Dr. Simon Iremonger and Mr. Gunnar DeBruijn. Dr Iremonger always demanded perfection throughout this work, and his valuable comments helped me bridge the gap between industry and academia. Mr. DeBruijn, with his immense knowledge, validated my research techniques and gave me insights into unexpected results which gave me confidence in my own research. I am also grateful for the committee members serving in my MSc final exam: Dr. Mustafa Gül, Dr. Ergun Kuru, Dr. Huazhou Li, Dr. Tayfun Babadagli and special thanks to Mr. Gunnar DeBruijn for agreeing to read my thesis, providing his review comments and attending my exam as an external observer.

This research work has been supported by the Natural Sciences and Engineering Research Council of Canada (NSERC RGPIN-2022-02956 Kuru) and the Petroleum Technology Alliance Canada.

My sincere thanks go to Mr. John F Czuroski, Dr. Ke Hu, and Mr. Liam Abrams for their technical support during this project. I would also like to thank my friends, Yufei Liu, Weishen Yan, and Chunkui Mu for providing me support during my research.

And finally, I would like to thank my parents for their belief in me. I could have not come this far in life without their support and words of encouragement.

Table of Contents

List of Tables

List of Figures

Chapter 1 Introduction

1.1 Overview

When a well reaches the end of its life cycle, it must be permanently plugged and abandoned [1]. The abandoned wells are usually filled with cement, which forms a barrier between the production zone and the surface. A good cement system should be capable of providing zonal isolation of the well throughout its life cycle. However, the loss of zonal isolation at any time during the well's life span can lead to severe economic loss, environmental pollution, and even loss of life in some cases. Figure 1-1 shows the possible fluid pathways in a cemented section of wellbore [2].

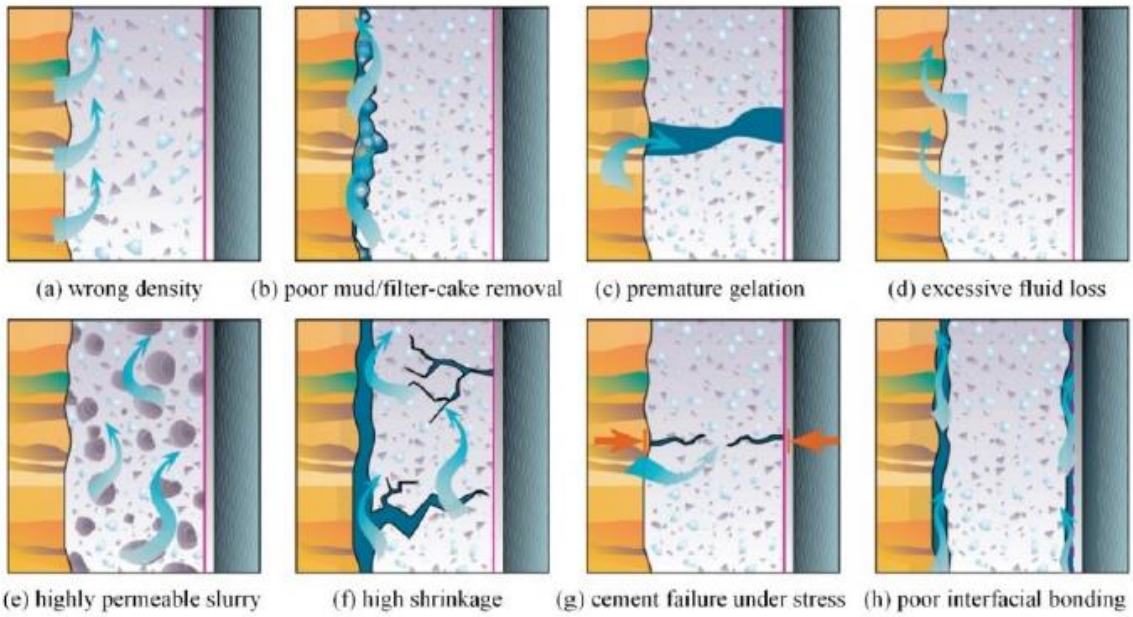

Figure 1-1: Possible fluid pathways in a cemented section of a wellbore [2]

Watson and Bachu [3] analysed data from over 316,000 wells in Alberta and determined that about 4.5% of all oil wells showed gas migration or surface casing vent flow. Fugitive emissions reported in the literature usually combine all types of wells, so the individual leakage rates of abandoned wells and suspended wells are not clear. The main problem associated with loss of well integrity is the leakage of greenhouse gases such as methane, which is 80 times more potent in warming the atmosphere when compared to carbon dioxide over a 20-year time period [4].

As of 2024, there are approximately 496,309 registered petroleum wells in Alberta [5]. The number of abandoned wells in Alberta continues to increase year on year and it is vital to ensure that the wells are abandoned in a proper manner. If leakage is reported in any of these wells, remedial action needs to be taken to fix these wellbore integrity issues.

1.2 Statement of the Problem

The main purpose of well abandonment is to permanently isolate all subsurface formations penetrated by the well and all permeable zones [6]. Portland cement has been commonly used as the recommended sealant for abandoning wells in the oil and gas industry [7]. The ability of Portland cement to provide an effective long-term seal is aided by designing the blend to the given well conditions, required chemical compatibility, optimal cement expansion, chemical compatibility, and correct field operations to ensure optimal placement. The use of suboptimal cement designs or placement will significantly increase the risk of well integrity issues in the long term, as they can increase the risk of flow paths [7].

Before the 1950s, most wells that were drilled for oil and gas exploration and production were not sufficiently documented, making abandonment process at a later date more difficult [8]. These wells were also not plugged with cement when the operator decided to abandon them and in fact some operators even ended up filling these abandoned wells with dirt [8]. These early abandonment techniques (filling with dirt) resulted in lots of wells leaking [8]. Since the 1950s, significant improvements in well abandonment techniques have occurred, although not at the same pace as how drilling and completion technology evolved. To reduce the likelihood of wellbore leaking, it is critical that continued enhancements to plugging materials and placement methods occur.

There have been several papers published in the literature discussing the effects of subsurface conditions when designing an abandonment plug. However, generally, there is a lack of data and studies when it comes to testing cemented wells under relevant abandonment pressure and temperature conditions.

The main cause of well leakage has predominantly been blamed directly on the cement properties [9], as cement tends to shrink after setting. Work done by Thiercelin et al. [10] showed that the cement system as a whole needs to be evaluated rather than pinpointing the cause of leakage

directly on cement. The cement system comprises many individual components, such as the bottom hole conditions, casing, formation, and the interfaces between all these elements.

Many studies have been carried out to investigate cement integrity with regards to abandoned wells in the past two decades [11-18]. However, many if not all of these studies, investigated just one or two components of the cement system rather than treating the cement system as a whole. While investigating things like compressive strength of the cement or bond strength of the cement can give valuable insights into the integrity of the cement system, there has been little to no studies investigating the permeability of the system. In order to prevent hydrocarbon leakage to the atmosphere, the key parameter that needs to be investigated is the permeability of the entire system.

There have also been numerous studies investigating the effect of cement contamination in the wellbore on cement integrity [19-30]. However. many of these studies do not replicate actual downhole conditions. The main contaminants used in these contamination studies are drilling mud. Drilling mud contamination is more relevant to primary cementing. The most common contaminant found in a well that is about to be abandoned is either formation water or residual oil. No studies have been carried out investigating the effect of residual oil.

Once well leakage issues have been reported in petroleum wells, the well needs to be remediated. There have been lots of studies investigating the penetration potential of conventional cements, microfine cements, engineered microfine cements, and resins [30-43]. However, most, if not all, of these experiments, have some limitations associated with them, such as not replicating field conditions. These limitations include not replicating typical squeeze pressures, squeezing cement through a metal-metal interface and squeezing through filter papers which would promote slurry dehydration. Furthermore, Dusseault et al. [9] stated that a micro annulus in the range of 10-20 microns can cause well leakage; however, the smallest gap size investigated in the literature is 120 microns. Most of the studies focus on the penetration capabilities of cement through different gap sizes. Meek and Harris [33] squeezed cement through two metal plates with various gap sizes and Ewort et al. [39] tested the penetration of cement through sand particles. Although penetration capability is a good metric to test the effectiveness of a remedial job, the penetration potential of the cement slurry is not the only deciding factor to determine if the cement job was successful or not. The penetration potential in combination with the permeability of the remediated sample needs to be investigated.

1.3 Objective and Scope of the Study

Upon reviewing the literature [11-43], it became evident that a comprehensive test design for assessing abandoned well integrity is essential, particularly under conditions that closely mimic typical abandonment scenarios, including relevant pressure and temperature conditions. There is also an obvious knowledge gap in the literature when it comes to investigating the effect of oil and water contamination in cement slurries and on cement permeability testing after remediation. For the remediation experiments, narrower gap widths should be investigated as well as replicating field conditions such as squeeze pressure and squeezing slurry in between a cement-cement interface.

The wellbore simulator used in this study allows us to simulate wellbore conditions relevant to typical abandonment operations with the ability to control far more variables than in previous studies [11-30]. Curing pressure, confining pressure, injection pressure and temperature can be controlled using the experimental setup.

The objectives of this research are as follows:

i-) Conduct small scale experiments:

- Curing and testing the permeability of a small-scale bulk cement core.
- Curing and testing the permeability of a small-scale cement core inside a metal pipe.

ii-) Conduct wellbore simulator experiments using optimally placed cement plugs.

- Curing and testing the permeability of optimally placed abandonment plugs using the wellbore simulator.
- Compare the zonal isolation performances of two different cement blends: Neat G cement, as this the regulatory requirements for abandonment operations, and an engineered cement blend with enhanced sealing properties.

iii-) Conduct wellbore simulator experiments using contaminated cement plugs.

- Investigate the effect of water contamination on the cement system.
- Investigate the effect of oil contamination on the cement system.
- Investigate the role of stress which can induce the formation of a micro annulus.
- Identify the primary leakage pathways for abandoned wells.

iv-) Conduct remedial cementing experiments.

- Investigate the remediation capabilities of three types of cement slurries: Class G cement, Portland limestone cement and Microfine cement.
- Investigate the isolation capabilities of the remediated samples.
- Determine the fracture width that the remedial blends can penetrate into.

1.4 Organization of the Dissertation

This MSc thesis is comprised of the following 5 chapters:

Chapter 1 provides a brief introduction into the topic that is being investigated, followed by the problem statement which identifies the shortcomings and knowledge gaps in the literature. The objectives of the study are then stated.

Chapter 2 discusses the results of the permeability tests conducted by using small-scale samples made from neat G cement. The second part of this chapter discusses the permeability test results and the shear bond strength results of the optimally placed abandonment plugs using the wellbore simulator. For the wellbore simulator experiments, two types of cements were used, i.e., the class G neat cements and the class G cement with additives used to enhance the sealing potential of cement.

Chapter 3 discusses the effects of the introduction of contaminants into the cement slurry. Two different types of contaminants were used in this study. The cement was contaminated with 12.5% and 25% of water by cement volume. Then the cement was contaminated with 2.5% of light crude oil by cement volume. The permeability and shear bond strength of the samples were measured and compared.

Chapter 4 discusses the remediation capabilities of three cement blends, i.e., Class G cement, Portland Limestone Cement (PLC), and microfine cement. The penetration capabilities of the cement were determined by varying the fracture widths of the sample. The water conductivity of the remediated cores was also measured and compared to that of the open fracture.

Chapter 5 summarizes the key conclusions of the study and provides recommendations for future work.

1.5 References

[1] Schiffner, D., Kecinski, M. and Mohapatra, S., 2021. An updated look at petroleum well leaks, ineffective policies and the social cost of methane in Canada's largest oil-producing province. Climatic Change, 164(3), pp.60.

[2] Bonett, A. and Pafitis, D., 1996. Getting to the root of gas migration. Oilfield Review, 8.

[3] Watson, T.L. and Bachu, S., 2009. Evaluation of the potential for gas and CO2 leakage along wellbores. SPE Drilling & Completion, 24(01), pp.115-126.

[4] Forster, P., Storelvmo, T., Armour, K., Collins, W., Dufresne, J.L., Frame, D., Lunt, D., Mauritsen, T., Palmer, M., Watanabe, M. and Wild, M., 2021. The Earth's energy budget, climate feedbacks, and climate sensitivity. Chapter 7 of IPCC Sixth Assessment Report.

[5] AER, June 2024. Number of licensed wells in each stage of the life cycle, https://www.aer.ca/providing-information/data-and-reports/data-hub/well-status

[6] Khalifeh, M. and Saasen, A., 2020. Introduction to permanent plug and abandonment of wells (p. 273). Springer Nature.

[7] Barclay, I., Pellenbarg, J., Tettero, F., Pfeiffer, J., Slater, H. and Staal, T., 2001. The beginning of the end: a review of abandonment and decommissioning practices. Oilfield Review, 13(4), pp.28-41.

[8] Achang, M., Yanyao, L. and Radonjic, M., 2020. A review of past, present, and future technologies for permanent plugging and abandonment of wellbores and restoration of subsurface geologic barriers. Environmental Engineering Science, 37(6), pp.395-408.

[9] Dusseault, M.B., Gray, M.N. and Nawrocki, P.A., 2000, November. Why oilwells leak: cement behavior and long-term consequences. In SPE International Oil and Gas Conference and Exhibition in China, SPE-64733-MS. SPE.

[10] Thiercelin, M.J., Dargaud, B., Baret, J.F. and Rodriquez, W.J., 1998. Cement design based on cement mechanical response. SPE Drilling & Completion, 13(04), pp.266-273.

[11] Ozyurtkan, M.H., Altun, G., Mihcakan, I.M. and Serpen, U. An experimental study on mitigation of oil well cement gas permeability, In IPTC 2013: International Petroleum Technology Conference, pp. cp-350, European Association of Geoscientists & Engineers.

[12] Boukhelifa, L., Moroni, N., James, S.G., Le Roy–Delage, S., Thiercelin, M.J. and Lemaire, G., 2004, March. Evaluation of cement systems for oil and gas well zonal isolation in a full-scale annular geometry. In SPE/IADC Drilling Conference and Exhibition, Dallas, Texas, USA, SPE-87195-MS. SPE.

[13] Van Eijden, J., Cornelissen, E., Ruckert, F. and Wolterbeek, T., 2017. Development of experimental equipment and procedures to evaluate zonal isolation and well abandonment materials, In SPE/IADC drilling conference and exhibition, The Hague, The Netherlands, SPE-184640-MS. OnePetro.

[14] Corina, A.N., Opedal, N.V.D.T., Vrålstad, T. and Sangesland, S., 2019, June. Cement plug sealing studies of silica cement systems. In International Conference on Offshore Mechanics and Arctic Engineering, Glasgow, Scotland, UK, OMAE2019-95928. American Society of Mechanical Engineers.

[15] Opedal, N., Corina, A.N. and Vrålstad, T., 2018, June. Laboratory test on cement plug integrity. In International Conference on Offshore Mechanics and Arctic Engineering, Madrid, Spain OMAE2018-78347. American Society of Mechanical Engineers.

[16] Ogienagbon, A.A. and Khalifeh, M., 2023. Investigation of the hydraulic integrity of cement plug: Oilwell cementitious materials. Geoenergy Science and Engineering, 231, p.212261.

[17] Mabeyo, P.E., Ibrahim, Y.S. and Gu, J., 2020. Effect of high metakaolin content on compressive and shear-bond strengths of oil well cement at 80 C. Construction and Building Materials, 240, p.117962.

[18] Kamali, M., Khalifeh, M., Eid, E. and Saasen, A., 2022. Experimental study of hydraulic sealability and shear bond strength of cementitious barrier materials. Journal of Energy Resources Technology, 144(2), p.023007.

[19] Patel, A.D., Wilson, J.M. and Loughridge, B.W., 1999, February. Impact of synthetic-based drilling fluids on oilwell cementing operations. In SPE International Conference on Oilfield Chemistry, Houston, Texas, USA, SPE-50726-MS. SPE.

[20] Agbasimalo, N. and Radonjic, M., 2014. Experimental study of the impact of drilling fluid contamination on the integrity of cement–formation interface. Journal of Energy Resources Technology, 136(4), p.042908.

[21] Clark, C.R. and Carter, G.L., 1973. Mud displacement with cement slurries. Journal of Petroleum Technology, 25(07), pp.775-783.

[22] Zuiderwijk, J.J.M., 1974, May. Mud displacement in primary cementation. In SPE Europec featured at EAGE Conference and Exhibition, Amsterdam, Netherlands, SPE-4830-MS. SPE.

[23] Coleman, J.R. and Corrigan, G.L., 1941. Fineness and water-cement ratio in relation to volume and permeability of cement. Transactions of the AIME, 142(01), pp.205-215.

[24] Goode, J.M., 1962. Gas and water permeability data for some common oilwell cements. Journal of Petroleum Technology, 14(08), pp.851-854.

[25] Aughenbaugh, K., Nair, S., Cowan, M. and van Oort, E., 2014, September. Contamination of deepwater well cementations by synthetic-based drilling fluids. In SPE Deepwater Drilling and Completions Conference, Galveston, Texas, USA, SPE-170325-MS. SPE.

[26] Li, M., Ou, H., Li, Z., Gu, T., Liu, H. and Guo, X., 2015. Contamination of cement slurries with diesel-based drilling fluids in a shale gas well. Journal of Natural Gas Science and Engineering, 27, pp.1312-1320.

[27] Li, Z., Liu, H., Guo, X., Ou, H. and Gu, T., 2016. Contamination of cement slurries with oil based mud and its components in cementing operations. Journal of Natural Gas Science and Engineering, 29, pp.160-168.

[28] Bourgoyne, A.T., Scott, S.L, and Manowski, W., 2000. A review of sustained casing pressure occurring on the OCS, Bureau of safety and environmental enforcement.

[29] Scrivener, K.L., Crumbie, A.K. and Laugesen, P., 2004. The interfacial transition zone (ITZ) between cement paste and aggregate in concrete. Interface Science, 12, pp.411-421.

[30] Nelson, E.B. and Guillot, D., 2006. Well cementing, 2006. Schlumberger, Sugar Land, Texas, USA.

[31] Todorovic, J., Raphaug, M., Lindeberg, E., Vrålstad, T. and Buddensiek, M.L., 2016. Remediation of leakage through annular cement using a polymer resin: a laboratory study. Energy Procedia, 86, pp.442-449.

[32] Manceau, J.C., Hatzignatiou, D.G., De Lary, L., Jensen, N.B. and Réveillère, A., 2014. Mitigation and remediation technologies and practices in case of undesired migration of CO2 from a geological storage unit—Current status. International Journal of Greenhouse Gas Control, 22, pp.272-290.

[33] Meek, J.W. and Harris, K., 1993. Repairing casing leaks using small-particle-size cement. SPE Production & Facilities, 8(01), pp.45-50.

[34] Rike, J.L. and Pledger, T.M., 1981, March. Clean Fluids Improve Completion Results. In SPE Oklahoma City Oil and Gas Symposium/Production and Operations Symposium, SPE-9752. SPE.

[35] Bradford, B. and Reiners, B., 1985. Analysis gives successful cement squeeze. Oil & Gas Journal, 83(13), pp.71-74.

[36] Goodwin, K.J. and Phipps, K., 1984. Salt-Free Cement An Alternative to Collapsed Casing in, Plastic Salts (includes associated papers 12952 and 13012). Journal of Petroleum Technology, 36(02), pp.320-324.

[37] Nasional, B.S., 2002. SNI 13-6910-2002 Drilling Operation for Safe Conduct of Onshore and Offshore in Indonesia-Implementation.

[38] Normann, A.S., 2018. The most common causes for leaks in oil wells and 8 questions to consider before you select solution.

[39] Ewert, D.P., Almond, S.W. and Bierhaus, W.M., 1991. Small-particle-size cement. SPE Production Engineering, 6(02), pp.213-216.

[40] Slater, H.J., Stiles, D.A. and Chmilowski, W., 2001, February. Successful sealing of vent flows with ultra-low-rate cement squeeze technique. In SPE/IADC Drilling Conference and Exhibition, Amsterdam, Netherlands, SPE-67775. SPE.

[41] Wu, B., Arjomand, E., Tian, W., Dan, B. and Yan, S., 2020. Sealant technologies for remediating cement-related oil and gas well leakage. CSIRO.

[42] Farkas, R.F., England, K.W., Roy, M.L., Dickinson, M., Samuel, M. and Robert, E.H., 1999, October. New cementing technology cures 40-year-old squeeze problems. In SPE Annual Technical Conference and Exhibition, Houston, Texas, USA, SPE-56537-MS. SPE.

[43] Gong, F., Babadagli, T., Huang, H. and Li, H., 2024. Resolved CFD-DEM simulation of proppant aggregating and bridging mechanisms in a narrowing fracture. Powder Technology, 437, p.119548.

Chapter 2 Experimental Investigation of Well Cement Integrity in Abandoned Oil and Gas Wells

2.1 Abstract

This research is focused on testing the limits of cement abandonment plugs, evaluating their isolating capabilities under severe conditions. The results will be used to understand possible failure modes and ensure long term effectiveness of wellbore abandonment operations of different cement systems. In this study, small-scale bulk cement and abandonment plug (i.e. cement in casing) samples were optimally cured under 50°C and 1000 psi for a period of 7 days and tested for their permeability to understand the basic behavior of the cement. Water and Nitrogen permeability tests for all small-scale samples were conducted using a typical core flow setup. From the small-scale experiments, it was observed that bulk cement on its own had exceptionally low permeability. The small-scale abandonment plug exhibited relatively higher permeability than the bulk cement. Nitrogen flow was observed in the small-scale abandonment plug experiments, possibly through the cement-casing interface. A set of permeability experiments were also carried out using a physical wellbore simulator, which allowed cement curing and subsequent permeability testing under elevated pressure and temperature. The setup is designed to simulate abandoned wellbore section with variable fluid injection pressure, confining pressure and temperature conditions. Cement shear bonding strength was also determined after each experiment. Two different cement blends were tested using the wellbore simulator; Neat G cement without any additives and a Class G cement with additives that has been engineered to enhance its sealing performance. The wellbore simulator experiments had shown that the Class G plus additives cement plug outperformed Neat G cement blend in every testing scenario. Although both cement systems were tested in severe conditions, both performed adequately. The class G plus additives cement blend also resisted the formation of a micro annulus better than the Neat G cement. Results also indicate an inverse relationship between the shear bond strength of the cement plug and the permeability of the cement system, indicating that stronger mechanical bonding also delivered improved resistance to gas flow. Data measured from these experiments will form the baseline for future experiments where other crucial parameters are to be investigated.

2.2 Introduction

As of 2021, there are approximately 81,182 inactive wells in Alberta that have not been abandoned and about 74,482 abandoned wells [1]. As of March 25, 2021, 54.8 per cent of all currently inactive oil and gas wells on Alberta's list have been inactive for more than five years while 29.2 per cent have been so for more than a decade [2]. The main environmental concerns associated with inactive and abandoned wells are the potential risks of contamination of surface water and groundwater and the release of methane, a potent greenhouse gas [3, 4]. Watson and Bachu [5] analysed data from over 316,000 wells in Alberta and determined that about 4.5% of all oil wells showed gas migration/surface casing vent flow. Fugitive emissions reported in the literature usually combine all types of wells, so the individual leakage rates of abandoned wells and suspended wells are not clear.

The main purpose of well abandonment is to permanently isolate all subsurface formations penetrated by the well and isolate all permeable zones [6]. Portland cement has been commonly used as the recommended sealant for abandoning wells in the oil and gas industry [7]. The ability for Portland cement to provide an effective long-term seal is aided by designing the blend to the given well conditions, required chemical compatibility, optimal cement expansion and correct field operations to ensure optimal placement. Use of suboptimal cement designs or placement will significantly increase the risk of well integrity issues in the long term as they can increase the risk of flow paths [7]. In addition, the cement may be exposed to fluctuations in downhole pressure due to nearby hydraulic fracturing operations or temperature variations from thermal processes (such as steam-assisted gravity drainage operations), which can negatively affect cement integrity or cause debonding [7]. Local in-situ stress variation can also occur. These may include large-scale stresses such as plate tectonics, which can affect the tangential and radial stresses in the wellbore. They may also include small-scale stress changes in the form of pore pressure variation due to production and abandonment [8]. These changes can have a negative impact on the integrity of cement, resulting in fluid migration or loss of zonal isolation, even if the cement initially provided a good seal [7, 9]. When zonal isolation is lost, wellbore fluids such as methane may travel through these deficiencies and end up making their way to the surface. Figure 2-1 shows the leakage pathways that these pollutants potentially migrate across.

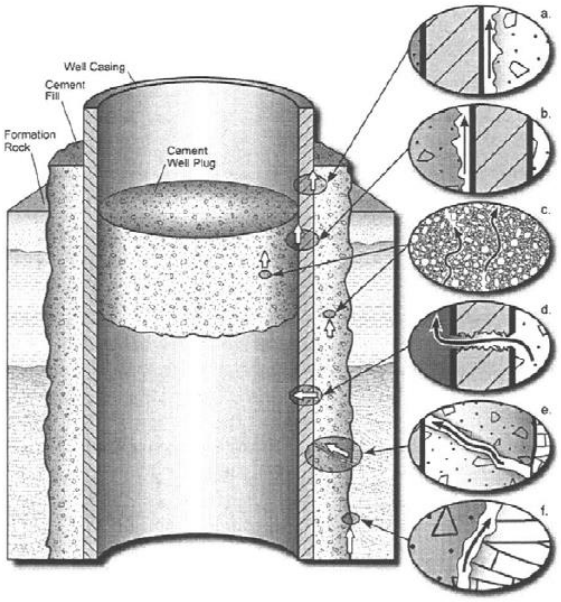

Figure 2-1: Potential leakage pathways in an abandoned well [10]

The technical requirements for an abandonment operation may differ significantly depending on the type of well that needs to be abandoned [11]. The abandonment process usually starts with hole cleaning, if the casing and cement sheath is considered to provide zonal isolation. If not, then the casing would need to be milled to ensure direct contact with the formation. After cleaning the well, barriers in the form of mechanical plugs are placed near the production zone. Once mechanical plugs have been placed, primary and secondary barriers in the form of cement is placed at the target zone. Any zones above the production zone that are fluid bearing will undergo the same treatment. An environmental plug is placed closer towards the surface and the wellhead is finally cut and removed [6].

Before the 1950s, most wells that were drilled for oil and gas exploration and production were not sufficiently documented, making abandonment process at a later date more difficult [12]. These wells were also not plugged with cement when the operator decided to abandon them and in fact some operators even ended up filling these abandoned wells with dirt [12]. These early abandonment techniques (filling with dirt) resulted in lots of wells leaking [12]. Since the 1950s, significant improvements in well abandonment techniques have occurred, although not at the same pace as drilling and completion technology. To reduce the likelihood of wellbore leaking, it is

critical that continued enhancement to plugging materials and placement methods occur.

There have been several papers published in the literature discussing the effects of subsurface conditions when designing an abandonment plug. However, generally there is a lack of data when it comes to testing cemented wells under relevant abandonment pressure and temperature conditions.

Dusseault [3] concluded that one of the main reasons we see oil well leaking is a result of cement shrinkage. During curing, circumferential micro-fractures form and propagate upwards causing the slow accumulation of gas in the casing [3]. Gas accumulation in the casing below the cement column yields to sustained casing pressure (SCP). It is stated that SCP occurs in 60-70 % of all the wells in the Gulf of Mexico; although 90% of the SCP is below the casing strength values, the risk still exists during production or abandonment [13]. Sustained casing pressure issues have also been reported elsewhere around the world like Canada and Norway [14]; however, detailed statistical data are not available from both of these locations. Thiercelin et al. [15] stated that stresses induced in the cement through deformation of the cemented casing resulting from varying downhole conditions can cause mechanical damage to cement in the form of cement debonding or cement cracking. One of his main conclusions was that instead of just focusing on the properties of cement alone, we need to consider all components of the system such as the cement, bottom hole conditions, casing, formation, and the interfaces between all these elements.

Ozyurtkan et al. [16] tested permeability of the cement plug only and did not consider the effects of having a casing (interface) around the cement plug. Boukhelifa et al. [17] carried-out experiments testing the sealing performance of cements by subjecting the sample to various downhole conditions to understand cement failure mechanisms. Boukhelifa [17] then used his results to validate his numerical models. However, the cement samples used in both of these studies were cured under ambient temperature and ambient pressure. The pressure and temperature in a wellbore will be much higher than ambient conditions and the cement properties after placement will be governed by both the temperature it was cured under as shown by Poon et al. [18] and pressure as shown by Meng et al. [19].

Van Eijden et al. [20] devised an experimental setup with the intention of replicating downhole conditions. Nonetheless, as the project progressed, it was deemed costly and time-consuming to assess all parameters. Consequently, a simplified model was applied, focusing on gauging cement expansion and shrinkage.

This design was then taken and modified by Corina et al. [21, 22] to test the permeability of cement. However, the work done by Corina et al.[21, 22] has limitations in their research as they cured the cement using nitrogen rather than water. In a real wellbore, the hydrostatic pressure is supported by water and not by nitrogen. Moreover, nitrogen may also cause cement dehydration and associated bulk shrinkage. Flow rates measured in this study are extremely high for such a low-pressure differential condition (> 500 ml/min at just 15 psi pressure difference between injection side and the outlet side), suggesting that the cured cement column is no longer bonded to the inner casing. The cement hydration reactions that occur during setting result in a new volume reduction of the material which can result in bulk shrinkage being observed. Water can help compensate for some of the shrinkage through absorption into the matrix but if the cement has no access to water, the shrinkage will likely be even more severe than observed in a real wellbore. Furthermore, the apparatus used to measure the permeability did not have a confining pressure, which was not representative of the real-world scenarios. There is also a lack of experimental data when testing the permeability of cement under relevant abandonment conditions.

Ogienagbon and Khalifeh [23] investigated the hydraulic integrity of cement plugs by carrying out permeability experiments. They built a pressure cell which can cure and test the permeability of the cement plug continuously. However, in their study, they noted that during curing, as the pressure used to cure the cement is extremely high, the casing ballooned up to 35.18μm radially. This reiterates the importance of applying a confining pressure to the casing as cement cure.

The shear bond strength of the cement-casing is another key factor to consider when analyzing the cement integrity in the wellbore. Mabeyo et al [24] studied the effect of substituting a fraction of class G cement with metakaolin to understand the effects of shear bond strength between the cement-casing interface. The cement was cured at 80 °C under ambient pressure, and subsequent shear bond strength tests were conducted post-curing. It is crucial to note that in a wellbore, the

pressure exceeds ambient levels. Furthermore, the shear bonding strengths were directly measured after curing. In a real wellbore, the abandonment plug system will be subjected to various stress variations such as production from an adjacent well and a more dynamic approach may be required where the cement is stressed first and then tested.

Kamali et al. [25] investigated the hydraulic sealability and shear bond strength of cement plugs. They noted that the shear bond strength of the cement depends on parameters such as surface geometry, chemical and mechanical characteristics of both the cement and the casing. They also concluded that the shear bond strength data on its own cannot be used to quantify the sealing performance of the cement and other mechanical variables such as tensile strength and modulus of flexibility, should also be evaluated.

Upon reviewing the literatures, it became evident that a comprehensive test design of assessing abandoned well integrity is essential, particularly under conditions that closely mimic typical abandonment scenarios, including relevant pressure and temperature conditions.

The wellbore simulator used in this study allows us to simulate wellbore conditions relevant to typical abandonment operations with the ability to control far more variables than done in previous studies. Curing pressure, confining pressure, injection pressure and temperature can be controlled using the experimental setup. In this paper, we compare the performances of two different cement blends; Neat G cement and a class G cement that is engineered to enhance sealing properties by using additives.

By curing the cement under relevant abandonment pressure and temperature conditions, we were able to better mimic what would happen in the wellbore. The cement plug was cured with water simulating real wellbore conditions. By applying a confining pressure to the abandonment plug during curing, artifacts in the form of a micro-annulus between the cement and casing could be minimized contrary to what was shown by previous studies. It is difficult to replicate the long-term environmental conditions that an abandonment plug is expected to see owing to the exceptionally long timeframes involved (>>multiple decades). We propose to use a proxy for this long-time frame through utilizing severe stress conditions. While such severe pressures are not expected to

be commonly observed in abandoned wells, the relative performance of different cement plugs under these conditions would be broadly representative of longer-term performance under milder conditions. After testing the performance of each cement blend under severe testing conditions, the shear bond strength of the cement plug was also measured to further compare both the cement blends.

The study presented here has two main objectives. 1) Curing and testing the permeability of optimally placed abandonment plugs to establish a baseline for future experiments. 2) Compare the performances of two different cement blends; Neat G cement as this the regulatory requirements for abandonment operations and an engineered cement blend with enhanced sealing properties.

Much of the past research has only focused on Neat G cement-based plugs. On its own Neat G cement slurry (at ~1900 kg/m3) will show some settling of the cement particles and up to 5% free water at the top of the slurry. This will create a plug that is not homogenous or at the designed density, making interpretation of the results difficult. In this study, we would like to expand this to evaluate more real-world cement systems. Plugs are not commonly just cement but they are also carefully engineered cement-based systems with a range of additives to facilitate safe pumping, placement and provide enhanced performance when placed down hole.

2.3 Methodology

The first step of the study was to start simple and look at the properties of cement on its own and cement inside a metal pipe. A small 1 inch diameter by 1 inch height bulk cement sample was prepared alongside a similarly sized cement in a metal casing representing an abandonment plug. The experiment was then upscaled using a wellbore simulator to simulate abandonment conditions. Results from the small-scale experiments were used to design a test matrix to rank the performance of each cement blend. Therefore, the experimental framework is, therefore, divided into two sections: The use of the small-scale samples and the upscaled wellbore simulator.

2.3.1 Materials

Two types of cement blends were used for this study. The cement mixing ratios and additives for each blend are listed in Table 2-1.

Cement blend	Cement: water mixing ratio	Additives	Slurry density (kg/m^3)
0:1:0 G "Neat"	0.440	Defoamer	1901
0:1:0 G + Additives	0.434	Accelerator, Fluid Loss, Dispersant & Defoamer	1901

Table 2-1: Cement blends used for the study

The functions of different additives are summarized below:

Accelerator – Aids in the development of early strength at low temperature and aids in the stability of the slurry by preventing particle settling.

Fluid Loss – Prevents fluid loss from the cement slurry.

Dispersant – Lowers the viscosity of the slurry for easier mixing and pumping and enhances the performance of the fluid loss additive.

Defoamer – Reduces the entraining of air bubbles in the cement slurry, facilitating easier field operations.

2.3.2 Cement Mixing

The cement was mixed as per the API-10B-2 [26] standard. Cement and water were weighed in separate containers. The blender was first set to 4000 rotations per minute (RPM) and inserted into the container with water. Cement was added to the water vortex over 15 seconds. After 15 seconds, the blender was set to 12,000 RPMs for 35 seconds. Once 30 seconds had elapsed, defoamer was added to the slurry. After high speed mixing, the cement slurry was then mixed at 150 RPMs for a period of 30 minutes to condition the slurry.

2.3.3 Small Scale Sample Preparation

The cement slurry was poured into two different mould as shown in Figure 2-2. Two types of mould were used for this study. A PTFE pipe with a 1-inch inner diameter was cut into 1-inch

sections and used to make the bulk cement sample. An AISI 4130 steel alloy pipe with an outer diameter of 1 inch and inner diameter of 0.944 inches was cut into 1 inch length sections to form the mould for the abandonment plug.

Electrical tape was attached to the bottom end of the moulds and the mixed cement slurry was poured into each mould. Once the mould was filled with the cement slurry, a second electrical tape was used to cover the top side of the mould, sealing the cement in place. The sealed mould was then placed into a curing cell.

The curing cell was connected to a pump which was used to apply curing pressure while the curing cell was placed in the oven. The cement samples were then cured for a period of 7 days at 50°C and at a pressure of 1000 psi using water as the confining fluid.

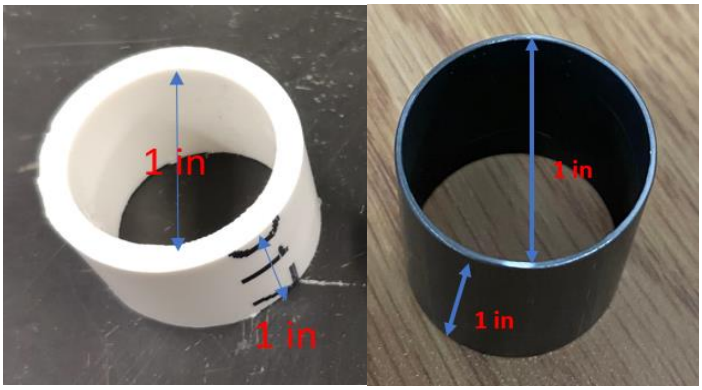

Figure 2-2: PTFE tube used to make bulk cement sample (left), metal pipe used to make abandonment plug (right).

After the curing process was completed, the curing cell was depressurized over 4 hours, this was done to prevent the formation of micro-cracks in the cement plug. The Teflon pipe surrounding the bulk cement sample was removed. The bulk cement sample was wrapped with electrical tape and placed into a core holder, ready for permeability assessment.

The abandonment plug was stored in a sealed bag while the permeability of the bulk cement plug was being assessed first. After the bulk cement permeability was measured, the cement sample was stored in a sealed bag. The samples were stored in a sealed bag to prevent the cement plug from dehydrating. Finally, the abandonment plug would be wrapped with electrical tape and placed

into the core holder, ready to be tested. Figure 2-3 shows both cement samples before permeability experiments.

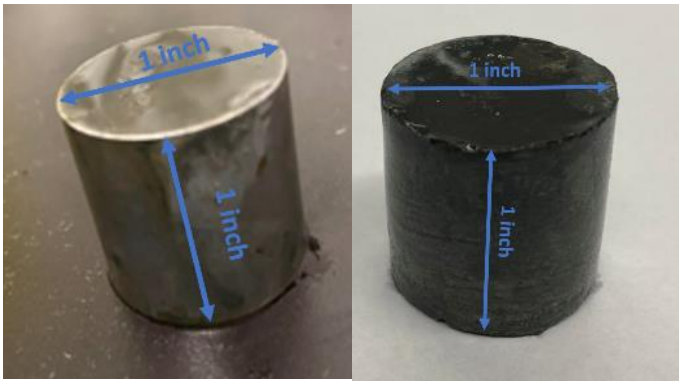

Figure 2-3: Abandonment plug using 4130 steel pipe (left) and bulk cement plug (right)

2.3.4 Permeability Measurements Using a Core Holder

The objectives of the small-scale sample experiments were to assess the permeability of the bulk cement samples and compare it to the permeability of the small-scale abandonment plug. The core holder used for permeability experiments can house a 1-inch by 1-inch cylindrical sample. There are two ports on each end of the core-holder, one port was used to flow the permeability testing fluid (nitrogen or water), and the secondary port was used to monitor the static pressure at both ends of the sample. The sample was housed inside a rubber sleeve connecting the inlet port to the outlet port. The rubber sleeve was needed to prevent fluid from bypassing the sample under high injection pressure. Two pressure transducers are connected to the secondary port to measure the absolute pressure differential at both ends of the sample. Two pumps are used to provide the confining pressure and inlet pressure. The schematic of the permeability measurement setup is shown in Figure 2-4.

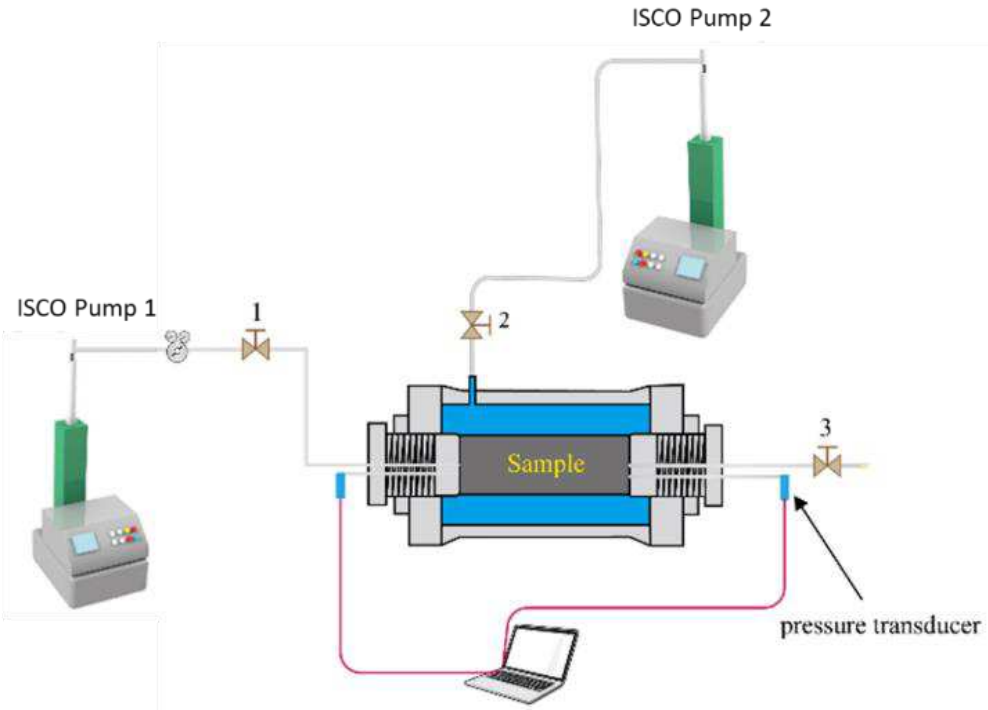

Figure 2-4: Schematic of the experimental setup used to measure permeability of small-scale samples.

The length and the diameter of the sample were first recorded, and the sample was then placed into the core holder. A confining pressure of 200 psi and injection pressure of 100 psi was first applied. Once this pressure has been achieved, all the flowlines are inspected for any signs of leakage. Once no leakage has been determined, the confining pressure and injection pressure are ramped up at a rate of 100 psi per minute. Once the confining pressure and injection pressure reached 1000 psi and 900 psi respectively, the pump was set to the constant pressure mode. Data from the pump and pressure transducer are recorded at every one-minute interval. To measure the nitrogen permeability, pump #1 is disconnected from valve #1 and replaced with a Nitrogen gas tank. A bubble flow meter is connected at the end of valve #3 to detect gas flow. Once the nitrogen gas tank was connected to the core holder, the procedure is repeated as described before for water flow. If a flow was detected, a stopwatch was used to measure the flow rate of the bubbles through the bubble flow meter.

2.3.5 Introduction to the Wellbore Simulator

A wellbore simulator previously designed and developed by Lin et al. [27] was used in this study (Figure 2-5). The main objective for designing such a device was to investigate the cement integrity by measuring the permeability of the cement column under elevated wellbore pressure and temperature conditions. The wellbore simulator can also mimic real world operations by allowing cement to be cured under the relevant wellbore conditions depending on the application of the cement. Figure 6 depicts all the essential components of the wellbore simulator. The inner casing (made from 4140 steel) is connected to valves #1 and #3 while the annulus between two casings is connected to valves #2 and #4. Pressure is applied to the wellbore simulator by connecting a Teledyne ISCO syringe pump 100DX to any of the 4 valves. The pump is an extremely sensitive device capable of measuring and recording flow rate as low as 0.0000001 ml/minute. The top and bottom caps both have a piston extension with O-rings embedded into the piston to prevent any fluid exchanges between the inner and outer casing. There is also an O-ring embedded in between the cap flange and the outer casing flange (shown in orange on Figure 2-6). This O-ring will seal in the fluids inside the annular space between inner and outer casings and prevent any fluid leakage to the atmosphere. Both the top and bottom caps are connected to the outer-casing by AISI 4140 steel screws as shown in Figure 2-5. The bottom and top plugs shown in yellow on Figure 6 were made from 4140 steel. The bottom and top plugs can be placed into the inner casing to isolate the cement slurry from the flow lines during the cement curing stage. To know more about the wellbore simulator design considerations and types of materials used, one can refer to Lin et al. [27].

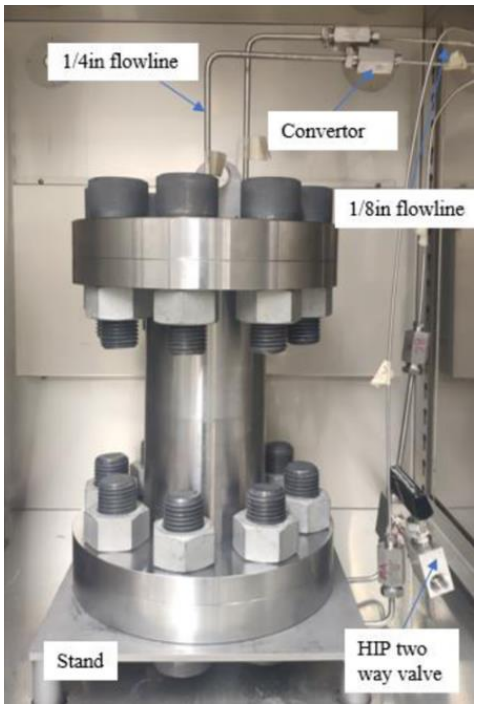

Figure 2-5: Wellbore simulator placed inside an oven [27].

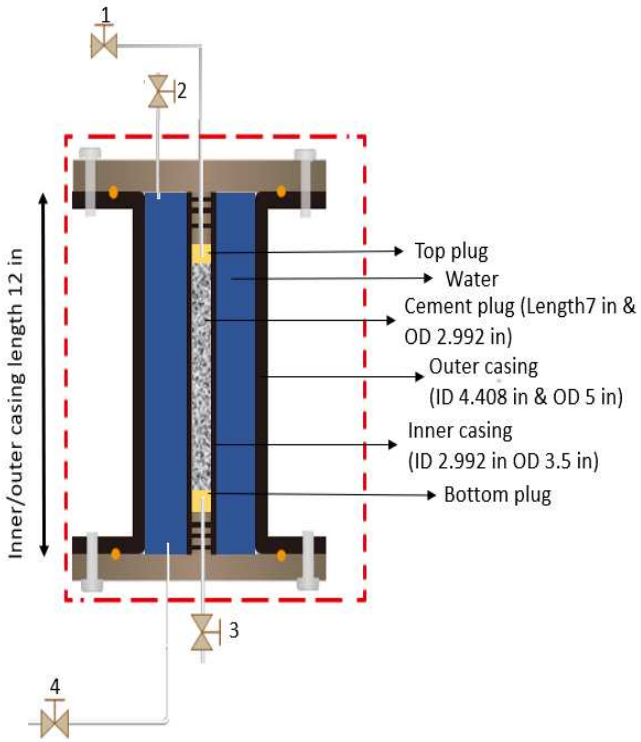

Figure 2-6: Schematic of the wellbore simulator

2.3.6 Wellbore Simulator Sample Preparation

The cement was mixed as per the API 10B-2 [26] standard. 800 milliliters of cement slurry was prepared and poured into the inner casing of the wellbore simulator to achieve the desired cement column height of 7 inches. After pouring the cement into the wellbore simulator, 50 ml of water was then slowly poured on top of the cement column to mimic wellbore conditions as shown in Figure 2-7.

The wellbore simulator was sealed up and the flow lines are connected. Both the annular pressure and inner casing pressure was ramped up to 1000 psi at a rate of 100psi/minute.

The cement was then allowed to cure at room temperature for 7 days. Water was used to provide the curing pressure and was injected from the top of the cement column; this was done to mimic the hydrostatic pressure in the wellbore.

After curing, the wellbore simulator was depressurized over 4 hours to the atmospheric conditions. This was done to prevent the formation of microcracks on the cement-casing interface. The wellbore simulator was then disassembled to remove the steel bottom plug which was used to isolate the flowlines from the cement slurry.

Once the bottom plug was removed, a Vernier caliper was used to measure the height of the cement column. This was done to confirm no settling of the cement column had occurred. The inner casing was then mounted back onto the wellbore simulator. Now the cement plug is ready for permeability assessment.

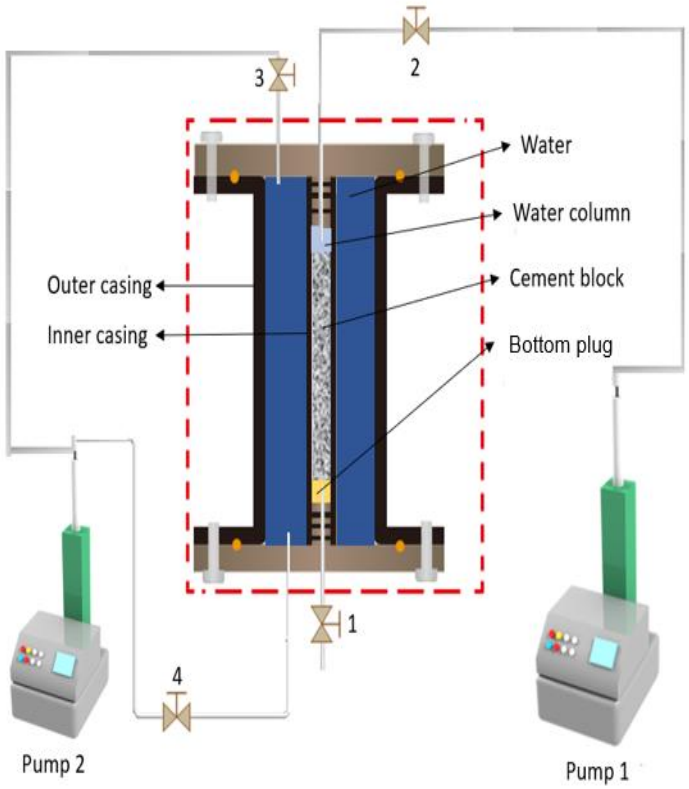

Figure 2-7: Schematic of the wellbore simulator during cement curing

2.3.7 Designing the Test Matrix

When a well is abandoned, the abandonment plug will be stressed laterally due to the effect of confining pressure and gas/hydrocarbon build-up pressure from the bottom of the plug. These stresses may change over time as a result of natural causes like seismicity or human-caused effects such as hydraulic fracturing operations in adjacent wells or oil and gas production.

Experiments conducted in this study aim to rank the performance of the cement systems by subjecting the abandonment plugs to severe testing conditions. One of the test matrix design's objectives is to create conditions, which potentially cause formation of a micro annulus and quantify the cement blend's performance.

The preliminary test matrix is summarized in table 2-2 and figure 2-8. A preliminary test matrix was designed where we would first test the water permeability for two days followed by testing the nitrogen permeability for one day. Once both tests were completed, we would reduce the annulus pressure by 250 psi and repeat same experiment to see if a micro-annulus would form

between the cement-casing interface. This process was repeated until the confining pressure was reduced all the way down to atmospheric condition and the objectives of the test matrix were still not met. The test matrix was then modified to only inject nitrogen rather than both fluids (as shown in Figure 2-8 on day 14). The injection pressure was also increased in a step wise manner.

The results from the preliminary test matrix were then used to design the final test matrix shown in table 2-3 figure 2-9. Water permeability was tested for 2 days followed by nitrogen permeability tests for 1 day (figure 2-9).

The confining pressure was reduced in a step wise manner at a rate of 250 psi per day and only the nitrogen permeability tests were carried out. The injection pressure was kept constant and the annulus pressure was reduced until the annulus pressure was at atmospheric conditions. A water permeability test was then carried out when the annulus pressure was at atmospheric levels (Step 7, Table 2-3).

A final water permeability test was carried out until the water flow rate stabilized. A final nitrogen permeability test (Step 8, Table 2-3) was conducted, but this time both the injection pressure (1000 psi) and confining pressure (15 psi) were kept constant until a gas breakthrough was observed.

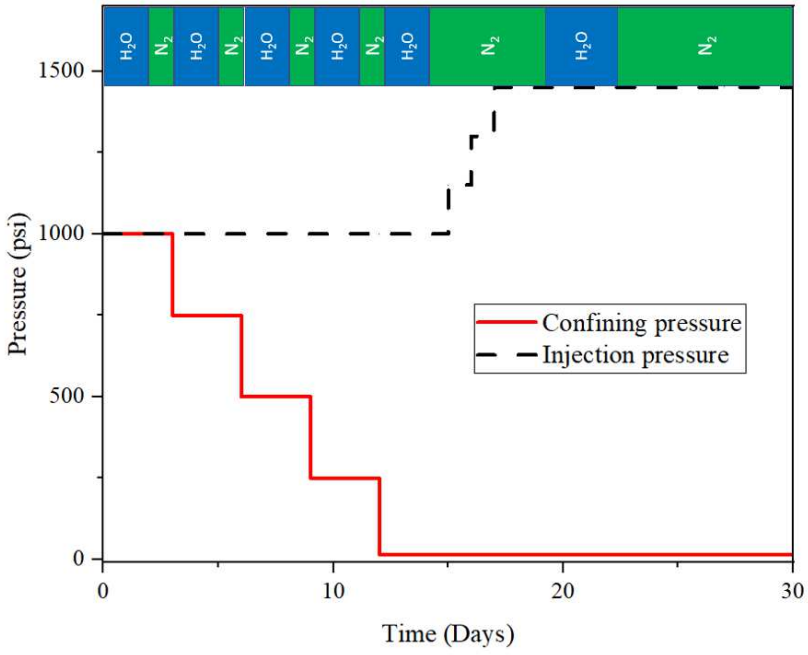

Figure 2-8: Preliminary test matrix design

Step #	Injection pressure (psi)	Confining pressure (psi)	Duration (days)
1	1000 (water)	1000	2
2	1000 (N_2)	1000	1
3	1000 (Water)	750	2
4	1000 (N_2)	750	1
5	1000 (Water)	500	2
6	1000 (N_2)	500	1
7	1000 (Water)	250	2
8	1000 (N_2)	250	1
9	1000 (Water)	15	2
10	1000 (N_2)	15	1
11	1150 (N_2)	15	1
12	1300 (N_2)	15	1
13	1450 (N_2)	15	1
14	1450 (Water)	15	Until stable flow rate
15	1450 (N_2)	15	Until gas breakthrough

Table 2-2: Preliminary test matrix

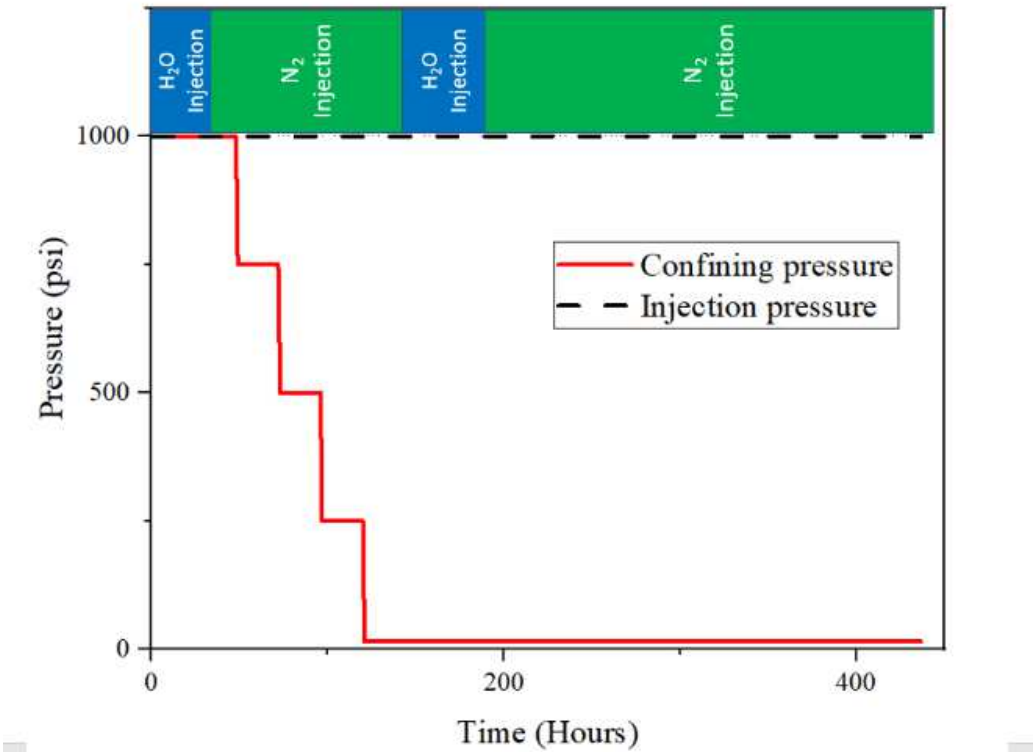

Figure 2-9: Final test matrix

Step #	Injection pressure	Confining pressure	Duration (Days)
1	1000 (Water)	1000	2
2	1000 (N2)	1000	1
3	1000 (N2)	750	1
4	1000 (N2)	500	1
5	1000 (N2)	250	1
6	1000 (N2)	15	1
7	1000 (Water)	15	Until stable flow rate
8	1000 (N2)	15	Until gas breakthrough

Table 2-3: Final test matrix

2.3.8 Ramp Up and Ramp Down Procedure Using the Wellbore Simulator

The annulus pressure and injection pressures were first ramped up to 150 psi. All the flowlines were inspected to ensure no leakage was occurring. Once all the flow lines were secure, the pressure was ramped up at a rate of 100 psi per minute until the target pressure of 1000 psi was reached. Once at 1000 psi, both pumps were set to constant pressure mode. Injection pressure was applied from the bottom as shown in Figure 2-10. Flow rate data were then recorded by the pump at a rate of 1 reading every 10 minutes. The pump was filled with either water or nitrogen depending on the objectives of the permeability test. Once the permeability test was complete, depressurization of the wellbore simulator took place over a period of 2 hours. This was done to prevent the formation of micro cracks in the cement plug.

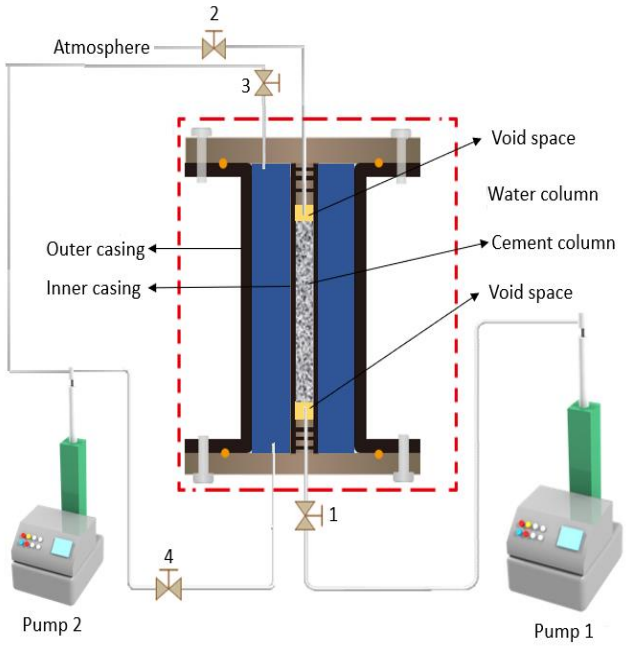

Figure 2-10: Schematic of the wellbore simulator during permeability measurement

2.3.9 Shear Bond Strength Measurements

The last step of the experiment was to determine the shear bond strength between the cement and the inner casing. The shear bond strength measured in these experiments gives us an idea of shear bond strength which can be used to compare the performance of each cement blend rather than

measure the true shear bond strength of the cement. This is because the rate at which the force is applied by the hydraulic press onto the cement column is not controlled.

The inner casing was removed from the wellbore simulator and placed on a hydraulic press as shown in Figure 2-11. The inner casing was lined up underneath the ram assembly and secured in place using an inner casing stabilizer. An aluminum piston with diameter of 2.85 inches was used to push the cement plug out of the inner casing. The force needed to displace the cement was read directly from the load gauge. The cement plug that falls out of the inner casing was collected and examined further. The shear bond strength was then determined by calculating the force needed to break the shear bond divided by the contact area between the cement and inner casing.

$$SBS = F/(2 * \pi * \mathrm{r} * \mathrm{h}) \qquad (1)$$

SBS – Shear bond strength (Pa)

F – Force (N)

r - Radius of cement column (m)

h – Height of cement column (m)

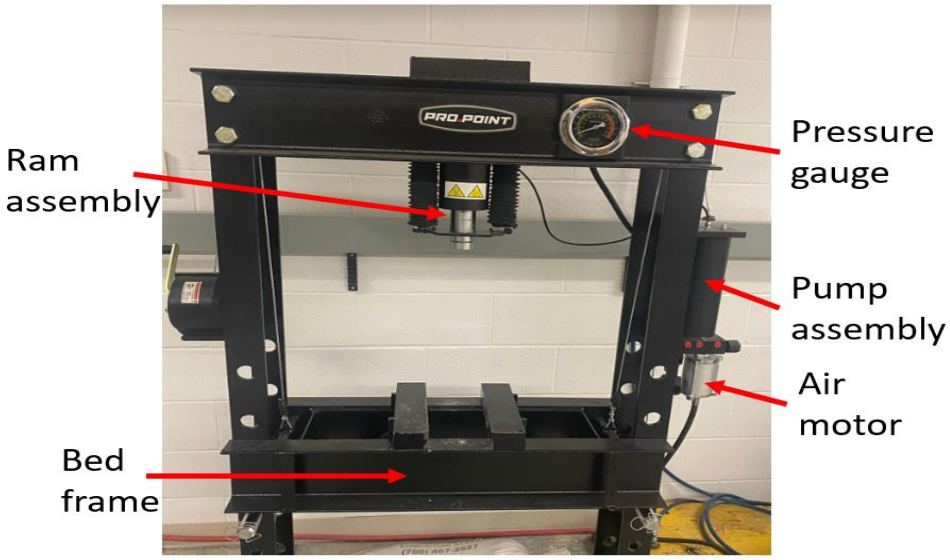

Figure 2-11: Hydraulic press used to measure the shear bond strength of the cement.

2.4 Results and Discussion

2.4.1 Small-Scale Bulk Cement Test

Bulk cement water permeability experiment was conducted using constant injection and confining pressure. Neat G cement was used for the small-scale experiments. An injection pressure of 900 psi and a confining pressure of 1000 psi were used for this test. There was no water breakthrough observed during the water permeability tests. However, minor volumetric changes in the pump over the testing period was observed and recorded as a function of time. The average water volumetric change was determined by subtracting the volume of water remaining inside the pump at every 10-minute interval. The maximum water injection rate recorded by the pump over a two-day period was only 0.0003 ml/minute. The water injection rate (ml/min) into the bulk cement sample as a function of time is shown in Fig 2-12.

No water breakthrough was observed throughout the experiment. However, minor volumetric changes were being recorded by the pump. This water loss could be a result of cement hydration reactions or due to volumetric changes of the cement plug rather than permeability. The water flow rate was initially high, but towards the back end of the experiment, minimal water was being consumed. The flow rate was initially higher as the bulk cement was charging, but as the experiment progressed, water saturation increased and flow rates declined to negligible levels.

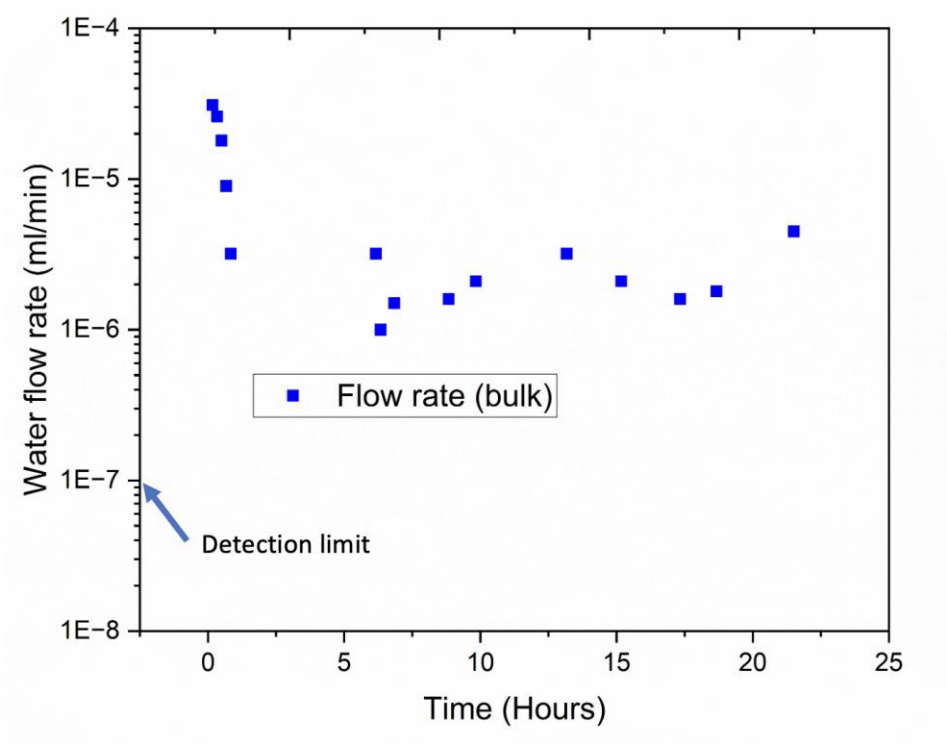

Figure 2-12: Bulk cement - water injection rates

After the water permeability experiment, Nitrogen permeability test was carried out using the same injection (900 psi) and confining (1000 psi) pressures for a period of three days and no gas breakthrough was observed.

2.4.2 Small-Scale Abandonment Plug Test

The abandonment plug water permeability experiment was also conducted using constant injection and confining pressure. The maximum water injection rate recorded by the pump over a period of one day was 0.0018 ml/minute. The total volume of water loss from the pump was recorded as 0.21 ml over the one-day testing period. From figure 2-13, it can be seen that the initial water injection rates were relatively high, but the average water injection rate stabilized after 200-minutes of injection time at around 0.0001ml/minute. An injection pressure of 900 psi and a confining pressure of 1000 psi were used.

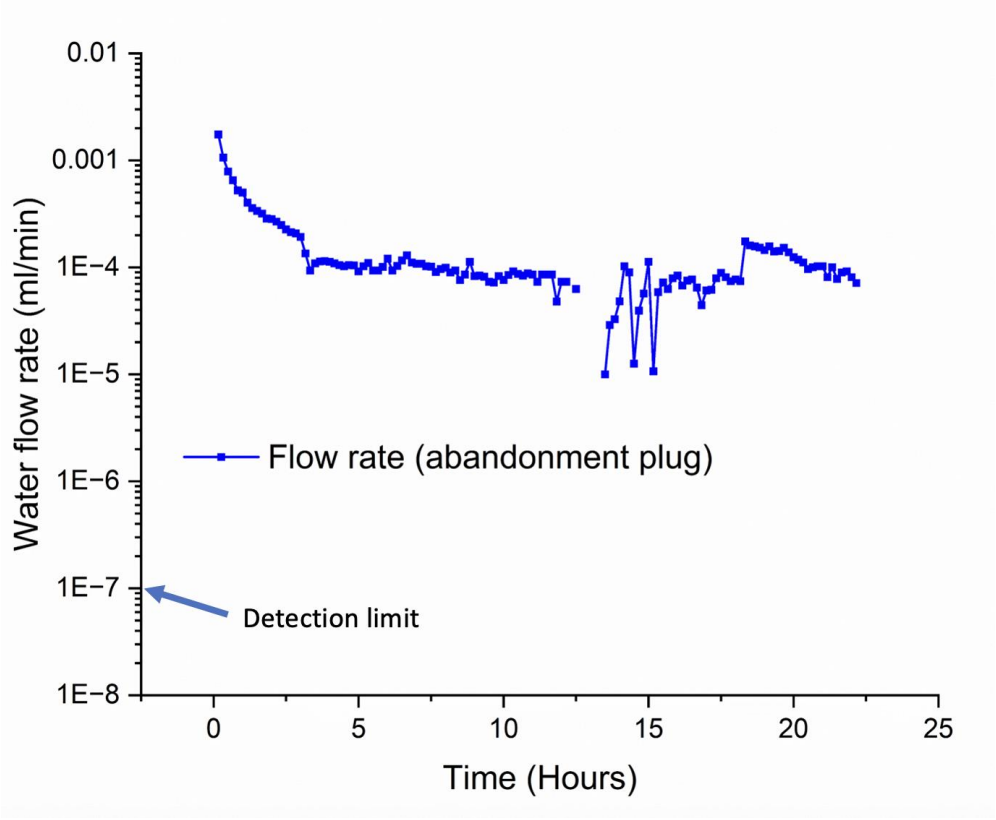

Figure 2-13: Abandonment plug – water injection rates

After the water permeability experiment, nitrogen was injected for 2 days. Initially no gas flow was detected, but after 2 days of continuous nitrogen injection, a gas breakthrough was observed. A flow rate of 400 ml/min was recorded at 1000 psi injection pressure.

After completing the permeability measurement experiment, the small-scale abandonment plug sample was taken out of the core holder. The small-scale abandonment plug showed signs of de-bonding from the metal pipe. The images of the abandonment plug before and after the experiments (Figure 2-14) confirms that debonding took placed during the experiment.

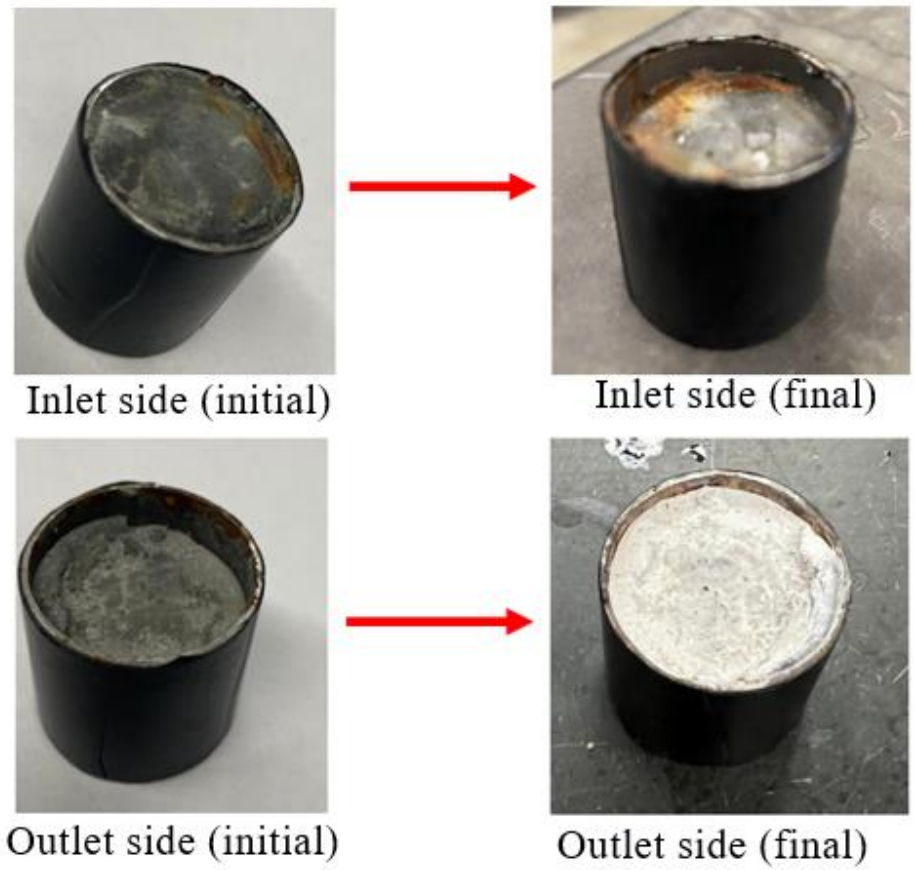

Figure 2-14: Abandonment plug before and after nitrogen permeability experiment

2.4.3 Comparison of the Water/Nitrogen Flowability Test Results - Bulk Cement Versus Abandonment Plug

From the small-scale core flow experiment results, it was observed that both bulk cement and abandonment plug cement samples had low water permeabilities. Since there was no water breakthrough in either experiments, we could only compare the water injection rates in both experiments. As shown in Fig.2-15, a relatively higher water injection rate was observed in small scale abandonment plug experiment when compared to the bulk cement. It is possible that more water was consumed by the abandonment plug as water could have traveled along the cement-casing interface. The addition of up to 1000 psi confining pressure in these tests may have induced surface deformation and or micro cracks to form at the interface, but these pathways may not be in full communication with each other, hence we did not get water break through but observed elevated water injection rates.

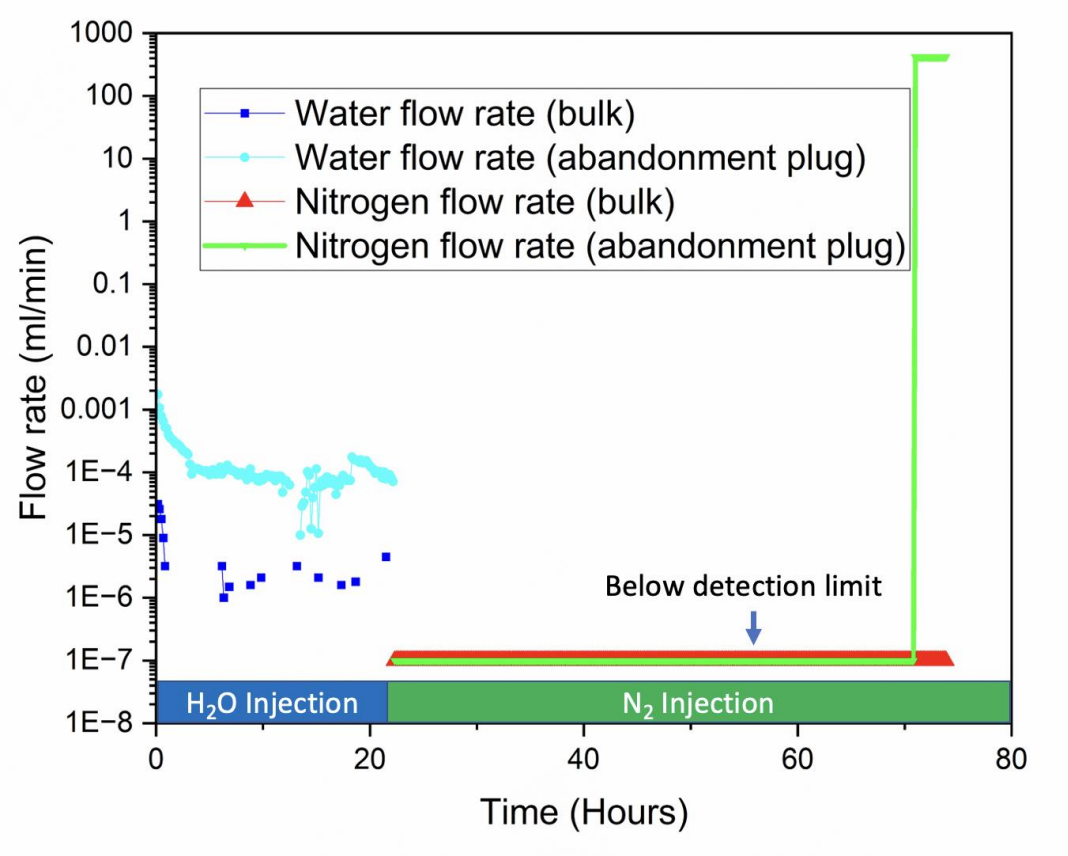

Figure 2-15: Flowability comparisons - bulk cement versus abandonment plug

There was no Nitrogen flow breakthrough observed in the bulk cement sample. However, significant Nitrogen flow (breakthrough) was eventually (after 70 hours) observed in abandonment plug tests. When nitrogen injection started, the water saturation in the cement plug would have been high; but with prolonged exposure to dry nitrogen at high pressures, cement dehydration could have taken place, causing minor bulk shrinkage in the cement. This minor dehydration induced bulk shrinkage could have developed a micro annulus, causing gas to breakthrough after two days rather than instantaneously. It is important to note that shrinkage induced by dehydration process is not expected to be prevalent in the field as any downhole formation gas would be water saturated owing to the presence of the pore fluid. Bulk shrinkage of the cement could also reduce the radial stress applied by the cement plug onto the metal pipe, reducing the bond strength at the interface. As we were using high pressures, this reduction in the bond strength due to bulk shrinkage might have caused the cement plug to migrate through the metal pipe.

It is noteworthy that even though debonding took place, the cement plug still maintained some level of shear bond strength, suggesting that debonding was partial rather than complete.

2.4.4 Wellbore Simulator Test Results

Preliminary test matrix results: One of objectives when designing the test matrix was to simulate downhole pressure conditions that would potentially induce a micro annulus and rank the performance of different cement blends under these conditions. In order to determine an optimum test matrix, we conducted preliminary permeability experiments using Class G plus Additive Cement. Figure 2-16 summarizes the preliminary test matrix (also shown in Table 2-2) and the Nitrogen and water flowability test results.

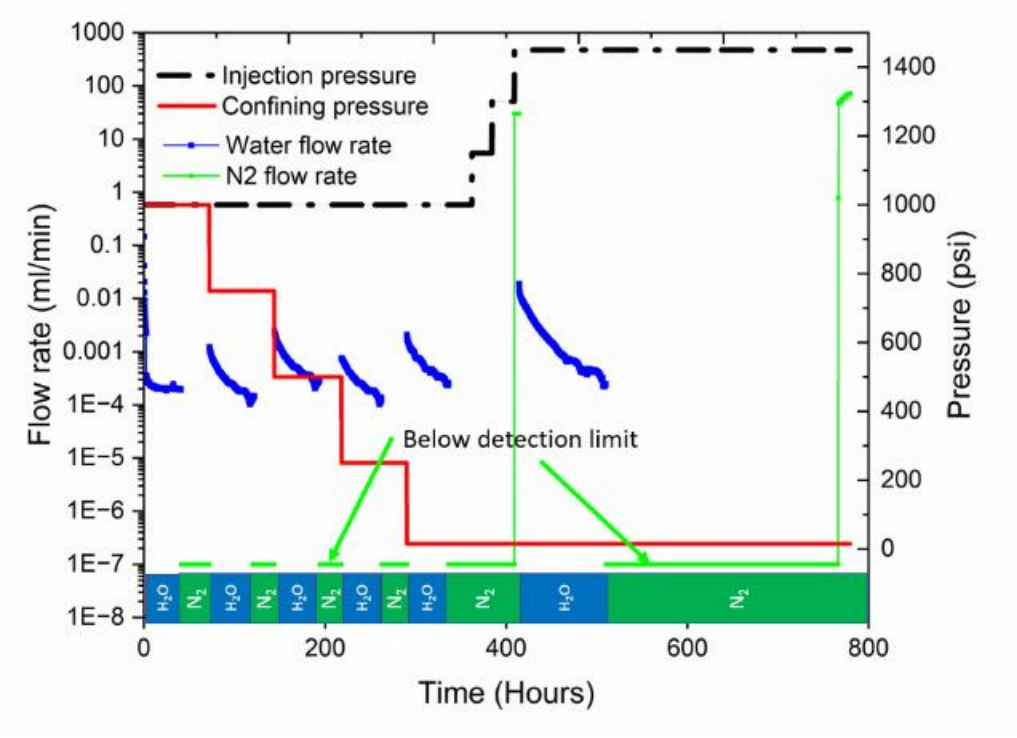

Figure 2-16: Preliminary test matrix using G plus additives - water/nitrogen injection rates.

As per the test matrix (Figure 2-16), the first step of the wellbore simulator experiment was to test the water permeability of the abandonment plug at an injection pressure of 1000 psi and a confining pressure of 1000 psi. The water injection rate was stabilized at 0.00025 ml/min; however, no water breakthrough was observed. Nitrogen was then injected for a period of 1 day and no gas breakthrough was observed. The next step was to reduce the confining pressure to 750 psi and see

if that would result in the formation of a micro annulus. Similar water injection rate readings were recorded but again no water or gas breakthrough was observed. This process was repeated several times until the annulus pressure was reduced to atmospheric pressure. Even at atmospheric (confining) pressure, no water or gas breakthrough was observed, clearly demonstrating the robustness of the cement plug and its excellent isolating capabilities.

During this process, we observed a certain trend in the water injection rate as a function of time. The water injection rates at the start of the experiment (0.005 ml/min) was generally higher, by order of 1 or 2 magnitudes than the water injection rate at the end of the experiment (0.0001 ml/min). Clearly, there was a larger intake of water into the cement matrix at the start of the experiment. This may be because cement was being dehydrated by the injection of dry nitrogen gas and following that, the injected water was rehydrating the cement plug. From the first five sets of water injection tests, anywhere between 1.5ml to 2ml of water was being used to rehydrate a cement column with volume of 700 ml. The test matrix was then changed to only inject nitrogen and increase the injection pressure to see if that would result in a gas breakthrough as shown in Figure 2-16 (at 370 hours). After three continuous days of Nitrogen injection, a gas breakthrough was observed at an injection pressure of 1450 psi. The Nitrogen breakthrough flow rate was measured as 30 ml/s.

Once we have induced a micro annulus, the next logical step was to check if we could flow water through this artificially induced micro annulus. Water was injected at 1450 psi injection pressure and atmospheric confining pressure. A maximum flow rate of 0.02 ml/min was recorded, which was the highest flow rate recorded throughout the experiment. However, after 3 days of water injection, water injection rate declined back to the preliminary levels and no water breakthrough was observed. A relatively larger volume of water (12.29 ml) was consumed (compared to steps 1, 3, 5, 7 and 9 in Table 2-2) to close up the micro annulus space (i.e. rehydration of the cement).

A final nitrogen permeability test was conducted while keeping the injection pressure constant at 1450 psi and confining pressure at atmospheric levels. Nitrogen breakthrough took place after 11 days of constant nitrogen injection. A flow rate of 42 ml/min was recorded. Based on these preliminary test results, we finalized the test matrix (Table 2-3) to be used for the rest of the experiments.

Neat G cement tests: Permeability tests of the neat G cement was conducted as per the test matrix shown in Table 4 and Figure 10. The first step of the experiment was to test the water permeability of the neat G abandonment plug at an injection pressure of 1000 psi and a confining pressure of 1000 psi. Variation of the water injection rates over time during step 1 is shown in Figure 2-17. Water breakthrough was observed as soon as the experiment commenced. The maximum flow rate recorded by the pump was 0.105 ml/minute over a one-day testing period. As seen in Figure 2-17, water flow rates were initially high, but the average flow rate steadily declined over the experiment. The average water flow rate during the last 6 hours of the experiment was calculated as 0.04 ml/min, forming the baseline for water permeability experiments using Neat G cement. Water was also collected from the outlet side, indicating that water had indeed bypassed the Neat G abandonment plug through a micro annulus.

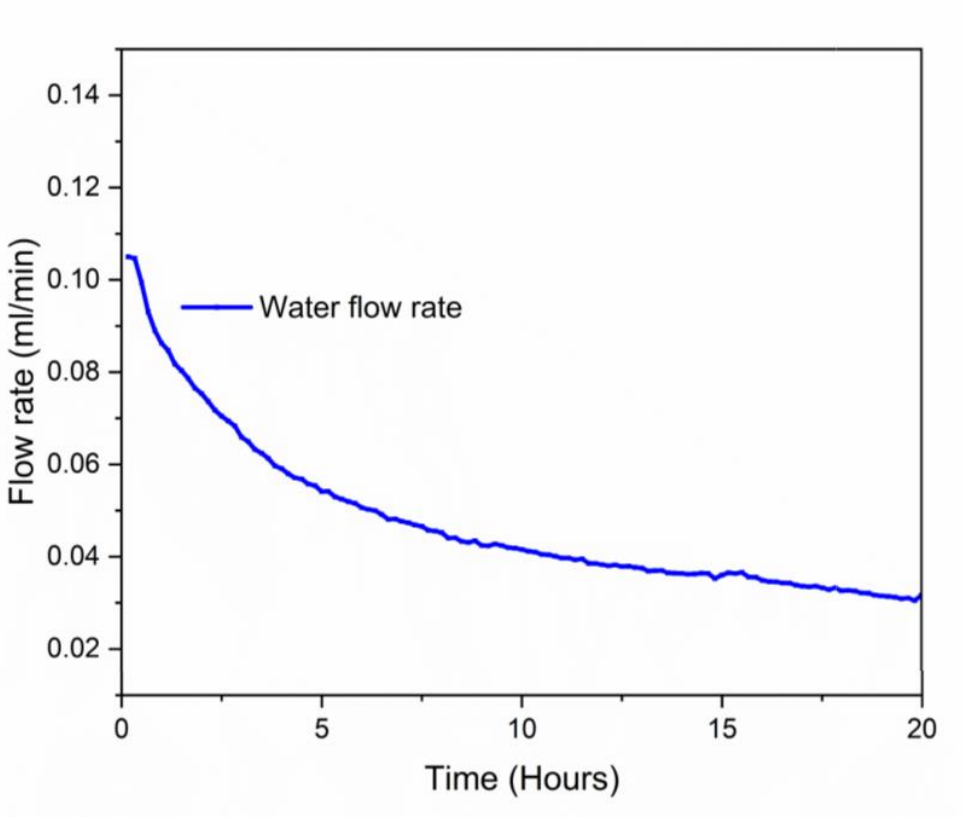

Figure 2-17: Water flow rate through the neat G cement column, step 1

After the water permeability experiment (step 1), nitrogen was injected at 1000 psi injection pressure and 1000 psi confining pressure. Nitrogen breakthrough was observed immediately. A

nitrogen breakthrough flow rate was measured as 154 ml/min forming the baseline for nitrogen permeability experiments using Neat G cement. The water permeability and nitrogen permeability tests were repeated as per the test matrix (Table 2-3, Figure 2-10). As we reduced the confining pressure, the nitrogen flow rates rapidly increased above our detection limit (> 600 ml/min) as shown in Figure 2-18.

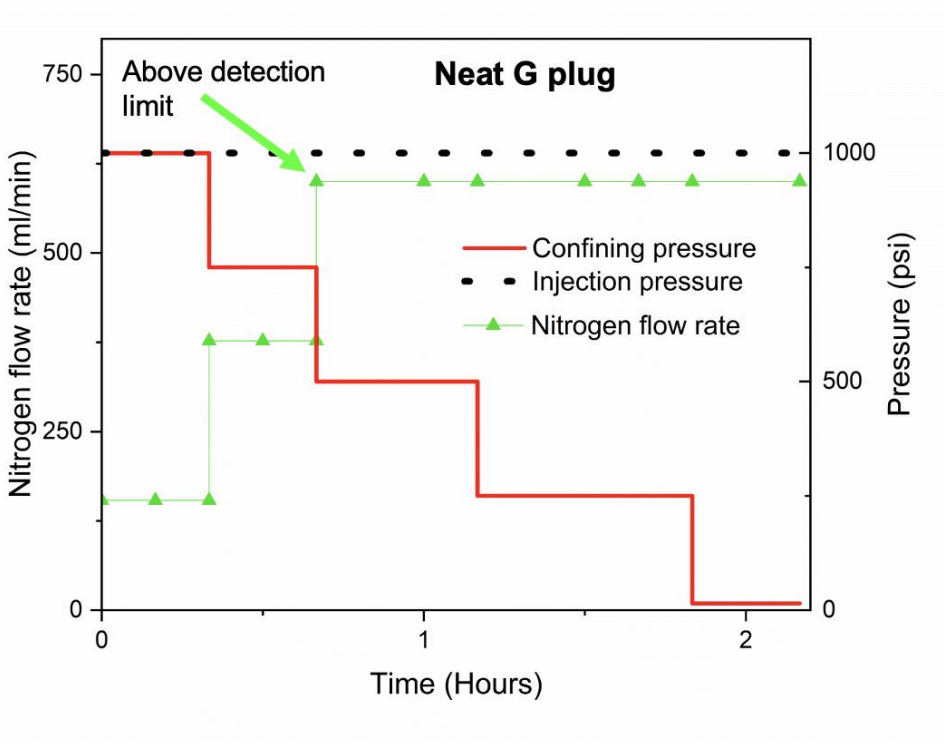

Figure 2-18: Nitrogen flow rate summary using neat G cement

After the nitrogen permeability experiment, Water was now injected at an injection pressure of 1000 psi and a confining pressure of 15 psi (step 7). The average water flow rates were measured at 0.25 ml/min (6 times higher than the water flow rate measured at step 1). Figure 2-19 summarizes the full schedule of the experiment conducted using Neat G cement.

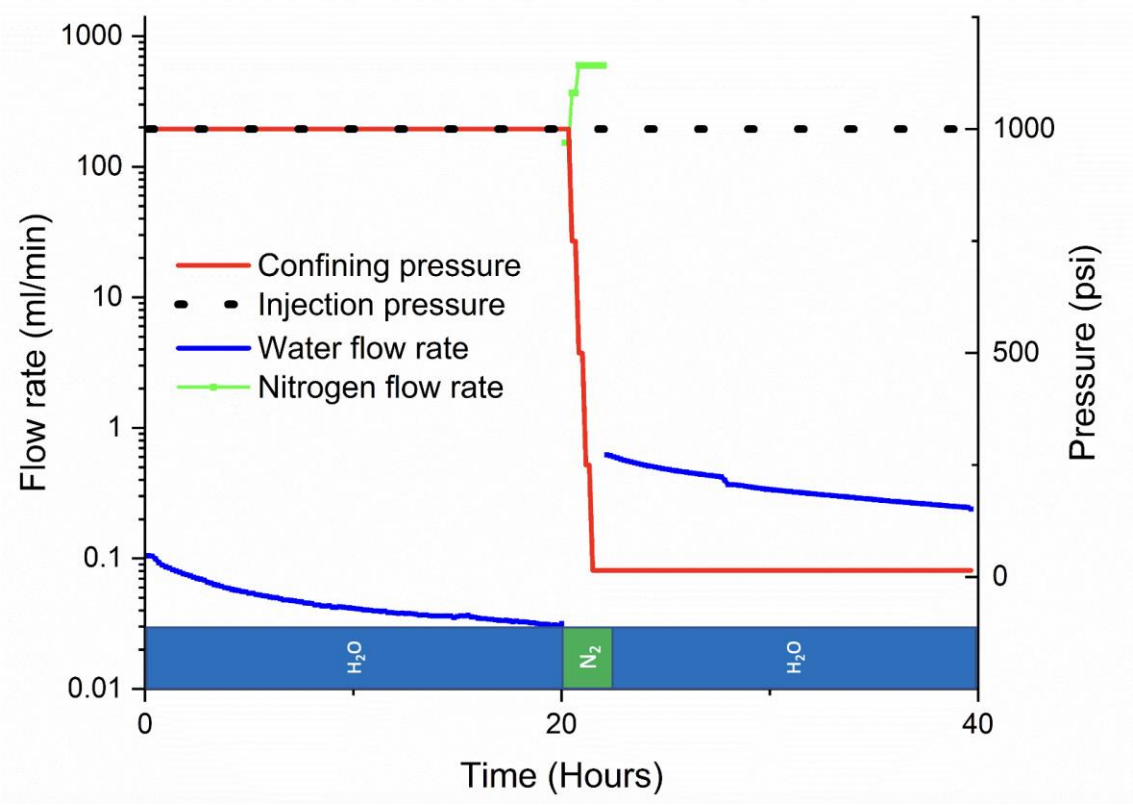

Figure 2-19: Full schedule of water/nitrogen flow rate results using neat G cement

Class G plus additives tests: Full test schedule and the recording of Nitrogen and Water flow rates during the Class G plus additives cement experiments are shown in Fig 2-20.

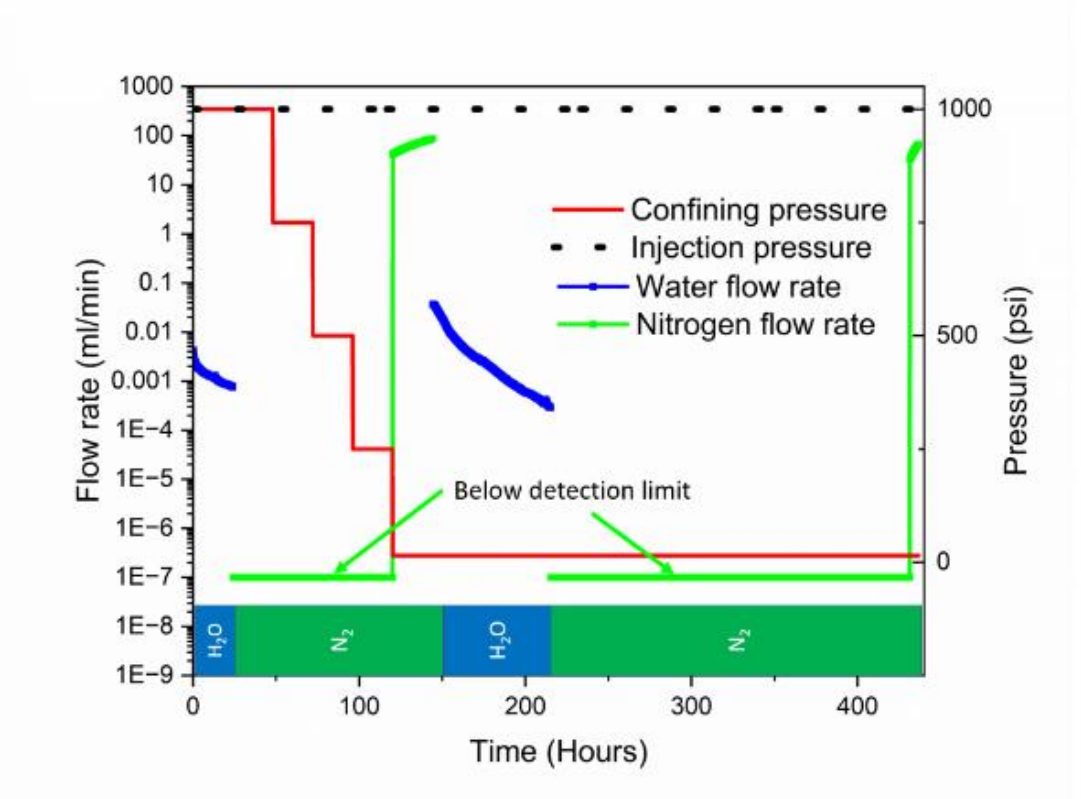

Figure 2-20: Full schedule of water/nitrogen injection rate results using G plus additive cement

As per the test matrix (Table 2-3, Figure 2-10), the first step was testing the water permeability at an injection pressure of 1000 psi and a confining pressure of 1000 psi. There was no water breakthrough observed during the two-days testing period. However, minor volumetric changes (1.92 ml of water consumed) were recorded by the pump. Detailed variation of the water injection rates as a function of time during step 1 is shown in Figure 2-21. The maximum water injection rate recorded over the two-day testing period was 0.004 ml/min. The water injection rates declined steadily over time and stabilized around 0.0008 ml/min forming the baseline for class G plus additives cement blend (Figure 2-21).

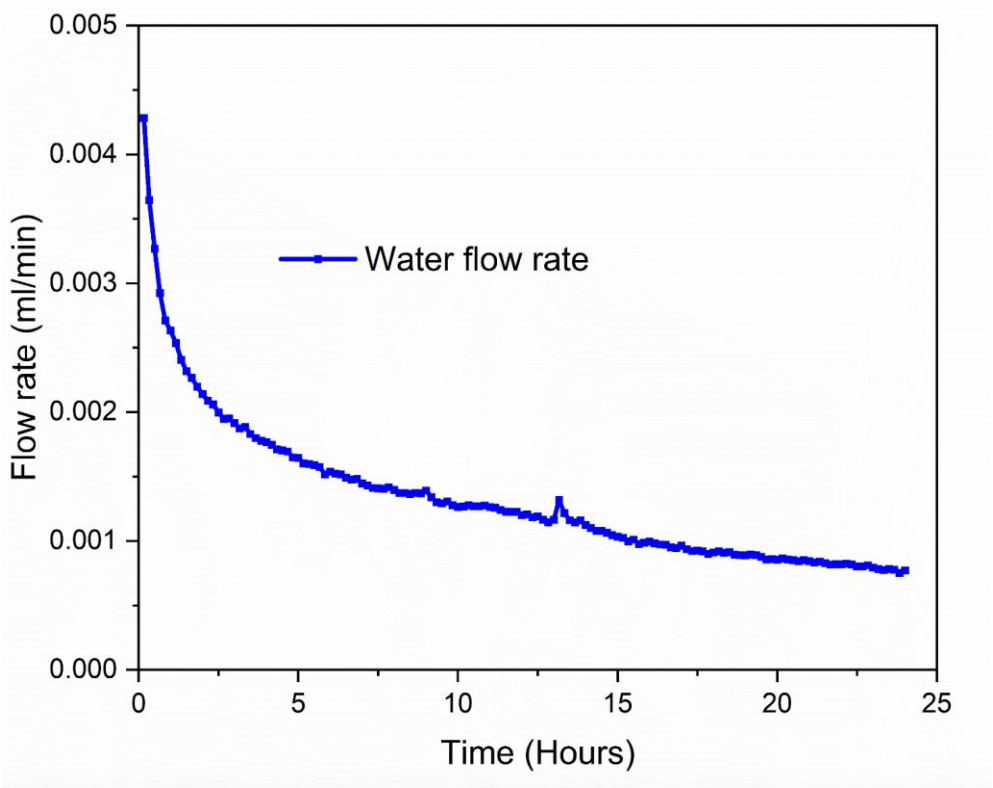

Figure 2-21: Water injection rates into the class G plus additives cement column, step 1

After the water permeability test (Step-1), the pump was filled with nitrogen. Nitrogen was then injected at an injection pressure of 1000 psi and a confining pressure of 1000 psi. Initially, no nitrogen gas breakthrough was observed. The experiment was continued without changing the initial injection and confining pressures for 24 hours. After 24 hours, no gas breakthrough was observed. The injection pressure was kept constant, the annulus pressure was reduced to 750 psi, and the experiment carried on for another 24 hours. Once again, no gas breakthrough was observed, then the annulus pressure was further dropped down to 500 psi and this process was repeated until the annulus pressure was at atmospheric pressure.

Gas breakthrough was observed as soon as the annulus pressure was reduced to atmospheric pressure. Detailed summary of the Nitrogen flow rates are shown in Figure 2-22 (also in Figure 2-20), Results shown in Figure 2-22 illustrate that nitrogen breakthrough in the abandonment plug cement column was not observed until the confining pressure was reduced to atmospheric levels. Nitrogen breakthrough flow rate was measured as 42 ml/min.

The confining pressure drop in the annulus allowed the inner casing to expand in combination with dry nitrogen dehydrating the cement plug, most likely creating micro channels between cement column and casing. Nitrogen bypassed the abandonment plug through the micro annulus space and was measured as 42 ml/min using a bubble flow meter. A second permeability test was conducted 24 hours after gas breakthrough was initially observed. Nitrogen flow rate of 87 ml/min was recorded after 24hrs, indicating a progressive increase in the permeability of the Class G plus additives abandonment cement plug. This phenomenon could be attributed to cement dehydration. As the cement was dehydrating, the micro-annular space could widen further, allowing more nitrogen to bypass the sample.

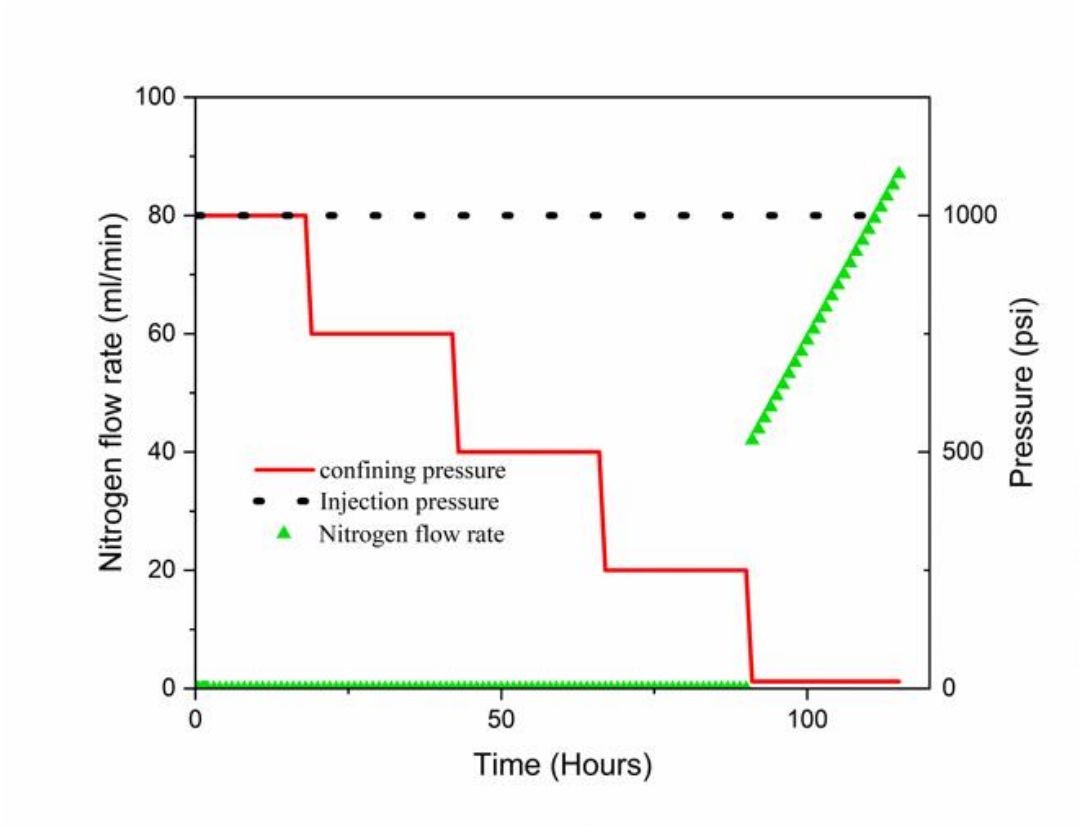

Figure 2-22**:** Nitrogen flow rate summary using class G plus additives cement blend (step 2 to step 6).

After gas breakthrough was observed, the next step as per the test matrix (table 2-3, Figure 2-10) was to investigate if water would now flow through the artificially induced micro-annulus. The confining pressure was kept at atmospheric pressure and water was injected at an injection pressure

of 1000 psi. No water breakthrough was observed even when a micro annulus was artificially induced during the Nitrogen permeability experiment.

However, minor volumetric changes in the water injection rate was recorded by the pump. Detailed variation of the water injection rate as a function of time is shown in Figure 2-23.

As shown in Figure 2-23, the initial water injection rate recorded by the pump was 0.037 ml/min. This injection rate was one order of magnitude larger than the initial water injection rate recorded for this experiment during step 1 (Figure 2-21). Although the water injection rate was initially much higher than the water injection rate recorded during Step-1, the flowrate declined sharply over the first day of water injection. During the last 6 hours of the experiment, the flow rates recorded by the pump were identical to the flow rates recorded at the start of the experiment in Step-1 (Figure 2-21) (0.004ml/min). These results indicated that the large initial water injection rates could be attributed to cement rehydration reactions. A total of 21.33 ml of water was consumed by the cement plug for cement hydration reactions. Cement rehydration reactions closed the micro annulus that was created by both reducing the confining pressure and cement dehydration that might have occurred during nitrogen injection test.

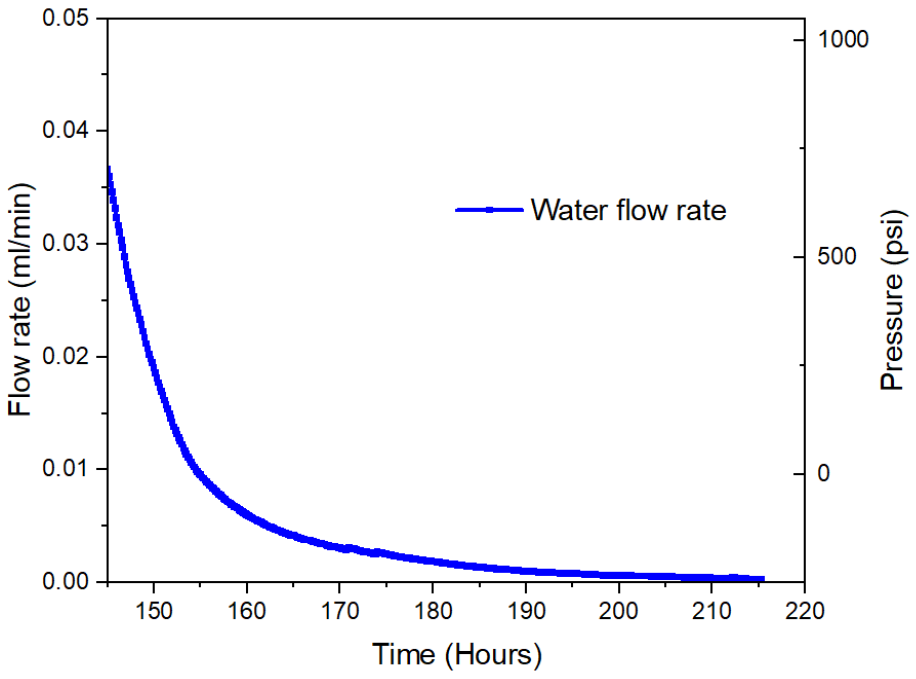

Figure 2-23: Water injection rates into the class G plus additives cement column, step 7.

A final nitrogen permeability test was carried out as per the test matrix (table 2-3, Figure 2-10). The nitrogen injection pressure was set at 1000 psi and the confining pressure remained at atmospheric levels. The set up was left undisturbed and the volume of the pump was checked every day to identify if gas breakthrough occurred. On the 9th day of continuous nitrogen injection, a gas breakthrough was observed. Nitrogen flow rate of 66 ml/min was recorded. Based on the results of the second Nitrogen permeability experiment, it can be inferred that a micro annulus formed mainly due to cement dehydration. Prolonged exposure of the abandonment plug to dry nitrogen gas caused the cement to dehydrate, forming a micro-annulus. The dehydration effect is also reversible.

Comparisons of the Neat G vs Class G plus additives cement test results

Figure 2-24 shows the comparison of the water injection rates into the neat G cement and the class G plus additives cement at 1000 psi injection pressure and 1000 psi confining pressure. The water flow rates recorded in the neat G cement were between one to two orders of magnitude higher than the water injection rates associated with the class G plus additives cement blend. It is possible that as the neat Class G blend had no accelerators, its degree of reaction was delayed relative to the G plus additives and hence relatively more hydration/reaction was occurring during the experiment. The dispersant in the G plus additives blend also allows cement grains to pack in a more orderly manner, further reducing the flowability of water across the G plus additives cement plug. Water breakthrough was also observed when testing neat G cement whereas no water breakthrough was seen when testing the class G plus additives cement blend demonstrating that, as expected, the engineered G plus additives cement blend showed superior isolating abilities and stress resilience in relation to the neat G system.

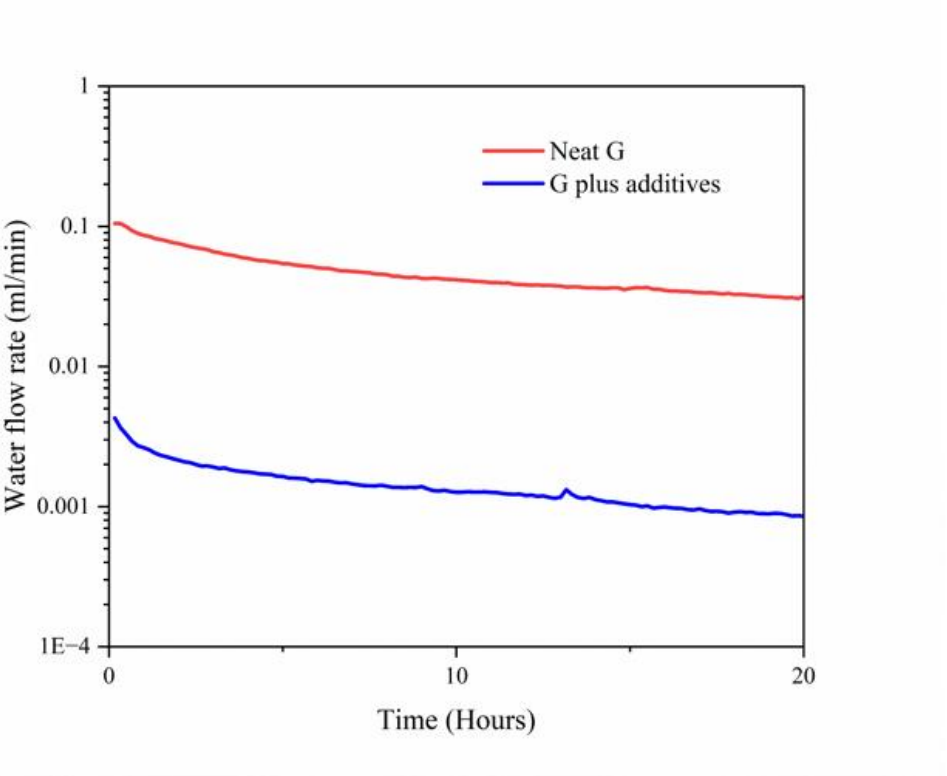

Figure 2-24: Step 1 water injection rates comparisons (injection pressure 1000 psi confining pressure 1000 psi)

Figure 2-25 shows a side-by-side comparison of the Nitrogen flow experiments in the neat G and G plus additives cement blend. A direct comparison could not be made as the time scale of these two experiments are significantly different. However, each individual step can be compared.

Nitrogen breakthrough in neat G cement was instantaneous under our severe test condition and flow rate of 154ml/min was recorded. However, at the same pressure conditions (1000 psi inlet and 1000 psi confining pressure), gas breakthrough was not observed with the G plus additives cement blend.

When the confining pressure was reduced to 750 psi, nitrogen flow rates in the neat G experiments spiked to 376 ml/min, whereas, no gas breakthrough was observed with the G plus additives blend. When the confining pressure was dropped to 500 psi, the nitrogen flow rate went above the detection limit (>600 ml/min) for the neat G cement. However, there was still no Nitrogen flow detected in the G plus additives cement plug. Finally, a gas breakthrough was observed when the confining pressure was dropped all the way down to atmospheric pressure (42 ml/min) with the G

plus additives cement blend. In addition to this the G plus additives blend was subjected to a substantially longer stress cycle lasting over 80 hours in comparison to the neat G blend <3 hour total test duration.

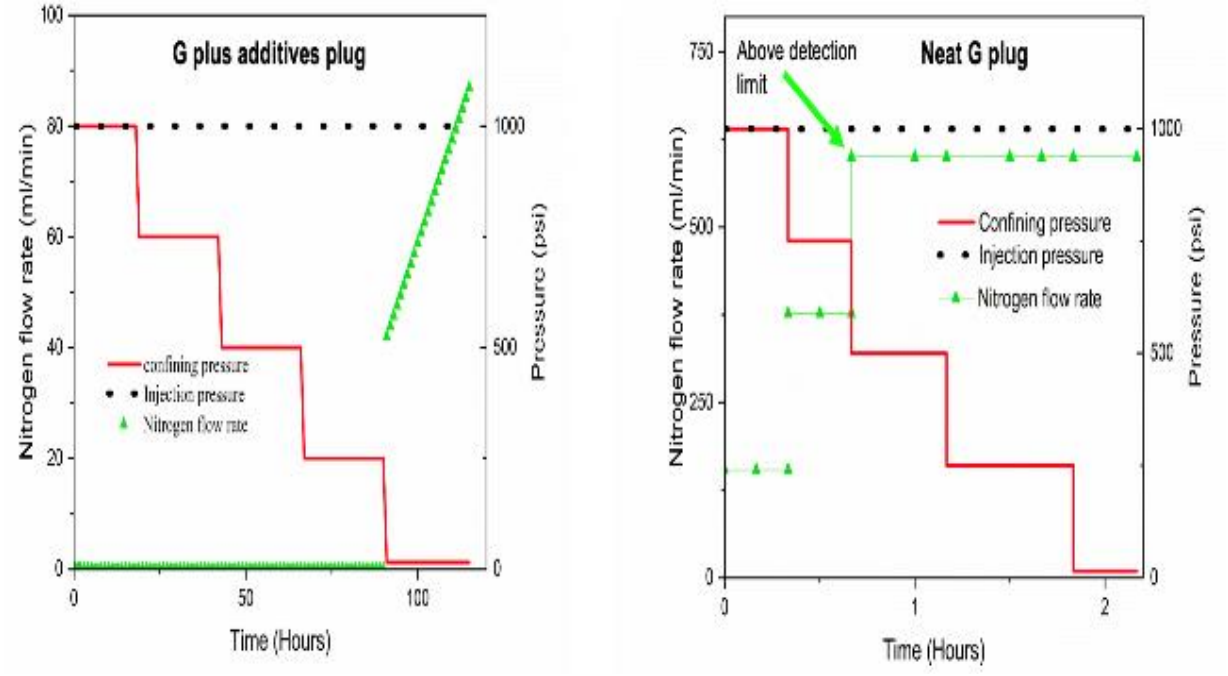

Figure 2-25: Nitrogen flowability comparisons – G plus additives (left), neat G (right).

The water flow rates recorded through the neat G cement during step 7 (1000 psi injection and atmospheric confining pressure) was between two to three orders of magnitude higher than the flow rates recorded through the G plus additives cement blend (Figure 2-26).

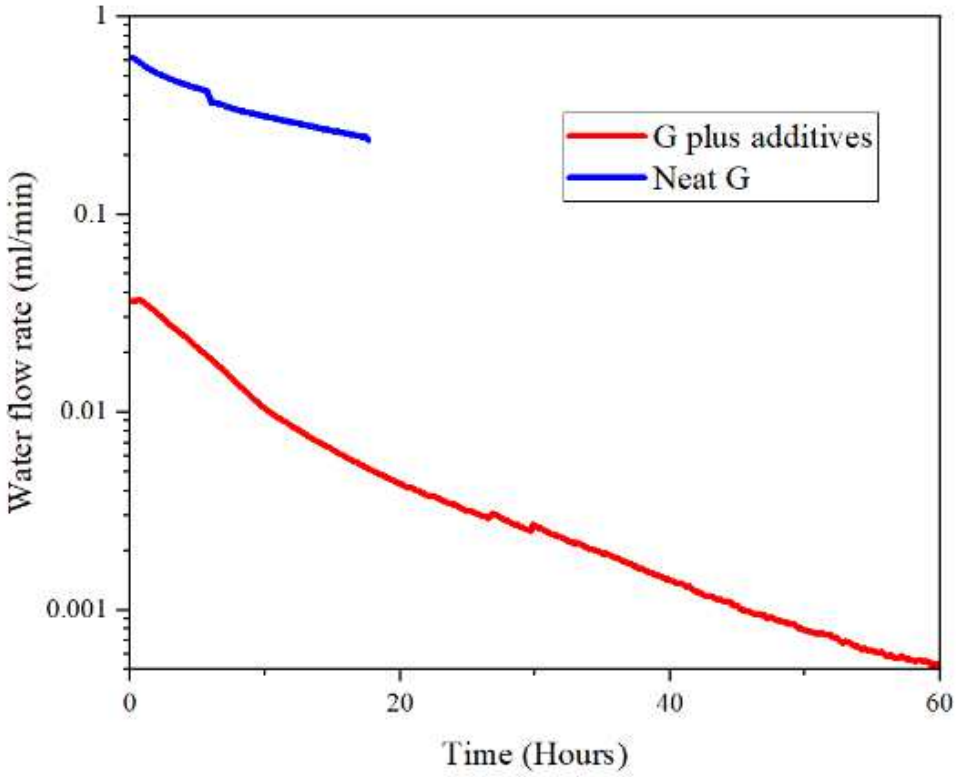

Figure 2-26: Step 7 - water injection rates comparisons (injection pressure 1000 psi confining pressure 15 psi)

Water injection rate into the G plus additives showed rapid decline over the course of the test period and no water breakthrough was observed. The neat G sample also showed some evidence of water injection rate decline but the injection rate was stabilized at around 0.25 ml/min. Water was also being collected at the outlet, but now in much larger volumes as there is a lack of a confining pressure for the neat G cement. Table 2-4 shows a side-by-side comparison of the water and nitrogen injection/flow rate data for both samples.

Test Matrix Step #	**Neat G flow rate (ml/min)**	**G plus additives flow rate (ml/min)**
Step 1 (H_2O)	0.04	0.0008
Step 2 (N_2)	154	(< 1E-7)
Step 3 (N_2)	376	(< 1E-7)
Step 4 (N_2)	(> 600)	(< 1E-7)
Step 5 (N_2)	(> 600)	(< 1E-7)
Step 6 (N_2)	(> 600)	42
Step 7 (H_2O)	0.25	0.004
Step 8 (N_2)	(> 600)	66

Table 2-4**:** Comparison of the nitrogen and water injection test results

2.5 Shear Bonding Strength Test Results

Experiment	**Shear Bond strength (MPa)**	**Total experiment duration**
Preliminary test (G plus additives)	5.37	31 Days
Neat G	1.76	2 Days
G plus additives	4.76	19 Days

Table 2-5: Shear bond strength comparison results

Table 2-5 summarizes the shear bond strengths that were measured after each wellbore simulator experiment. The shear bond strength measured in this experiment is an estimate of the cement bonding strength rather than the actual measurement of the cement bond strength as the force applied to break the shear bond is done in an uncontrolled manner. The results from these experiments can be used to compare the bond strength between each cement blend to rank the performance of each abandonment plug system.

Neat G cement (finalized test matrix): The shear bonding strength of Neat G cement was the lowest measured shear bond strength between the three experiments. A shear bond strength of 1.76 MPa was recorded. The water and nitrogen permeability values were the highest for this cement blend, indicating an inverse relationship between the shear bonding strength and permeability (i.e. lower the shear bond strength, the higher the permeability).

Class G plus additives (finalized test matrix): The shear bonding strength was measured significantly higher at 4.76 MPa in comparison to the Neat G blend at 1.76 MPa . Cement hydration reaction took place at an injection pressure of 1000 psi and a confining pressure at atmospheric levels, forming the baseline for future experiments. The experiment lasted a total of 19 days, during which water was injected for a total period of four days.

Class G plus additives (preliminary test matrix): The shear bonding strength was measured as 5.37 MPa. Cement hydration reactions took place at an injection pressure of 1450 psi. The cement absorbed more water at this pressure and the cement-casing bond was enhanced. The experiment lasted for 31 days, during which water was injected for 13 days.

Two experiments were carried out using the class G plus additives cement blend (an experiment using the preliminary test matrix, and an experiment using the finalized test matrix). The higher shear bond strength measured after completing the preliminary experiment can be attributed to a combination of longer total test time and higher water injection pressures, both of which would allow the cement hydration reactions to progress further delivering improved bonding.

2.6 Conclusions and Future Work

Results of the small-scale bulk cement sample experiments have shown that bulk cement on its own has exceptionally low permeability (below the detection limit of 0.1×10^{-6} ml/min). The small-scale abandonment plug experiments, with cement in a metal casing, have shown that addition of the cement-metal interface results in a slight increase in the water injection rates from an average flow rate of 0.1×10^{-5} ml/min to 0.1×10^{-3} ml/min. The cumulative water flow volume during the bulk cement experiments was negligible (<0.01ml) when compared to the total water flow volume during the abandonment plug experiments (0.21ml).

The severe test conditions for the abandonment plug where the annulus pressure was reduced likely created a flow path for nitrogen to bypass the abandonment plug through a micro annulus between the casing and the cement plug. Further nitrogen flow could have caused cement dehydration to occur resulting in a rapid increase in the observed flow rate. It is critical to note that processes such as this are not expected to occur in the well bore owing to the ready availability of pore fluid creating a high humidity environment which would not result in dehydration of the cement matrix.

The small-scale experiments were upscaled to simulate real wellbore conditions to assess the integrity of the cement plug using our wellbore simulator. From the initial experiments, it was seen that the permeability of both cement blends was exceptionally low with the engineered cement blend showing enhanced performance over the Neat G cement in every testing scenario.

No water breakthrough was observed when testing the G plus additives cement blend while water breakthrough was observed when testing the neat G cement. The water injection rates for the G

plus additives were two orders of magnitude lower than neat G, at 0.004 ml/min and 0.25 ml/min respectively, indicating that a carefully engineering blend can enhance the isolation performance of a standard product. Gas breakthrough was instantly observed when testing the neat G cement while no gas breakthrough was observed initially when testing the G plus additives blend. Over time, the G plus additives blend did show gas breakthrough although this is attributed to the prolonged injection of dry nitrogen, causing the cement plug to dehydrate, most likely inducing a micro annulus between the cement and casing interface. As the duration of nitrogen injection increased, the gas flow rates (from 42 ml/min to 87 ml/min in one day) also increased as the cement plug likely further dehydrated allowing more gas to bypass the cement plug. As indicated previously, dehydration induced micro annulus is not expected to occur in real wells due to the presence of formation fluid.

The shear bond strength measurement completed after the N2 and water permeability tests showed that the engineered blend maintained a significantly stronger bonding relative to the neat G (4.76 MPa vs 1.76MPa) and a slight enhancement in bonding was observed in the engineered blend with increased curing time and pressure. This demonstrates the importance of allowing cement to cure for sufficient time before pressure tests or other operations that may stress the cement plug.

Overall, this work clearly shows that cement blends that are ideally mixed and optimally placed in ideal casing are incredibly effective and resilient barrier materials. Further to this, optimization of the blend with the addition of carefully designed additives provides further enhancement to this performance, delivering a significant improvement in isolation resilience and well integrity.

Such perfect cements, placement, and casing conditions are more difficult to achieve in real wells as contamination of the cement plug during placement and suboptimal conditions of the casing will create a scenario far from the conditions replicated in this study.

Work is already underway to prepare cement samples under more challenging real well conditions (e.g., contaminations of the slurry or casing interface by wellbore fluids) and compare the results to the baseline that has been established in this work.

2.7 References

[1] Schiffner, D., Kecinski, M. and Mohapatra, S., 2021. An updated look at petroleum well leaks, ineffective policies and the social cost of methane in Canada's largest oil-producing province. Climatic Change, 164(3), p.60.

[2] Goodday, V. and Larson, B., 2021. The Surface Owner's Burden: Landowner Rights and Alberta's Oil and Gas Well Liabilities Crisis. The School of Public Policy Publications, 14.

[3] Dusseault, M.B., Gray, M.N. and Nawrocki, P.A., 2000, November. Why oilwells leak: cement behavior and long-term consequences. In SPE International Oil and Gas Conference and Exhibition in China, SPE-64733. SPE.

[4] Kang, M., Kanno, C.M., Reid, M.C., Zhang, X., Mauzerall, D.L., Celia, M.A., Chen, Y. and Onstott, T.C., 2014. Direct measurements of methane emissions from abandoned oil and gas wells in Pennsylvania. Proceedings of the National Academy of Sciences, 111(51), pp.18173-18177.

[5] Watson, T.L. and Bachu, S., 2009. Evaluation of the potential for gas and CO2 leakage along wellbores. SPE Drilling & Completion, 24(01), pp.115-126.

[6] Khalifeh, M. and Saasen, A., 2020. Introduction to permanent plug and abandonment of wells (p. 273). Springer Nature.

[7] Barclay, I., Pellenbarg, J., Tettero, F., Pfeiffer, J., Slater, H. and Staal, T., 2001. The beginning of the end: a review of abandonment and decommissioning practices. Oilfield Review, 13(4), pp.28-41.

[8] Mainguy, M., Longuemare, P., Audibert, A. and Lécolier, E., 2007. Analyzing the risk of well plug failure after abandonment. Oil & Gas Science and Technology-Revue de l'IFP, 62(3), pp.311-324.

[9] Garnier, A., Saint-Marc, J., Bois, A.P. and Kermanac'h, Y., 2008, October. A singular methodology to design cement sheath integrity exposed to steam stimulation. In SPE International Thermal Operations and Heavy Oil Symposium, SPE-117709. SPE.

[10] Celia, M.A., Bachu, S., Nordbotten, J.M., Gasda, S.E. and Dahle, H.K., 2005. Quantitative estimation of CO2 leakage from geological storage: Analytical models, numerical models, and data needs. In Greenhouse Gas Control Technologies 7 (pp. 663-671). Elsevier Science Ltd.

[11] Vrålstad, T., Saasen, A., Fjær, E., Øia, T., Ytrehus, J.D. and Khalifeh, M., 2019. Plug & abandonment of offshore wells: Ensuring long-term well integrity and cost-efficiency. Journal of Petroleum Science and Engineering, 173, pp.478-491.

[12] Achang, M., Yanyao, L. and Radonjic, M., 2020. A review of past, present, and future technologies for permanent plugging and abandonment of wellbores and restoration of subsurface geologic barriers. Environmental Engineering Science, 37(6), pp.395-408.

[13] Bourgoyne, A.T., Scott, S.L, and Manowski, W., 2000. A review of sustained casing pressure occurring on the OCS, Bureau of safety and environmental enforcement.

[14] Xu, R. and Wojtanowicz, A.K., 2017. Pressure buildup test analysis in wells with sustained casing pressure. Journal of Natural Gas Science and Engineering, 38, pp.608-620.

[15] Thiercelin, M.J., Dargaud, B., Baret, J.F. and Rodriquez, W.J., 1998. Cement design based on cement mechanical response. SPE Drilling & Completion, 13(04), pp.266-273.

[16] Ozyurtkan, M.H., Altun, G., Mihcakan, I.M. and Serpen, U., 2013, March. An experimental study on mitigation of oil well cement gas permeability. In IPTC 2013: International Petroleum Technology Conference (pp. cp-350). European Association of Geoscientists & Engineers.

[17] Boukhelifa, L., Moroni, N., James, S.G., Le Roy–Delage, S., Thiercelin, M.J. and Lemaire, G., 2004, March. Evaluation of cement systems for oil and gas well zonal isolation in a full-scale annular geometry. In SPE/IADC Drilling Conference and Exhibition, SPE-87195. SPE.

[18] Poon, C.S., Wong, Y.L. and Lam, L., 1997. The influence of different curing conditions on the pore structure and related properties of fly-ash cement pastes and mortars. Construction and Building Materials, 11(7-8), pp.383-393.

[19] Meng, M., Frash, L.P., Carey, J.W., Li, W., Welch, N.J. and Zhang, W., 2021. Cement stress and microstructure evolution during curing in semi-rigid high-pressure environments. Cement and Concrete Research, 149, p.106555.

[20] Van Eijden, J., Cornelissen, E., Ruckert, F. and Wolterbeek, T., 2017. Development of experimental equipment and procedures to evaluate zonal isolation and well abandonment materials, In SPE/IADC drilling conference and exhibition, SPE-184640-MS, OnePetro.

[21] Corina, A.N., Opedal, N.V.D.T., Vrålstad, T. and Sangesland, S., 2019, June. Cement plug sealing studies of silica cement systems. In International Conference on Offshore Mechanics and Arctic Engineering (Vol. 58875, p. V008T11A056). American Society of Mechanical Engineers.

[22] Opedal, N., Corina, A.N. and Vrålstad, T., 2018, June. Laboratory test on cement plug integrity. In International Conference on Offshore Mechanics and Arctic Engineering (Vol. 51296, p. V008T11A071). American Society of Mechanical Engineers.

[23] Ogienagbon, A.A. and Khalifeh, M., 2023. Investigation of the hydraulic integrity of cement plug: Oilwell cementitious materials. Geoenergy Science and Engineering, 231, p.212261.

[24] Mabeyo, P.E., Ibrahim, Y.S. and Gu, J., 2020. Effect of high metakaolin content on compressive and shear-bond strengths of oil well cement at 80 C. *Construction and Building Materials*, *240*, p.117962.

[25] Kamali, M., Khalifeh, M., Eid, E. and Saasen, A., 2022. Experimental study of hydraulic sealability and shear bond strength of cementitious barrier materials. Journal of Energy Resources Technology, 144(2), p.023007.

[26] The American Petroleum Institute., 2013. Recommended practice for testing well cement, API recommended practice 10-B2, Second edition.

[27] Lin, Z., Kuru, E., Iremonger, S., Yang, X., Fisher, B. and Spence, J., 2022. Design and Development of a High Pressure-High Temperature Wellbore Simulator for Investigation of the Impact of Cyclic Stresses on the Integrity of Wellbore Sections with Cement/Casing Interfaces, In SPE Annual Technical Conference and Exhibition, Houston, Texas, USA, SPE-210223-MS, SPE.

Chapter 3 Experimental Investigation of Well Cement Integrity in Abandoned Oil and Gas Wells – The Effect of Water and Oil Contamination

3.1 Abstract

The rapid increase in water cut marks the end of the life cycle OF an oil and gas well. When a well reaches this stage, the well is usually abandoned. During abandonment, the formation water present in the well can mix with the cement, reducing its designed density, which can lead to issues with regards to the isolation performance of the abandonment plug. Improper cleaning practices during the preparation for well abandonment can also cause residual oil to remain on the surface of the inner casing of the wellbore. This residual oil can mix with the cement slurry and impact the sealing performance of the cement plug. In this study, we investigated the sealing performance of the cement plug contaminated with water and oil to understand the effects of improper cleaning before well abandonment on the sealing effectiveness of the abandonment plug.

Two water contamination experiments were carried out, where the cement was contaminated with 12.5% and 25% water by volume of cement slurry. The sealability of the contaminated cement set in the wellbore simulator has been tested by using water flow tests. For the neat G cement, it was observed that as the water contamination increased, the isolation capability of the cement decreased. The water flow rates associated with the 25% contaminated neat G cement was an order of magnitude higher than the flow rates associated with the plug that had no contamination.

The fluid pathways were also identified visually by opening the wellbore simulator after the water flow test. Nitrogen flow was used to inspect the leakage pathways. Large volumes of nitrogen gas could be seen flowing through the Neat G plug at the cement-casing interface.

The class G with additives blend was contaminated with 12.5% and 25% water by volume of slurry. Water flow tests have indicated that the isolation capabilities of both cements have been reduced. The flow rates associated with the 12.5% contaminated plug were between 1 and 2 orders of magnitude higher than those of the original uncontaminated cement. The water flow rates associated with the 25% contaminated plug were 2 to 3 orders of magnitude higher than that of the uncontaminated cement plug. The wellbore simulator was opened up, and nitrogen flow test was

conducted to investigate the fluid pathways after the water flow test. A large volume of nitrogen gas flow was observed flowing through the matrix of the cement. The fluid loss additives used in the slurry most likely prevented the cement from expelling the excess water out of the slurry. This excess water might have been trapped in the cement matrix, forming larger pores. These larger pores then possibly formed migration pathways for the nitrogen flow used for checking the presence of possible leakage pathways after the water flow tests.

For the oil contamination experiments, the cement was contaminated with 2.5% light crude oil. Since the objective of these tests were to determine the effect of the residual oil, the contamination volume was kept low. Water flow tests were conducted to investigate the sealability of the oil contaminated cement column. The results were compared to water flow test conducted using original (uncontaminated) cement.

For the neat G cement, it was observed that a 2.5% oil contamination had little to no effect on the isolation capabilities of the cement as long as the entire cement system was left undisturbed (i.e., keeping the stress conditions same as the ones used during cement curing). As soon as the effective stresses acting on the cement changed (e.g. reducing the confining stress), the sealing capability of the contaminated cement against water flow reduced drastically. When the confining pressure of the wellbore simulator was reduced to atmospheric pressure condition, a micro annulus was very likely created. The observed water flow rate associated with the contaminated neat G cement plug was 1.5 times higher than that of the uncontaminated cement plug. This indicated that the contaminated cement plug forms a micro annulus more readily, when compared to the uncontaminated cement plug. The nitrogen flow rates were slightly lower than that of the uncontaminated sample, which could be due to the three-phase gas-oil-water flow occurring in the oil contaminated cement/casing microchannel as opposed to only two-phase gas-water flow in the uncontaminated cement/casing microchannel. The nitrogen needs to displace both the oil and water in the former case, causing the observed Nitrogen flow rates to be slightly lower.

For the oil contamination experiments carried out using class G cement with additives, a similar trend could be observed. As long as the effective stresses acting on the cement column were unchanged from curing conditions, the isolation capabilities against the flow of water for both the contaminated and uncontaminated cement systems were identical. Any changes to the effective stress (e.g. reducing the confining stress) drastically reduced the sealing capabilities of the

contaminated cement plug against water flow. The isolation capability of the contaminated cement column against Nitrogen flow, however, was reduced greatly. Gas breakthrough was immediately observed for the contaminated sample. Conversely, for the uncontaminated sample, no gas breakthrough was observed initially.

Even though the isolation capabilities of the contaminated class G cement with additives was reduced, its isolation capabilities were far better than the uncontaminated neat G cement. The water flow rate through the contaminated G plus additives cement/casing section was one order of magnitude lower than that of the uncontaminated neat G cement/casing section. The shear bond strength of the G plus additives plug was also higher than that of the neat G cement.

3.2 Introduction

Well abandonment marks the end of the life cycle of an oil or gas well. The objective of an abandonment operation is to isolate all the fluid bearing zones from the surface. The abandonment operations can also be very costly and needs to provide zonal isolation for centuries until natural barriers can form once more. The main environmental concerns associated with inactive and abandoned wells are the potential risks of contamination of surface water and groundwater and the surface release of methane, a potent greenhouse gas [1, 2].

Portland cement has been commonly used for abandonment operations and far too often leakage related issues in well abandonment are directly attributed to the cement properties such as shrinkage [1], failure to prove a seal during placement [3], and cement deterioration due to significant temperatures and pressure changes [3]. Research has shown that when a cement plug has been tailored to the given well conditions and placed optimally, a 6-inch plug with a diameter of 3 inches is capable of withstanding a pressure differential in excess of 1000 psi, forming an excellent barrier [4] material in the context of abandonment. If the cement is not optimally designed, placed sub optimally or is contaminated, then the risk of inducing a potential leakage pathway increases greatly [3].

Cement integrity tests carried out in laboratories normally assume that the cement is placed under perfect conditions; however, this may not always be the case. Cement contamination in the wellbore can lead to various integrity issues with regards to zonal isolation. These contaminants include formation fluid mixing with the cement, drilling fluid mixing with the cement, residual oil mixing with the cement, etc. Before cementing operations begin, the wellbore needs to be cleaned. The spacer that is pumped ahead of the cement needs to clean the inner casing and change the properties of the casing from oil wet to water wet.

An oil-based drilling fluid is commonly composed of oil in the continuous phase and water as a fraction in the dispersed phase. It also contains thickening agents, surfactant and emulsifiers. Before cementing operations, the oil-based drilling fluid needs to be cleaned due to its oil wetting characteristics. This can be done using spacer fluids. The spacer needs to be designed in such a way that it cleans the casing from the drilling fluid and changes the casing from oil wet to water wet [5]. The displacement efficiency in a wellbore can range from 37% to 99% depending on the

wellbore conditions [6-9]. The residual components in the wellbore can contaminate the cement that is placed, altering its sealing properties. A large number of studies have been carried out, investigating the effect of drilling fluids (mainly oil-based) contamination on the integrity of cement [6, 10-15].

Goode [10] conducted gas and water permeability tests on the dried and wet cement samples. He reported that cement samples, which contained a moderate amount of Bentonite, seemed to have higher permeability values. His results suggested that the wellbore would need to be cleaned properly before cementing as the residual drilling fluid could react with cement, causing leakage through the cement plug.

Aughenbaugh et al. [11] investigated the integrity of various cement slurries when mixed with synthetic based drilling fluid by assessing the cement compressive strength. They formulated 6 different slurries and contaminated them by replacing a part of the cement slurry with synthetic based drilling fluid. Their methodology involved testing the compressive strength of the original cement and then contaminating the slurry with 5%, 10% and 15% synthetic based drilling fluid [11]. The slurry was then cured for 2 days and the compressive strength test was carried out. They noted that at just 5% contamination, the compressive strength of the cement samples reduced to anywhere between 20% to 60 % of the original compressive strength [11]. This massive reduction in compressive strength inhibits the ability of the cement to hold pressure, posing a serious threat to zonal isolation [11]. A control test was carried out where silica (sand) was added instead of the synthetic based drilling fluid, and these results showed very minor changes in compressive strength. Aughenbaugh et al. [11] stated that the reduction in compressive strength could be attributed to osmosis of water from the cement slurry to the synthetic drilling fluid. Aughenbaugh et al. [11] suggested that by increasing the salt content in the slurry, this effect could be reduced. They concluded that the contamination does not interfere with the cement hydration process itself, but limit the extent to which hydration takes place [11].

Aughenbaugh et al. [11] then compared the effect of preparing synthetic based drilling fluid with brine versus synthetic based drilling fluids prepared from fresh water. They observed a reduction in compressive strength for the synthetic based drilling fluids prepared from brine when compared to the drilling fluid prepared from fresh water [11]. They stated that this could be a result of osmosis dehydration, where the synthetic based drilling fluid is absorbing the water from the cement slurry

[11]. They then tried to add various additives to counteract some of the negative effects that they observed with limited success. The only additive that showed promise was an alkali which was presumed to disrupt the invert emulsion [11].

Li et al. [12] investigated the integrity of the cement slurry when the cement was contaminated with diesel-based drilling fluids. They investigated key parameters such as rheological properties and compressive strength. They also imaged the microscopic structure of the contaminated products. The tools used in this study to image the microstructure of the contaminated cement included Scanning Electron Microscope (SEM), X-Ray Diffraction (XRD), Thermogravimetry (TG) and Energy Dispersive Spectrometer (EDS) [12]. Class G cement was mixed as per the API guideline and a fraction of the cement was replaced with a diesel-based drilling fluid. Contamination levels of 0%, 5%, 25% and 50% were investigated [12].

Li et al. [12] noted that the compressive strength rapidly decreased when increasing the contamination fraction in the cement up until 50% contamination, at which point the compressive strength was completely lost. They noted that there was an increase in compressive strength as the curing time increased; however, this was insignificant [12]. More experiments were carried out using different contamination values (at increments of 5%) and both the bond strength and the compressive strength was measured. From their results, they identified three critical contamination ranges. When the contamination is less than 15%, there is a reduction in compressive strength [12]. Between 15% to 20% there is a significant reduction in compressive strength. Above 20%, there is almost no compressive strength associated with the cement [12].

Data from the SEM, XRD and EDS were analyzed to understand the reduction in compressive strength and the interaction between the cement grain and the oil-based fluid. From their CT scans, they found that for the neat cement with no contamination, the matrix was very dense with only a few small pores [12]. When the oil contamination was increased to 5%, honey comb structures started to appear, a slight reduction in density was observed, and the number of pores also increased [12]. When contaminated with 25% drilling fluid, the honeycomb structures became larger and even more pores were visible [12]. For the 25% contaminated sample, oil-based fluids appeared to surround the cement grains, explaining why the compressive strength of the cement was significantly lower [12].

Li et al. [12] concluded that the introduction of oil-based drilling fluid hinders cement hydration reaction, resulting in incomplete hydration and the formation of honeycomb structures [12]. Li et al. [12] used surfactants to try to negate this problem. From their experiments, they found that the compressive and bond strengths were improved significantly with the addition of surfactants.

Li et al. [13] in a later study then suggested that the oil-based drilling fluid does not hinder the hydration process of the cement slurry. But it does form holes in the solidified cement, destroy the structural integrity of the cement, and reduce the cement slurry's ability to consolidate [13]. They also noted an increase in the permeability and porosity of the consolidated cement sample [13].

Other possible contaminations in the wellbore include formation fluids mixing with the cement. The formation fluids (usually brine) can mix with the cement slurry, altering the intended design density at the surface. Bourgoyne et al. [14] reported that the interface between cement and the other components such as the casing and formation is more likely to form fluid pathways rather than the cement matrix itself. The cement-casing bond quality is probably related to the microstructural changes that occur in the interfacial transition zone at the cement-casing interface during cement hydration reactions [15].

Agbasimalo & Radonjic [6] investigated the effect of contamination on the cement/formation interface. They placed a half-core of Berea sandstone (300 mD) in a mould and filled the other half of the mould with class H cement [6]. Two experiments were carried out. One experiment served as the control while the other cement slurry was contaminated with 10% water-based drilling fluid [6]. The cement was cured for 24 hours, removed from the mould, and placed in tap water for 28 days [6]. Several core flooding experiments using brine were carried out. They used a confining pressure of 2100 psi and a back-pressure of 1350 psi [6]. The core flood experiments were carried out at a constant flow rate of 1 ml/min for 30 days [6]. The pH of the produced water was also measured. CT scans were carried out before and after the permeability experiments to understand the microstructural changes at the cement-formation interface. The CT scan showed that there was good bonding between the control slurry and the 10% contaminated slurry at the start of the experiment [6].

At the end of the core flooding experiments, smaller cores were drilled out of the inlet and outlet sides of the larger cores to improve CT resolution [6]. For the uncontaminated cores, the cement showed uniform density before core flooding [6]. After core flooding, cement close to the cement-rock interface was less dense than the cement further away from the interface [6]. The porosity of the original cement rock was 0.02%, and after core flooding, the reaction zone had a porosity of 6.67% [6].

For the 10% contaminated core, the cement exhibited higher porosity (0.65%) closer to the interface and moving further away from the interface, the original porosity of 0.02% was maintained [6]. After core flooding, the contaminated cement possessed large pores measuring 750 μm length and 150 μm in thickness which were not present in the neat cement [6]. The pores formed in areas which were previously occupied by fluid, and the porosity of that interfacial zone increased from 0.65% to 12.53% [6].

The pH of the influent brine was found to be 6.2 throughout the experiment and the effluent brine was collected and measured daily [6]. The pH of the effluent brine was much higher than the influent brine. For the uncontaminated sample, the pH increased from 6.2 to 9.49 and for the 10% contaminated sample, the pH increased from 6.2 to 9.78, indicating a higher dissolution rate when the cement was contaminated [6].

Aughenbaugh et al. [11] reported that brine mixed with cement can cause osmatic dehydration. Another parameter that changes due to dilution is the density of cement, which can also have an impact on the zonal isolation capabilities of cement.

Coleman & Corrigan [16] studied the effect of water-cement ratio as well as the particle size of the cement grains on the permeability of the cement samples. They used 4 types of cement with the same chemical composition but with varying grain sizes. The cement was cured in the annular space of two cylindrical pipe for a period of 72 hours at room temperature and pressure. They found that the set cement volume was inversely proportional to the water/cement ratio. They also found that fine cement could react with more water. After curing, 6 cores were cut from each sample, with three cores coming from the top of the sample and three cores coming from the bottom of the sample. This was done to understand the permeability variations across the sample.

The cores were then dried for a period of 6 hours and allowed to cool before testing the permeability.

Coleman & Corrigan's results indicated that there was minimal variation in the permeability between the cores cut from the top and bottom when the cement was mixed using a low water to cement ratio (40%) [16]. However, as the water to cement ratio was increased (60-70%), large variations could be observed between the permeability of the cores cut from the bottom of the sample and the top of the sample. Higher permeabilities were observed from cores cut from the top of the sample [16]. Coleman & Corrigan concluded that this was a result of excess free water which did not react with the cement, moving up the cement column and thus possible forming water channels or pockets towards the top end of the cement sample in combination with particle settling. They also noted that this effect was more severe with coarser grained cement [16].

All these studies carried out previously to investigate cement contamination have their own merits as well as limitations. Most studies, if not all, investigated the effect of drilling fluid on the integrity of cement. However, for an abandoned well, the presence of drilling fluid is less likely, and a more realistic testing condition would be to investigate the most common contaminant found in an a well that is being prepared for abandonment. These contaminants would be formation fluid and residual oil. Furthermore, the studies reviewed in this paper did not account for the wellbore conditions such as the additional stresses exerted on the cement column.

The wellbore simulator used in this study allows us to control more variables than in previous studies. It enables us to control the injection pressure, confining pressure, curing pressure and temperature. In this paper, we will compare the sealability performance of two cement blends, i.e., the neat G and a G plus additives that has been engineered to enhance the sealing potential through the use of additives. The effect of both oil contamination and excess water contamination will be investigated and compared with previously published results [4].

The main objectives of the study are as follows: 1) investigate the sealing potential of oil contaminated cements under wellbore conditions; 2) investigate the sealing potential of water contaminated cements under wellbore conditions; 3) compare the performance of the two different cement samples with each other; and 4) determine the most likely fluid flow pathway in the contaminated cements.

3.3 Methodology

One of the main objectives of the current study is to investigate the effect of bulk fluid contamination on cement sealing ability. The increase in water cut in a well marks the beginning of the end of the well life cycle. Remnants in the form of formation fluid can be left behind in the well and the possibility of this fluid mixing with the pumped cement slurry is high. So, in the first part of this study we investigated the effect of water contamination of the cement slurry on the cement/casing sealing performance. In the second part of this study we investigated the effect of oil contamination. An oil well can produce oil for multiple decades. Over the time, some amount of residual oil would be left in the well and/or on the inner casing making the casing oil wet. Improper cleaning techniques can cause some residual oil to mix with the cement leaving the casing oil wet. Therefore, the effect of oil contamination also needs to be studied.

3.3.1 Materials

Cement blends used in this study are listed in Table 3-1.

Cement blend	Cement: water mixing ratio	Additives	Contamination v/v %	Slurry density (kg/m^3)
0:1:0 G "Neat"	0.440	Defoamer	2.5% oil contamination	1875
0:1:0 G + Additives	0.434	Accelerator, Fluid Loss, Dispersant & Defoamer	2.5% oil contamination	1875
0:1:0 G "Neat"	0.544	Defoamer	12.5% water contamination	1800
0:1:0 G + Additives	0.529	Accelerator, Fluid Loss, Dispersant & Defoamer	12.5% water contamination	1800
0:1:0 G "Neat"	0.639	Defoamer	25% water contamination	1720
0:1:0 G + Additives	0.623	Accelerator, Fluid Loss, Dispersant & Defoamer	25% water contamination	1720

Table 3-1: Cement blends used for the contamination study

The functions of different additives are explained below:

Accelerator – Aids in the development of early strength at low temperature and aids in the stability of the slurry by preventing particle settling.

Fluid Loss – Prevents fluid loss from the cement slurry.

Dispersant – Lowers the viscosity of the slurry for easier mixing and pumping and enhances the performance of the fluid loss additive.

Defoamer – Reduces the entraining of air bubbles in the cement slurry, facilitating easier field operations.

3.3.2 Cement Mixing

For the bulk fluid contamination experiments, the cements were mixed as per the ratios set out in Table 3-1 and as per the API-10B-2 standard [17] described in Section 2.2 of Chapter 2.

For the oil contamination experiments, the high-speed mixing (4,000 RPM & 12,000 RPM) procedure was the same as in API-10B-2; but during low-speed mixing, the cement was allowed to mix for a period of 5 minutes first (150 RPM), before adding 20 milliliter of light crude oil directly into the mixing vortex. The light oil has a total acidic number of 1.3 mg/g, density and viscosity of 0.88 g/cm^3 and 11 cP at 25°C. The now contaminated cement was allowed to mix for a further 25 minutes and was ready to be poured into the wellbore simulator for curing.

3.3.3 Cement Sample Preparation in the Wellbore Simulator

The procedure used for preparing cement samples in the wellbore simulator has already been described in Sections 3.5 to 3.9 of Chapter 2. This procedure remained consistent throughout all the contamination experiments.

3.4 Results and Discussion

3.4.1 Water Contamination Experiments Using Neat G Cement

Two experiments were carried out with a water contamination of 12.5% and 25% using neat G cement.

Both contaminated cements were cured for a period of seven days at a pressure of 1000 psi and ambient temperature. For the 12.5 % water contaminated cement sample, the expected cement column height was 16.6 cm, but the measured cement height was only 15.4 cm. The cement slurry had compacted and shrunk by 7.2%. For the 25% water contaminated cement, the expected cement column height was 16.3 cm, but the measured cement height was only 13.7 cm. The cement slurry had compacted and shrunk by 16%. The 25% contaminated cement plug experienced more cement shrinkage than the 12.5% contaminated cement plug.

The water permeability for both contaminated cement plugs were tested at an injection pressure of 1000 psi and a confining pressure of 1000 psi. The water flow rates of both cement plugs and the uncontaminated cement plug are shown in figure 3-1. Water breakthrough was observed as soon as the experiment was started for both the contaminated cement plugs and the uncontaminated cement plug, however, the recorded flow rates for the contaminated plugs were much higher. For the 12.5% contaminated sample, the maximum water flow rate recorded at the start of the experiment was 0.15 ml/min; however, towards the end of the experiment, water flow rate declined to a low point of 0.066 ml/min. For the 25% contaminated experiment, the maximum water flow rate recorded at the start of the experiment was 0.28 ml/min. However, towards the end of the experiment, water flow rates declined to a low point of 0.25 ml/min

An increasing trend in the flow rate can be observed as the density of the abandonment plug was reduced. The optimally placed neat G plug (1900 kg/m3) had the highest sealing potential (flow rates as low as 0.03 ml/min). The flow rate associated with a 25% contaminated plug was an order of magnitude larger than the flow rate associated with the optimally placed abandonment plug.

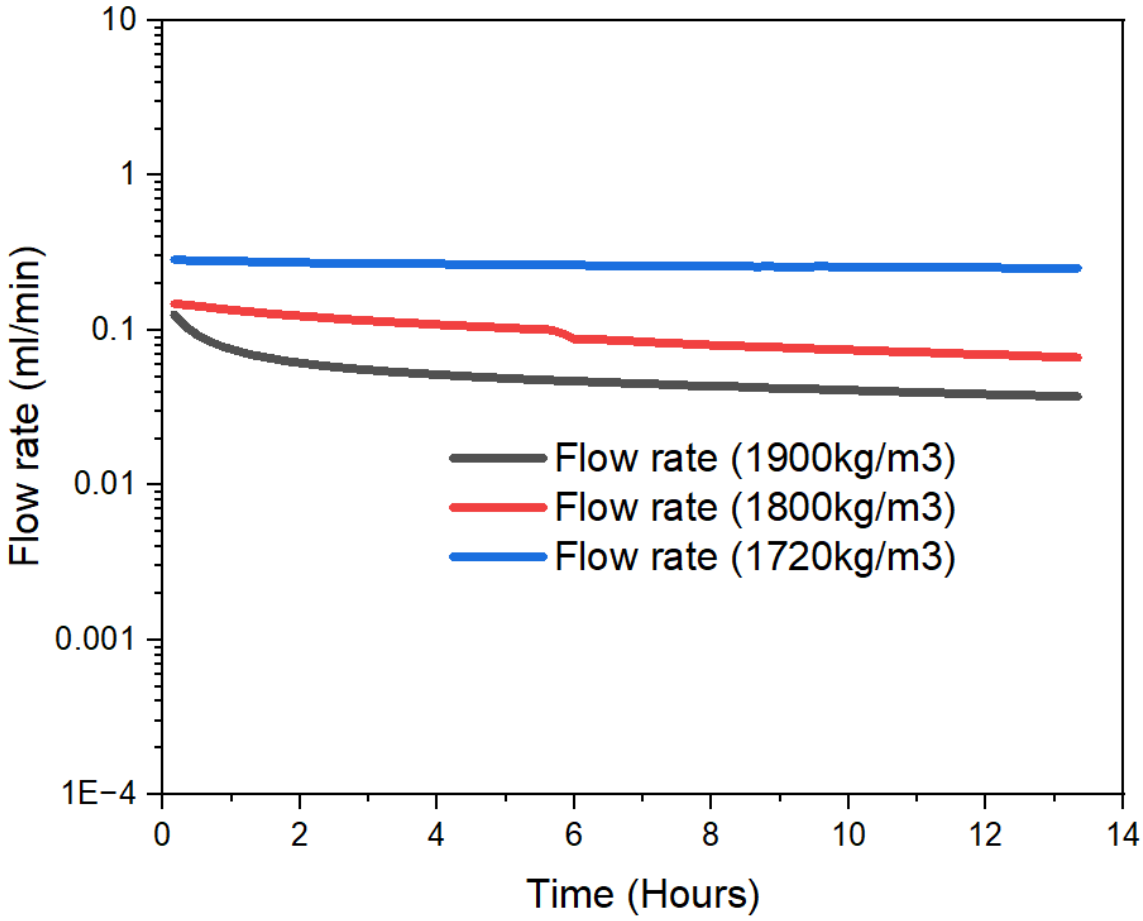

Figure 3-1: Water flow rate comparisons between the optimally placed cement plug and the contaminated cement plug (Injection and confining pressure of 1000 psi). (1900 kg/m^3; no contamination. 1800 kg/m^3; 12.5% contamination. 1720kg/m^3; 25% contamination).

After water injection experiments, Nitrogen was injected into the sample at an injection pressure of 1000 psi and confining pressure of 1000 psi. The nitrogen flow rates were well above our detection limit for both water contamianed cement plugs. The wellbore simluator was opened up to investigate the possible flow pathways. Once the wellbore simulator was opened, it was observed that the cement column for both experiments had migrated about 3.5 cm during the water permeability test. It appeared that reducing the density of the cement caused a reduction in the shear bond strength, which in turn caused debonding at the cement casing interface. In order to conduct a visual inspection of the flow paths, Nitrogen was injected (at a low injection pressure of 60 psi) at the bottom of the cement plug. Nitrogen bubbles were observed coming out of the

wellbore simulator, bypassing the abandonment plug through the cement casing interface as shown in figure 3-2.

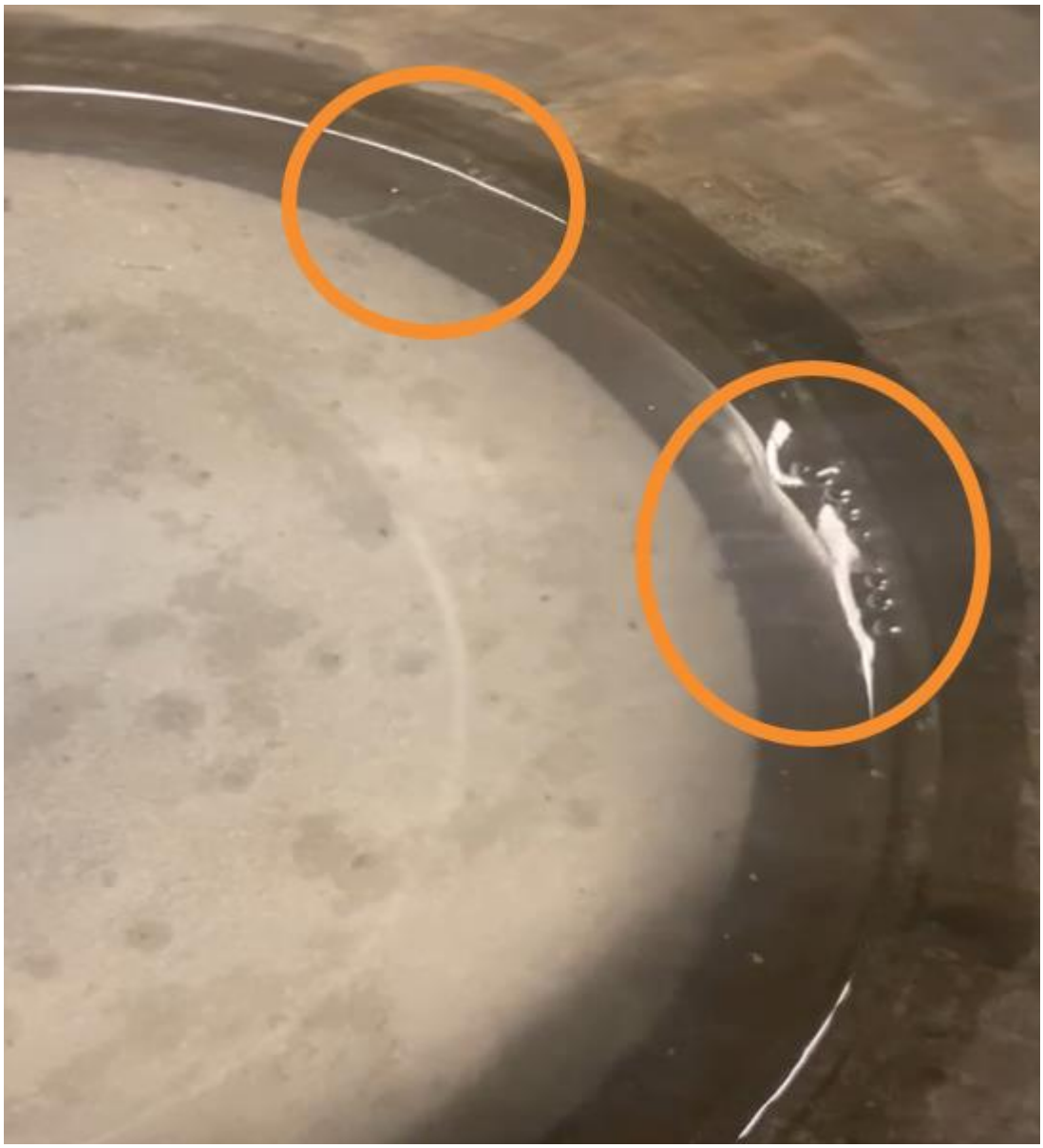

Figure 3-2: Visual inspection to determine the fluid flow pathway across the neat G cement plug with 25% water contamination.

The density of the Neat G abandonment plug at different locations was measured after completing the water and nitrogen permeability experiments to further understand why the shear bond failed between the cement and the casing as well as why we observed a 16% compaction of the cement plug. Figure 3-3 shows the measured results. Although the cement was mixed and placed with the intention of achieving a plug with uniform density of 1720 kg/m^3, this was not what happened. Due to the lack of additives present in neat G, water was expelled from the abandonment plug, causing this shrinkage. Particle settling was also observed and the density at the bottom of the plug was 160 kg/m^3 more than the density at the top of the plug.

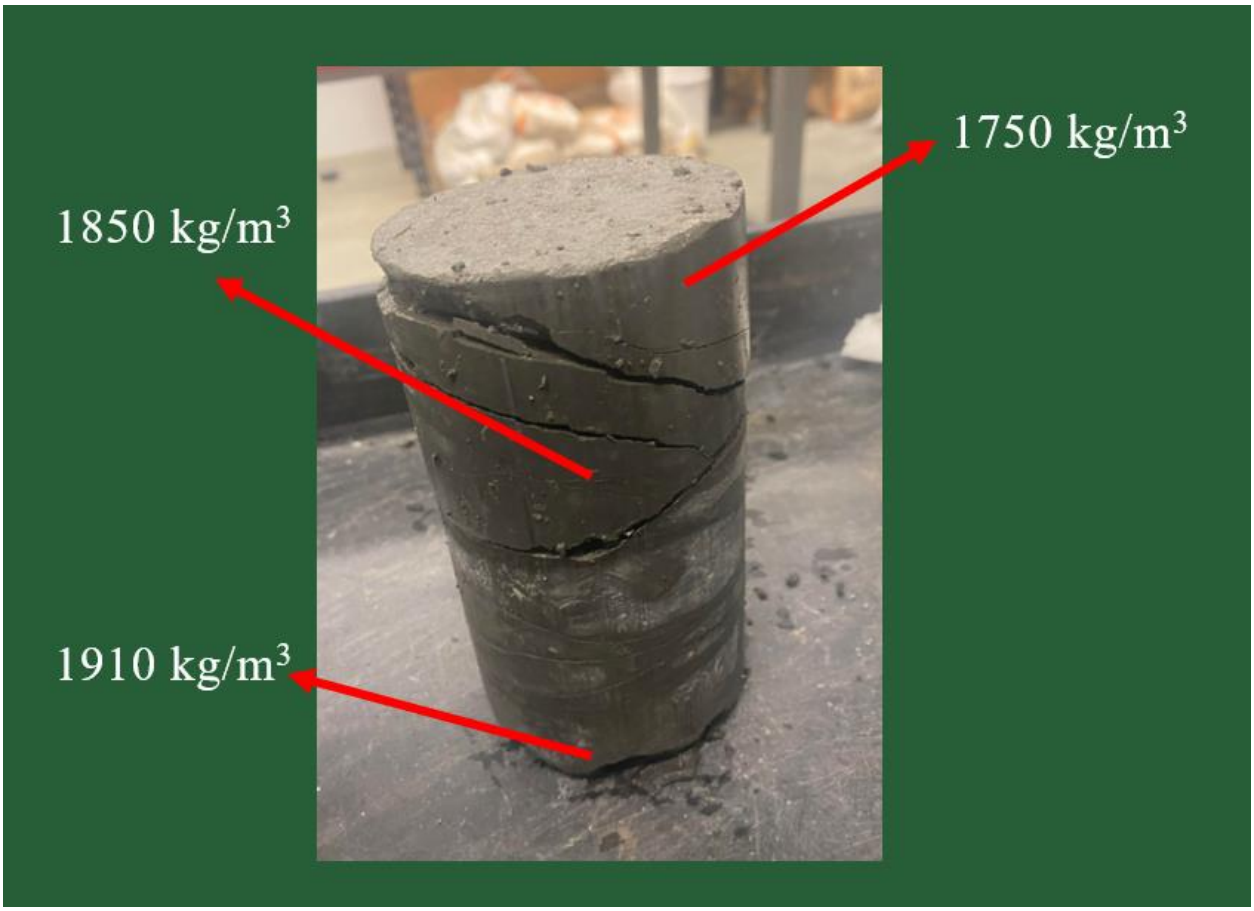

Figure 3-3: Density variation measured across the neat G cement plug with 25% water contamination.

3.4.2 Water Contamination Experiments Using Cement with G Plus Additives

Two experiments were carried out with a water contamination of 12.5% and 25% using class G cement with additives.

Both contaminated cements were cured for a period of seven days at a pressure of 1000 psi and ambient temperature. For the 12.5 % water contaminated cement sample, the expected cement column height was 16.7 cm, but the measured cement height was only 15.8 cm. The cement slurry had compacted and shrunk by a 5.4%. For the 25% water contaminated cement, the expected cement column height was 16 cm, but the measured cement height was only 14.3 cm. The cement slurry had compacted and shrunk by a 10.6%. The 25% contaminated cement blend experienced more shrinkage when compared to the 12.5% contaminated sample.

The water permeability for both contaminated cement plugs were tested at an injection pressure of 1000 psi and a confining pressure of 1000 psi. The water flow rates measured through both contaminated cement plugs and the water intake rate into the uncontaminated cement plug are shown in figure 3-4. Water breakthrough was observed as soon as the experiment was started for both cement plugs contaminated with water, but no water breakthrough was observed when testing the original uncontaminated sample. For the 12.5% contaminated sample, the maximum water flow rate recorded at the start of the experiment was 0.23 ml/min; however, towards the end of the experiment, water flow rates declined to a low point of 0.06 ml/min. For the 25% contaminated experiment, the maximum water flow rate recorded at the start of the experiment was 1.03 ml/min. Since the was flow rate was extremely high, the pump needed to be refilled twice, seen as drops and spikes in Figure 3-4 (at 2 hours and 5 hours). The flow rate stabilized at 0.36 ml/min. The performance of this cement blend was the worst among all the cement blends tested.

An increasing trend in the flow rate was observed as the density of the abandonment plug was reduced. The flow rate associated with a 25% contaminated plug was two to three orders of magnitude larger than the flow rate associated with the optimally placed abandonment plug.

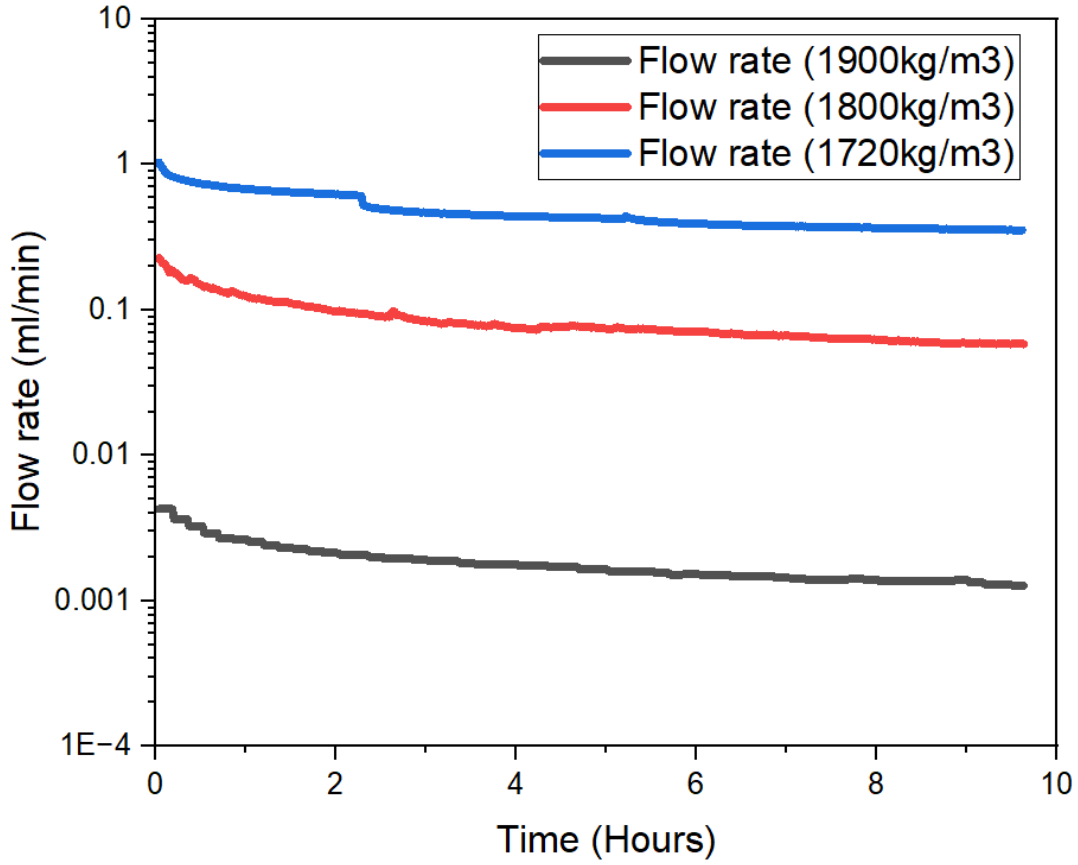

Figure 3-4: Water flow rate comparisons between the optimally placed cement plug and the contaminated cement plugs (Injection pressure and annulus pressure of 1000 psi). (1900 kg/m^3; no contamination. 1800 kg/m^3; 12.5% contamination. 1720kg/m^3 ; 25% contamination).

After water injection experiments, Nitrogen was injected into the sample at an injection pressure of 1000 psi and confining pressure of 1000 psi The nitrogen flow rates were well above our detection limit for both water contamianted cement plugs. The wellbore simluator was opened up to investigate the possible flow pathways. Once the wellbore simulator was opened, it was observed that the cement column for both experiments had migrated about 3.1 cm during the water permeability test. Reducing the density of the cement caused shear bond failure at the cement casing interface.

In order to conduct a visual inspection of the flow paths, Nitrogen was injected at a low injection pressure of 50 psi to the bottom of the cement plug. Nitrogen bubbles were observed coming out of the wellbore simulator, through the cement matrix as shown in figure 3-5.

Visual inspection confirmed that there were three individual pores located at the center of the cement plug, providing a flow path to the Nitrogen flow. Some minor flow was also detected at the cement casing interface. After removing the abandonment plug from the inner casing, the plug was broken into two halves and small pores could be seen across the plug. This confirmed that the nitrogen had indeed travelled through the matrix of the cement plug.

Figure 3-5: Visual inspection to determine the fluid flow pathway across the cement with G plus additives and 25% water contamination (1720 kg/m^3).

The density of the abandonment plug at different locations was measured after completing the water and nitrogen permeability experiments. Figure 3-6 shows the measured density results. Although the cement was mixed and placed with the intention of achieving a plug with uniform density of 1720 kg/m^3, this was not what happened. At the top of the cement plug, a density of

only 1510 kg/m^3 was observed. Particle settling was also observed in this case and the density at the bottom of the plug was 450 kg/m^3 more than the density at the top of the plug.

Due to the fluid loss additives present in this blend, the cement slurry could not expel the excess water out of the liquid slurry. This excess water might have travelled up the cement plug (due to lower density) and as the cement sets, it might have been trapped in the pore spaces, enlarging the pores. Once permeability experiments were initiated, these pore spaces acted as a pathway for fluid migration. These results indicated the importance of accounting for uncontrollable variables that could be found downhole.

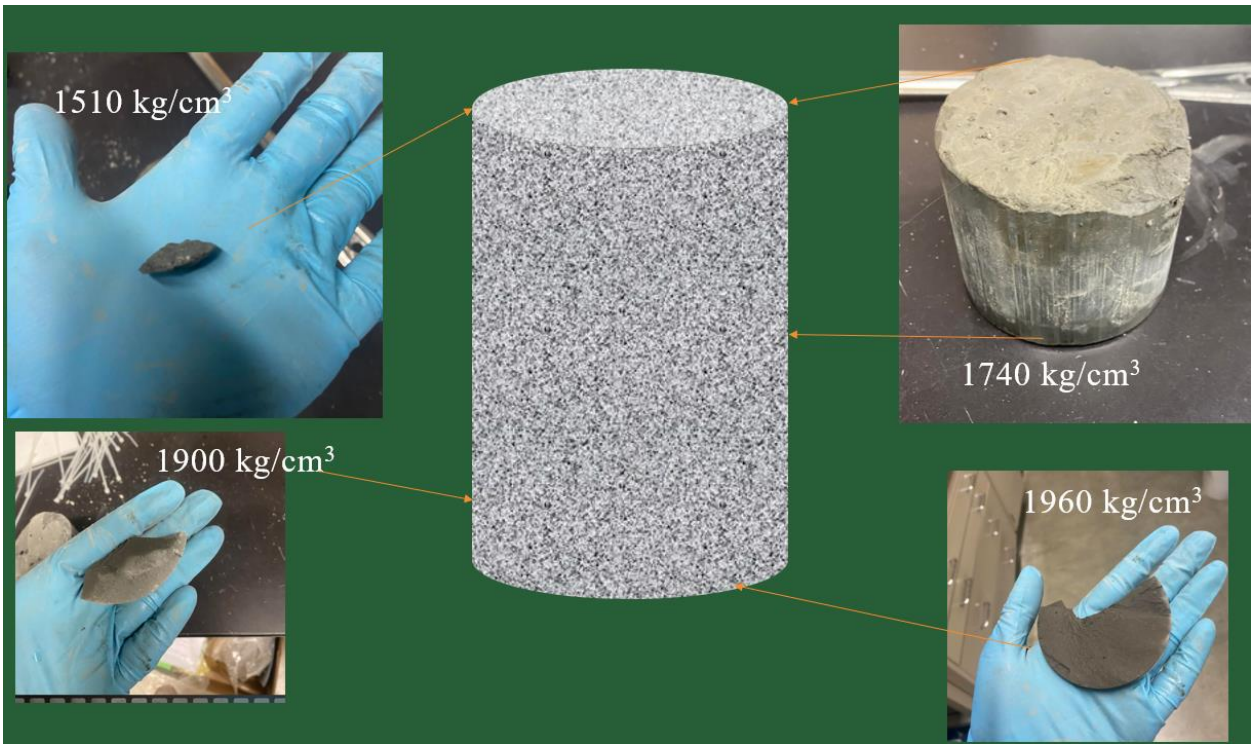

Figure 3-6: Comparison of the flow rate data obtained for the 3 neat G cement plugs

3.4.3 Flow-Rate Comparisons for Different Cement Blends with Water Contamination

The class G cement blend with additives showed more resistance to cement compaction and shrinkage than that of the Neat G plug (10.6% vs 16.0%). This was due to the presence of fluid loss additives. As the cement sets, the G plus additives cement blend tried to keep its original shape without expelling the excess water out of the slurry. This caused the plug to become less dense at the top as the heavy cement particles settled and water rose. Figure 3.7 shows a side by side comparison of the plug permeability for both neat G and G plus additives blends. It can be seen that the fluid contamination has a much more severe effect on the class G cement than that of the neat G cement. The permeability of the 25% contaminated G with additives blend is the worst among all the contamination experiments carried out. The class G cement with additives which was contaminated with 12.5% water had similar flow rates to the neat G cement plugs.

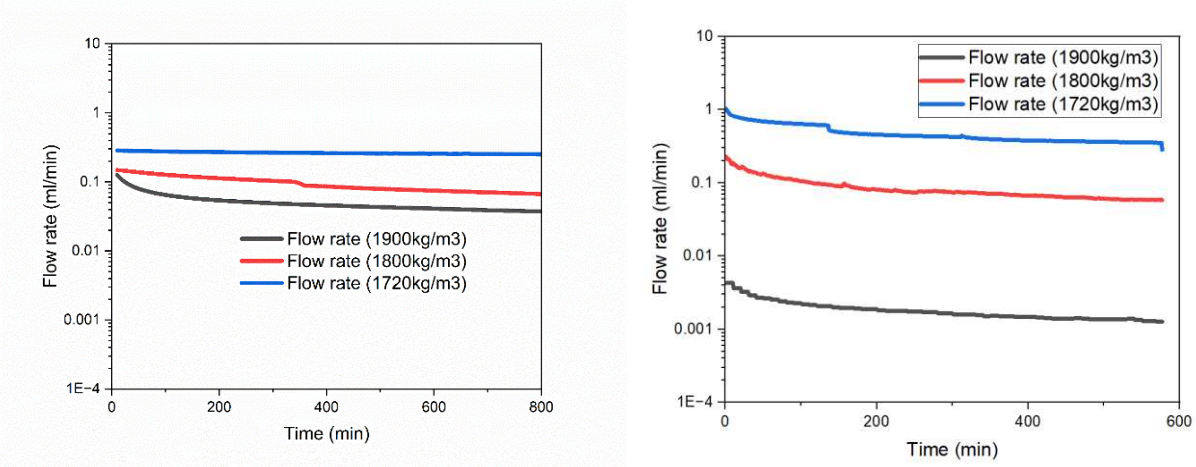

Figure 3-7: Comparison of the flow rate data recorded for the neat G cement blends with different levels of water contamination (left) and the class G cement plus additives with different levels of water contamination (right).

3.4.4 Oil Contamination Experiments Using Neat G Cement

Neat G cement was contaminated with 2.5% by volume of light crude oil. Figure 3-8 shows the flow rate comparison between the contaminated and uncontaminated samples. As per the test matrix described in Section 2.2.6, the first step was to test the water permeability of the cement plug at an injection pressure of 1000 psi and confining pressure of 1000 psi. Water breakthrough was observed as soon as the experiment commenced. The maximum flow rate recorded by the pump was 0.077 ml/min over a one-day testing period. The average water flow rate during the last 6 hours of the experiment was calculated as 0.037 ml/min. The water breakthrough in uncontaminated sample started with a higher flow rate (0.105 ml/min) as compared to the contaminated sample (0.077 ml/min). However, as the experiment progressed, the flow rate of the original sample declined below that of the contaminated sample. Overall, the flow rates through both cement plugs appeared to be similar in nature, with only very minor differences observed.

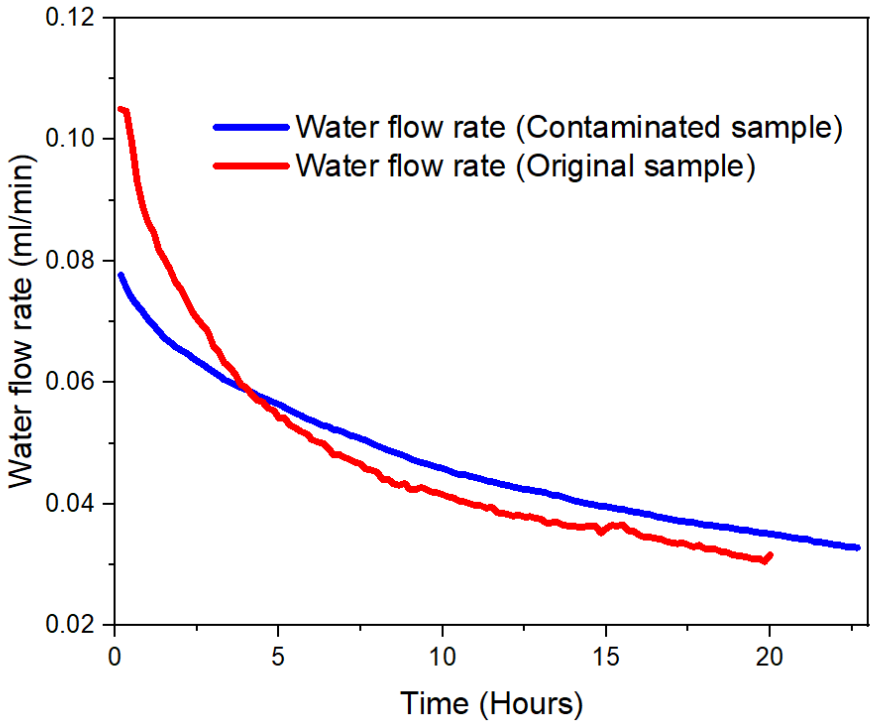

Figure 3-8: Water flow rates measured for the uncontaminated neat G cement and the oil-contaminated neat G cement at an injection pressure of 1000 psi and a confining pressure of 1000 psi.

After the water permeability experiment, nitrogen was injected at 1000 psi injection pressure and 1000 psi confining pressure. Nitrogen breakthrough was observed immediately in both cases. A nitrogen breakthrough flow rate 96 ml/min was measured, forming the baseline for nitrogen permeability experiments using uncontaminated Neat G cement. The water permeability and nitrogen permeability tests were repeated as per the test matrix. As we reduced the confining pressure, the nitrogen flow rates rapidly increased above our detection limit (> 600 ml/min). The shear bond of the cement started to fail after a confining pressure of 250 psi was reached. Nitrogen breakthrough was observed in both cases; however, the flow rate through the contaminated sample was slightly lower than the flow rate through the original (uncontaminated) sample. This might be due to having three phase flow with the contaminated sample as opposed to having two phase flow with the uncontaminated sample. For the contaminated sample, the nitrogen needed to displace both oil and water in the fluid pathway, causing the measured Nitrogen flow rate to be slightly lower. Overall, the nitrogen flow rate for both samples were similar, with both samples eventually exceeding the maximum flow rate detection capabilities of our apparatus. The nitrogen flow rate comparison is shown in figure 3-9.

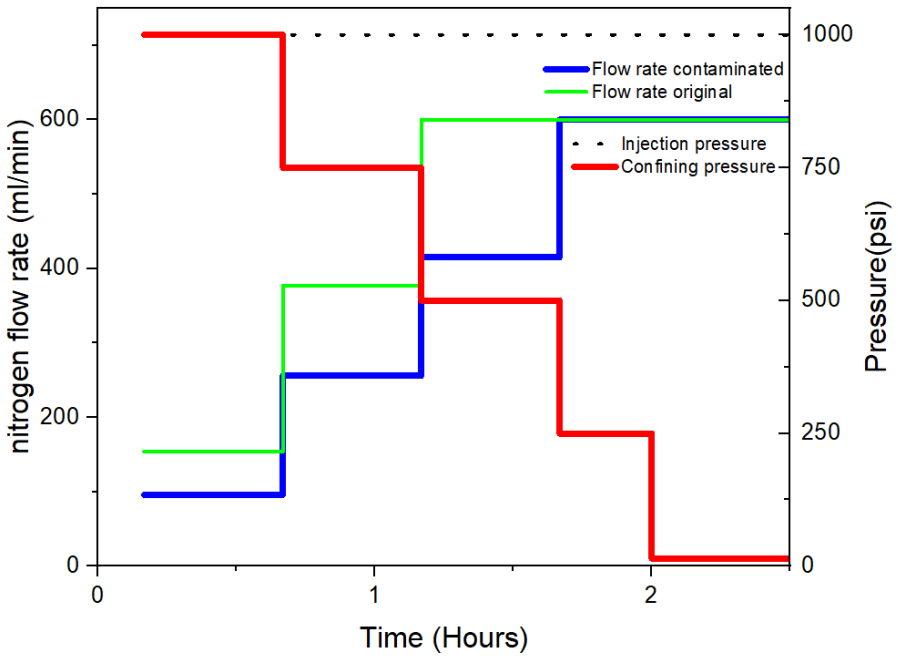

Figure 3-9: Nitrogen flow rates measured for the uncontaminated neat G cement and the oil-contaminated neat G cement at an injection pressure of 1000 psi and variable confining pressure.

After the nitrogen permeability experiment, water was injected again at an injection pressure of 1000 psi and a confining pressure of 15 psi (Figure 3-10). The average water flow rate through the oil contaminated sample was measured as 0.35 ml/min. The initial water flow rate through uncontaminated sample was higher than that of the contaminated sample, but as the experiment progressed, the water flow rate through the original sample started to decline below the water flow rate level observed through the contaminated sample. It might be the case that the water injected into the original (uncontaminated) sample after Nitrogen flow test would cause the cement to re-hydrate and reduce the size of the micro annuli (compensate for shrinkage). With the presence of oil contamination, however, this "self-healing" effect in the contaminated cement sample was diminished. It is possible that the oil present in the cement might be inhibiting the cement's ability to heal the micro annulus. Towards the end of the experiment, the water flow rate through the contaminated sample was almost 1.5 times higher than that of the original sample. The flow rates were similar initially but as the confining pressure was reduced, the sealing capability of the contaminated plug was reduced, suggesting that Micro annuli might have been formed more readily in the contaminated cement plugs.

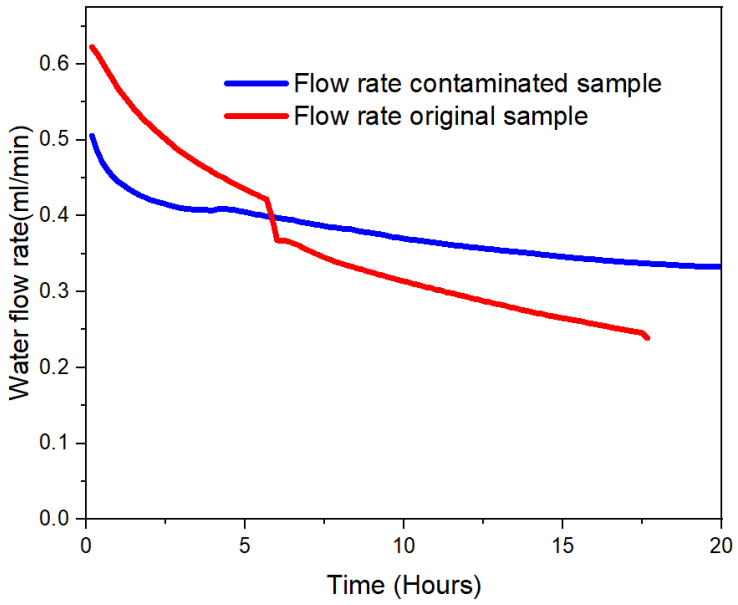

Figure 3-10: Water flow rate through the uncontaminated neat G cement and the oil-contaminated neat G cement plugs at an injection pressure of 1000 psi and a confining pressure of 15 psi.

3.4.5 Oil Contamination Experiments Using G Plus Additives

The G plus additives cement was contaminated by adding 2.5% by volume of light oil (20 ml) to the cement slurry. As per the test matrix described Section 2.3.7, the first step was to test the permeability of the cement plug using water flow. Figure 3-11 compares the water flow rates through the contaminated and uncontaminated class G cement with additives at an injection pressure of 1000 psi and a confining pressure of 1000 psi. Water flow rates were initially high for the contaminated sample, but the average flow rate steadily declined as more water was injected during the experiment. The average water flow rate into oil contaminated G plus additive sample during the last 6 hours of the experiment was determined as 0.00042 ml/min. No water breakthrough was observed during the experiment. The sealing performance of the two cement blends were very similar. It seemed that small amounts of oil did not affect the sealing capability of the cement slurry. The water flow rate curves obtained from both experiments almost perfectly overlapped one another.

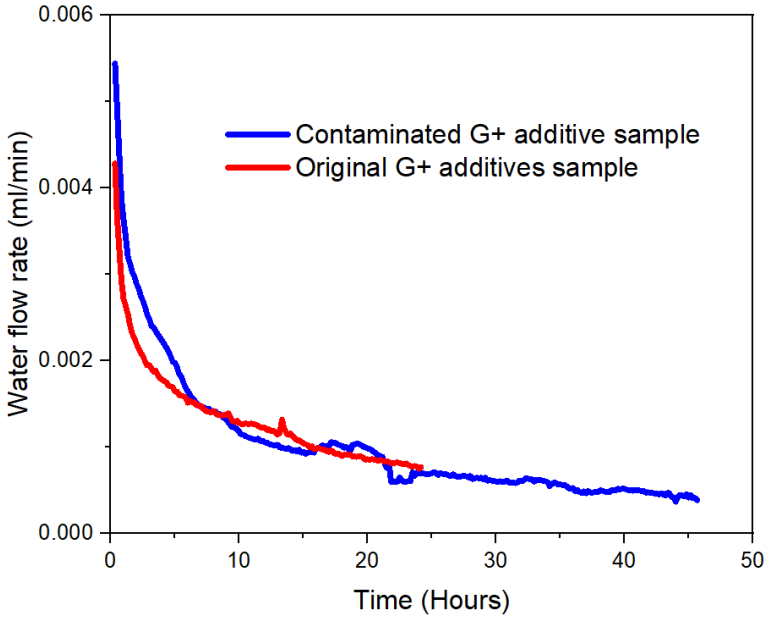

Figure 3-11: Comparison of water flow rates into the contaminated and uncontaminated class G cement with additives at an injection pressure and confining pressure of 1000 psi.

Figure 3-12 compares the Nitrogen flow rates between the contaminated and uncontaminated class G cement with additives at an injection pressure of 1000 psi and variable confining pressure. For the contaminated sample, immediate nitrogen breakthrough was observed and the flow rate kept increasing for 6 hours until the flow rate stabilized. The flow rate stabilized around 65 ml/min. As we reduced the confining pressure, the flow rate started to increase, until a point where the flow rate exceeded the detection limit of the experimental set-up. Nitrogen breakthrough was observed immediately for the oil contaminated cement sample while for the original (uncontaminated) sample it took more than 3 days, until the confining pressure was reduced to the atmospheric pressure level. Even the small volume of oil contamination caused the nitrogen flow rates to rapidly increase for the class G sample with additives.

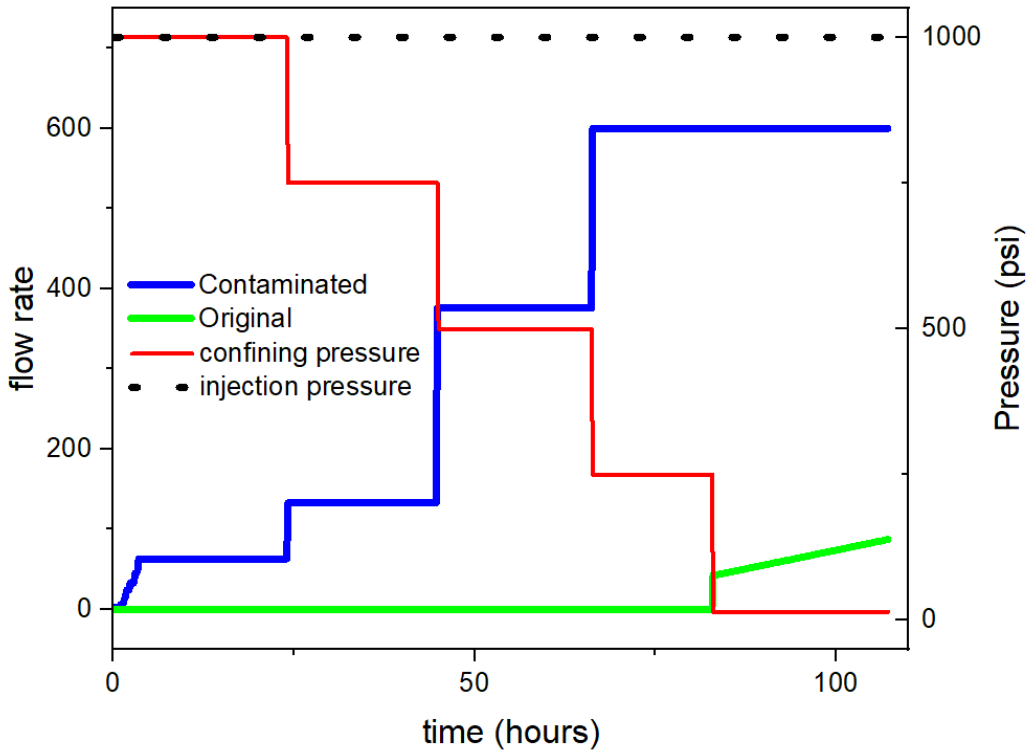

Figure 3-12: Comparison of nitrogen flow rates through the oil contaminated and uncontaminated class G cement with additives at an injection pressure of 1000 psi and varying confining pressure.

As per the testing matrix described in Section 2.3.7, the last step was to measure the water flow rate into the oil contaminated plug at an injection pressure of 1000 psi and atmospheric confining pressure. Figure 3-13 shows the test results. Water breakthrough was observed immediately with the oil contaminated sample, the average water flow rate for the last several hours of experiments were measured as 0.055 ml/min. The water flow rate was an order of magnitude higher than the flow rates observed in step 1.

No water breakthrough was observed with the original sample. Water flow rates into the original (uncontaminated) sample seemed to be about two to three orders of magnitude lower than those in the contaminated cement sample.

Results indicated that the cement sealability was not lost completely with the presence of a small amount of oil, but any disturbance to the effective stress causes the oil contaminated cement to lose its sealing capabilities very rapidly. These results reiterate the importance of cleaning the wells sufficiently before placing the cement plugs.

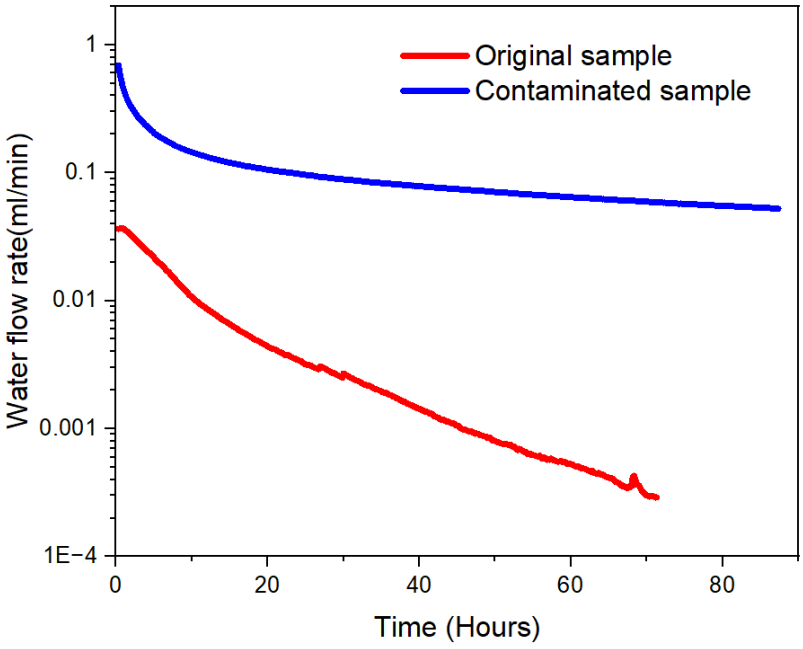

Figure 3-13: Comparison of the water flow rates through the contaminated and uncontaminated class G cement with additives at an injection pressure of 1000 psi and a confining pressure of 15 psi.

3.4.6 Comparison of Water Flow Rates Through the Original and Oil-Contaminated Cement Blends-Neat G vs G Plus Additives

Figure 3-14 compares the water flow rates through the original and oil-contaminated Neat G and G plus additive plugs at an injection pressure of 1000 psi and a confining pressure of 15 psi. The neat G blend contaminated with oil had the poorest sealing performance. The G plus additives blend with oil contamination had a better sealing performance than both original and contaminated neat G cement plugs. Although the sealing performance was reduced slightly, the flow rates into the contaminated G-plus additives blend was an order of magnitude lower than that of the neat G cement. The sealing performance of the cement was enhanced significantly with the addition of carefully selected additives. The sealing performance of the G-plus additives blend against water flow did not change significantly with oil contamination. But with some disturbance to the effective stress exerted on the cement, the sealing performance was significantly reduced.

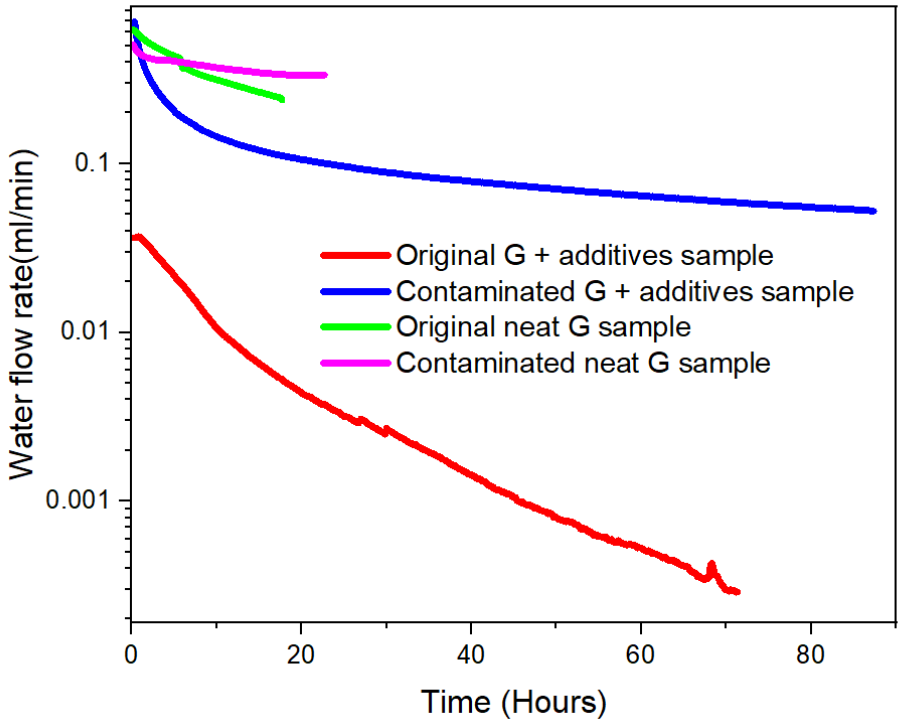

Figure 3-144: Comparison of water flow rates measured for all the original and oil-contaminated plugs at an injection pressure of 1000 psi and a confining pressure of 15 psi.

3.5 Shear Bond Strength

Table 3-2 summarizes the shear bond strengths that were measured after each wellbore simulator experiment. The shear bond strength measured in this experiment was done in an uncontrolled manner. This means that the results from these experiments is an estimate of the shear bond strength rather than the actual bond strength. The results from these experiments can be used to compare the bond strengths among different cement blends to rank their performance.

Cement blend	Shear bond strength (MPa)	Total test duration	Shear bond failure during experiment
Neat G (1900 kg/m3)	1.8	2	No
Neat G with 12.5% water contamination (1800 kg/m3)	1.4	1 Day	Yes
Neat G with 25% water contamination (1720 kg/m3)	1.2	1 Day	Yes
Cement with G plus additives (1900 kg/m3)	4.8	19 Days	No
Cement with G plus additives and 12.5% water contamination (1800 kg/m3)	1.1	1 Day	Yes
Cement with G plus additives and 25% water contamination (1720 kg/m3)	1.1	1 Day	Yes
Neat G with 2.5% oil contamination	1.2	2 Days	Yes
Cement with G plus additives and 2.5% oil contamination	2.8	9 Days	No

Table 3-2: Comparison of shear bond strengths of different cement blends

Shear bond strength of Neat G cement blend: The shear bond strength of the uncontaminated neat G cement plug was recorded as 1.8 MPa. When the cement slurry was contaminated with either water or oil, the shear bond between the cement and casing started to fail during the experiments. The cement column in these experiments usually moved up the inner casing (as pressure was applied from the bottom). Therefore, the shear bond values presented here refer to the force required to remove the cement plug from the inner casing as opposed to the actual strength needed to break the bond at the cement casing interface.

Shear bond strength of class G with additives: The shear bond strength of the uncontaminated class G cement with additives plug was recorded as 4.8 MPa. When the cement slurry was contaminated with oil, the shear bond between the cement and casing was reduced to 58% of the original shear bond strength. When the cement was diluted with water, the shear bond between the cement and casing failed during every experiment. The cement column in these experiments usually moved up the inner casing (as pressure was applied from the bottom). Again, the shear bond values presented here refer to the force required to remove the cement plug from the inner casing as opposed to the force needed to break the bond at the cement casing interface.

3.6 Conclusions

The reduction in cement density due to water contamination had a detrimental effect on the sealing capabilities of the cement plug. For all the water-contaminated experiments, the shear bond between the inner casing and cement plugs failed during the experiments. The cement plug could not withstand those severe testing conditions.

For the Neat G cement plugs, we identified that the dominant pathway for the test fluid was between the inner casing and the cement plug. The water flow rates through the 25% contaminated sample were an order of magnitude higher than the flow rates through the uncontaminated samples.

For the cement with G+ additives, the presence of excess water was far more detrimental to its isolation capabilities than the neat G cement plug. The shear bond for both the 12.5% and 25% water contaminated cement plugs failed during the experiments.

The dominant fluid pathway for the cement blends with G plus additives was through the cement matrix. The fluid loss additives used in this blend prevented the cement slurry from expelling excess water. This water was then trapped in the pore spaces of the cement matrix, forming larger pores. When fluids were injected at high pressure, these fluids flowed through these larger pores. The permeability of the cement blends with G plus additives with 25% water contamination was the highest among all four water-contaminated experiments.

For the neat G cement plugs, oil contamination had little to no effect on the permeability of the entire system as long as the permeability experiments were carried out at the pressure and temperature conditions same as the curing conditions. When the confining pressure was reduced, the permeability of the oil contaminated Neat G plug was 1.5 times higher than the permeability of the uncontaminated Neat G plug. This suggests that with oil contamination, the sensitivity of the plug to any minor stress changes was magnified, with the micro annulus forming more readily. The shear bond between the inner casing and cement plug also failed during the experiment.

For the class G cement with additives and oil contamination, a similar trend (as Neat G plug) was observed. As long as the permeability experiment were conducted at pressure and temperature conditions identical to the curing conditions, minimal changes in the flow rate data were observed. However, the type of fluid that was used to conduct the permeability tests did have an effect. When Nitrogen was injected at a pressure identical to the curing condition, gas breakthrough was observed immediately. Upon reducing the confining pressure, the nitrogen flow rates increased and exceeded the maximum detection limit.

When the water permeability test was conducted (following Nitrogen flow test) in an oil contaminated plugs at an injection pressure of 1000 psi and atmospheric confining pressure, the flow rates of the contaminated sample were between two and three orders of magnitude higher than the original sample. This validated the hypothesis that the sensitivity to the formation of a micro annulus was magnified in the presence of oil contamination. The shear bond of the sample did not fail during the pressure ramp up.

The water flow rates through the oil contaminated G plus additive plug was one order of magnitude lower than the neat G cement sample that had no contamination.

These results suggest that greater care needs to be taken when engineering cement blends. The engineered cement blend should account for the types of contaminants found in the wellbore and a “one glove fits all” methodology cannot be deployed in cementing practices.

3.7 References

[1] Dusseault, M.B., Gray, M.N. and Nawrocki, P.A., 2000, November. Why oilwells leak: cement behavior and long-term consequences. In SPE International Oil and Gas Conference and Exhibition in China, SPE-64733-MS. SPE.

[2] Kang, M., Kanno, C.M., Reid, M.C., Zhang, X., Mauzerall, D.L., Celia, M.A., Chen, Y. and Onstott, T.C., 2014. Direct measurements of methane emissions from abandoned oil and gas wells in Pennsylvania. Proceedings of the National Academy of Sciences, 111(51), pp.18173-18177.

[3] Barclay, I., Pellenbarg, J., Tettero, F., Pfeiffer, J., Slater, H. and Staal, T., 2001. The beginning of the end: a review of abandonment and decommissioning practices. Oilfield Review, 13(4), pp.28-41.

[4] Thaika, MA., Hu, K., Kuru, E., Li, H., Iremonger, S., Lin, Z., & DeBruijn, G., 2024. Experimental investigation of well cement integrity in abandoned oil and gas, In International Conference on Offshore Mechanics and Arctic Engineering, Singapore, OMAE2024-130296. American Society of Mechanical Engineers.

[5] Patel, A.D., Wilson, J.M. and Loughridge, B.W., 1999, February. Impact of synthetic-based drilling fluids on oilwell cementing operations. In SPE International Conference on Oilfield Chemistry, Houston, Texas, USA, SPE-50726-MS. SPE.

[6] Agbasimalo, N. and Radonjic, M., 2014. Experimental study of the impact of drilling fluid contamination on the integrity of cement–formation interface. Journal of Energy Resources Technology, 136(4), p.042908.

[7] Clark, C.R. and Carter, G.L., 1973. Fluid displacement with cement slurries. Journal of Petroleum Technology, 25(07), pp.775-783.

[8] Zuiderwijk, J.J.M., 1974, May. Mud displacement in primary cementation. In SPE Europec featured at EAGE Conference and Exhibition, Amsterdam, Netherlands, SPE-4830-MS. SPE.

[9] Nelson, E.B. and Guillot, D., 2006. Well cementing, 2006. Schlumberger, Sugar Land, Texas, USA.

[10] Goode, J.M., 1962. Gas and water permeability data for some common oilwell cements. Journal of Petroleum Technology, 14(08), pp.851-854.

[11] Aughenbaugh, K., Nair, S., Cowan, M. and van Oort, E., 2014, September. Contamination of deepwater well cementations by synthetic-based drilling fluids. In SPE Deepwater Drilling and Completions Conference, Galveston, Texas, USA, SPE-170325-MS. SPE.

[12] Li, M., Ou, H., Li, Z., Gu, T., Liu, H. and Guo, X., 2015. Contamination of cement slurries with diesel-based drilling fluids in a shale gas well. Journal of Natural Gas Science and Engineering, 27, pp.1312-1320.

[13] Li, Z., Liu, H., Guo, X., Ou, H. and Gu, T., 2016. Contamination of cement slurries with oil based fluid and its components in cementing operations. Journal of Natural Gas Science and Engineering, 29, pp.160-168.

[14] Bourgoyne, A.T., Scott, S.L, and Manowski, W., 2000. A review of sustained casing pressure occurring on the OCS, Bureau of safety and environmental enforcement.

[15] Scrivener, K.L., Crumbie, A.K. and Laugesen, P., 2004. The interfacial transition zone (ITZ) between cement paste and aggregate in concrete. Interface Science, 12, pp.411-421.

[16] Coleman, J.R. and Corrigan, G.L., 1941. Fineness and water-cement ratio in relation to volume and permeability of cement. Transactions of the AIME, 142(01), pp.205-215.

[17] The American Petroleum Institute, 2013. Recommended practice for testing well cement, API recommended practice 10-B2, Second edition.

Chapter 4 Squeeze Cementing Performance of Various Cement Blends

4.1 Abstract

Well leakage issues have been reported in many legacy wells around the world. The most popular method to fix well leakage issues is to carry out squeeze cementing operation. There have been many studies investigating the penetration capabilities of cement in the past, but many of these experiments do not replicate field conditions. In this study, three different cement systems were tested for both their sealing performance and penetration potential in narrow fracture gaps. These cement systems include class G cement (GC), Portland limestone cement (PLC) with grains smaller than class G cement, and finally microfine cement (MFC), which has the smallest grain size among the cement blends investigated in this study. Cement was cured and cut into halves with a diamond saw to create replicas of fractured cement samples. Metal shims of 200, 150, and 100 microns in thickness were used to control the gap size of the fractures. The fractured cement samples were imaged using micro-CT scanning technique before and after remediation to determine both the fracture width and the slurry flow pathway. It was observed that the Class G cement bridged at 200 microns. The cement slurry appeared to be deposited in a fingering pattern when the fracture width was in the range of 90 to 200 microns and cement filtrate could penetrate a fracture width a of 45 to 90 microns. For the Portland Limestone cement, we observed bridging occurred at 50 microns gap size, cement slurry fingering at a fracture gap size in the range of 35 to 50 microns and no penetration capabilities for fractures less than 35 microns. The microfine cement was able to penetrate fracture gap size as thin as 35 microns without any issues, making it the ideal blend for a typical squeeze cementing operation.

4.2 Introduction

As of 2024, Alberta has more than 469,306 registered petroleum wells [1]. 19.6% of these petroleum wells have already been abandoned and a further 16.6% of these wells are considered to be inactive [1]. The percentage of abandoned wells in Alberta is also increasing year on year. A study carried out by Watson & Baku in 2009 [2] showed that roughly 4.5% of all oil and gas wells showed some sign of leakage problems. When a well is cemented, it is expected that the barrier material isolates the production zone from the surface and the rest of the surroundings throughout the well's life span and even after abandonment. However, this is not always the case as the wells could experience numerous changes that could cause the barrier material to lose its zonal isolation capabilities from the time it was completed until the time it was abandoned. The well could experience fluctuations in downhole pressure and temperatures due to operations like hydraulic fracturing and steam assisted gravity drainage operations, causing well integrity issues [3]. These well integrity issues may include cement-casing or cement-formation debonding or the creation of cracks in the cement sheath [4]. The main problem associated with loss of well integrity is the leakage of greenhouse gases such as methane which is 80 times more potent at warming the atmosphere when compared to carbon dioxide over a 20-year time period [5]. Yang et al. [6] suggested that some small gaps in an oil and gas well may not provide an immediate communication pathway for fluids to migrate across but could act as a point of initiation for the formation of a micro annulus or fracture along the cement column due to stress concentrations. As this is a slow process, it is relevant to abandonment operations as these abandonment wells need to provide isolation for several decades or even centuries to come.

Remedial action needs to be taken to fix these wellbore integrity issues. These remedial techniques include squeeze cementing [4], plug cementing [7] and remediation through the use of polymer resin [8]. Squeeze cementing is by far the most popular method to remediate well integrity issues [7, 9]. Squeeze cementing is performed by perforating the casing and squeezing a sealant such as class G Portland cement behind the casing under pressurized conditions [8]. Squeeze cementing is commonly used to solve well integrity issues related to 1) seal lost-circulation zones, 2) repairing primary cement jobs, 3) eliminating water intrusions around the production zone, 4) altering the gas oil ratio or water oil ratio, 5) repairing casing leaks caused by corrosion or pipe breakage 6) abandon a depleted zone and 7) plug various zones in an injection well to direct the injection fluids

into the targeted intervals [7]. The viscosity of the squeezing cement slurry is typically lower than conventional cement [4, 10]. The slurry is mixed and pumped into the annulus or fracture space and then allowed to cure for a certain period [4]. When a squeeze job is initiated, the cement grains are too large to enter the matrix of the formation [7]. The filter cake accumulates along the perforation and eventually fills up the channel [7].

The squeeze job is generally divided into two categories: low-pressure squeezes and high-pressure squeezes. Low-pressure squeezes involve maintaining the bottom hole pressure below the fracture gradient and high-pressure squeezes involve exceeding the fracturing pressure [7]. The high-pressure squeezes induce fractures in the formation that allow cement to replace "dirty fluids" in the wellbore, whereas the low-pressure squeezes are the best option for squeezing into the pay zone [7]. The disadvantages of deploying a high-pressure squeeze involve using large volumes of slurry, difficulty in obtaining a filter cake, and difficulty in attaining high squeeze pressures [7]. The drawback of using low-pressure squeeze is that more careful design and execution is needed [7].

For low-pressure squeezes, the volume of slurry is usually small as the slurry is not being pumped into the formation [7]. The pressure must be constantly monitored and should never exceed the fracture pressure gradient [7]. It is also vital to ensure that the perforated channels are free of debris. It is generally accepted that low pressure squeeze operations are considered to be more successful [11-13].

The squeezing operation could be further separated into two methods: the running squeeze method and the hesitation squeeze method [4, 14]. Running squeeze technique involves squeezing the cement at the zone of interest until the target pressure is achieved [4]. The squeeze pressure is then monitored after squeezing to determine if the operation is successful. If the squeeze pressures start to drop, more slurry is squeezed into the target zone and the pressure is monitored again [4]. This process is repeated until the target zone is able to hold the squeeze pressure. The hesitation squeeze cementing technique involves pumping a set portion of the cement slurry and then immediately stopping in order to expose the cement slurry to differential pressure in the target zone [4]. The differential pressure forces the cement into zones that require repair and is done continuously until

all the cement slurry has been placed in the zone of interest [4].

Normann [15] stated that although squeeze cementing could be used to repair defects in the primary cementing jobs, it is not capable of remediating issues related to the formation of micro-annuli or micro fractures [15]. Normann [15] also stated that it is not possible to squeeze conventional cements into cracks in the range 300-500 µm and even engineered micro-fine cements cannot penetrate cracks smaller than 150 µm.

Ewort et al. [16] carried out experiments to investigate the cement penetration efficiency through various sand packs. A flow test under gravity was first conducted where a sand column of 6 inches in height of either 20/40 or 40/60-mesh sand was placed in a 1.25-inch diameter glass tube [16]. An equivalent amount of slurry was prepared and poured into the set up to test the penetration ability of the slurry [16]. A flow test under pressure was carried out as well. 20/40 or 40/60-mesh sand was placed into a 60 cm^3 syringe and a sand column height of 4 inches was obtained. A 2 inch column of slurry was placed above the sand and the pressure was applied by hand. The penetration capabilities of the slurry were monitored. The grain size of the slurries used in their experiment is shown in Table 4-1. The d_{90} term indicated that 90% of the grain diameters fell below the value listed in the table [16].

Sample	Grain size d_{90} (µm)	Grain size d_{50} (µm)	Grain size d_{10} (µm)
Class G	61.2	24.8	5.7
A	29.0	12.8	4.0
B	25.4	11.1	3.5
C	23.6	8.5	2.7
D	12.4	5.7	2.4
E	23.4	6.8	1.8

Table 4-1: Grain size distribution of the cement samples used in Ewort's study [16].

Sample A was class G cement that was grounded into finer particles. Samples B and C were ground from a clinker that was not chemically similar to class G cement. Sample D was a mixture of cement and slag to obtain a finer particle size and sample E was kiln dust. It was observed that the

typical class G cement could not pass any of the sand packs even when the cement water ratio was increased. Sample A was able to penetrate the 20/40 mesh sand pack under pressure after it was diluted with water. Sample B and all other samples with grain size less than that of sample B were able to flow across the 20/40 mesh sands [16]. As long as the mean diameter of the particles in a cement sample was less than 10 μm, the cement could penetrate both the 20/40 and 40/60-mesh sand. They also observed that by diluting the cement, the penetration potential was enhanced; however, the drawback of doing this was that the slurry became unstable due to its inability to suspend solids in the solution [16].

Microfine cements have been developed to remediate very small micro annuli between the cement and casing or the cement and formation. The micro annuli space could be as small as 10-20 μm [17] and it would be impossible for conventional class G cement to penetrate this fracture space. In order to penetrate very narrow gaps, the cement particle size must be very narrow, have efficient fluid loss control both in the axial and radial direction, form a very thin filter cake, low rheology, zero free water and no sedimentation under downhole conditions [18]. The cement slurry loses fluid as it is being forced into a gap [18]. As the cement slurry moves through a fracture, it loses fluid in the radial and axial direction, the large solid particles filter out on the formation face and the aqueous phase enters the formation matrix [18]. It is difficult to verify if the entire void space has been filled with cement before the slurry dehydrates (by losing fluids) and becomes unpumpable [18].

Ewort et al. [16] concluded their study by stating that the class G cements could not penetrate the different sandpacks due to the larger grains present in the Class G cement (100 μm -150 μm). Bridging and cement dehydration occurred when the slurry was forced through a gap size of 400 μm [16]. This study gives some great insights into the penetration capabilities of cement; however, the cement was not injected and cured under relevant wellbore conditions. Arbitrary pressures were used and there was no guarantee to get a uniform testing matrix. Furthermore, the experiments carried out by Ewort et al. [16] are testing the slurry filtration performance rather than squeezing cement to remediate microfractures.

Microfine cements have been commercially available for a long time but it was only in the early

1990's that the oil and gas industry started using microfine cements [19]. The increase in the use of microfine cements was due to the conventional thinking that reducing the grainsize would allow for further penetration capabilities. Meek & Harris [10] investigated the penetration capability of a micro-fine cement. They modified an API fluid loss testing cell by replacing the mesh at the bottom with two semi-circle plates connected with an adjustable screw. They were able to control the slot size to various widths ranging from 75 µm to 250 µm [10]. They tested 5 different cements with varying grain sizes. The properties of the cement are also listed in Table 4.2.

Sample	Grain size d_{90} (µm)	Grain size d_{50} (µm)	Grain size d_{10} (µm)
Microfine A	9.5	5.0	2.2
Microfine B	27.0	9.2	3.1
Class C	32.1	15.0	3.9
Class G	53	21.0	4.5
Class H	55.9	24.5	6.1

Table 4-2: Grain size distributions of the cement sample used in Meek & Harris's study [10, 19]

About 140 ml of slurry was placed into the cell and a pressure of 90 psi was applied to the slurry [10]. Any slurry that passed through the slot was collected. They observed that the cement bridged within a few seconds. After the experiment, the apparatus was disassembled and inspected for bridging.

At a slot size of 75 µm, minimal amounts (0-6% by volume) of slurry passed through the slot and bridging was observed in all cases [10]. At a slot size of 150 µm, anywhere between 36% to 96% by volume of cement were able to pass through the slot with slight bridging when tested with microfine cements. The performance of conventional cement was significantly lower (0% to 28%) and bridging was observed for all the conventional cements [10]. At the maximum slot size of 250 µm, anywhere between 43% to 99% by volume of cement penetrated the slot with no bridging observed when tested with microfine cements [10]. The performance of the conventional cement was slightly better with roughly 15% of the cement slurry passing the slot before bridging was observed [10]. The density of the collected slurry after the penetration experiment was also always lower than the initially injected slurry, indicating a filtration process occurring at the slot [10].

The experiments carried out by Meek & Harris [10] gave some great insights as to how cement

penetrates various fracture widths, however, there are some limitations associated with his experiment because the field conditions are not accurately represented. The objective of a squeeze job is to remediate a micro fracture (cement-cement interface) or remediate a micro annulus (cement-casing/formation interface). The cement slurry being squeezed between two metal plates does not replicate what is happening in a wellbore.

Slater et al. [18] investigated the penetration potential of a conventional microfine cement and an enhanced microfine cement. They argued that the conventional microfine cement was not good enough to seal the smallest fracture space (a few microns) because the conventional microfine cement had a particle size distribution between 13 to 30 μm. In addition to the cement itself, water was used to fill the pore spaces, and the water typically accounts for 30 to 35% of the cement volume [18].

Meek & Harris's [10] study showed that fluid loss additives to microfine cement reduced the penetration potential of the slurry due to an increase in viscosity. Slater et al. [18] decided to make a more optimized microfine cement. The microfine cement used in their studies had a maximum particle diameter of 7 to 10 μm. Instead of filling the pores with water, they decided to fill the pores with solid non-cement particles of two distinct smaller sizes. One of these particles had a maximum diameter range between 0.5 to 1 μm, while the other one had a maximum diameter of 1nm. By filling the pore space of the micro cement with other solids, the water requirements were significantly reduced [18].

They carried out penetration tests using a custom-built apparatus. The setup consisted of a porous plate on the bottom, a filter paper attached to the porous plate, spacers placed above the filter paper and covered by a plexi-glass [18]. The setup was held together by C-clamps. An injection port was attached to the plexi-glass and was connected to a syringe housing the slurry [18]. The gap was set at 120 μm and the cement was squeezed at an injection rate of 5 ml/min.

Slater et al. [18] observed that the conventional microfine cement lost all of its water very quickly and bridged after the slurry had only penetrated a distance of 30 mm. The conventional microfine cement also formed fingering patterns that did not fully isolate the gaps. The optimized microfine cement system filled the entire apparatus with no fingering observed [18]. The test carried out by

Slater et al. [18] involved using a hand syringe to squeeze the slurry into the fracture space (arbitrary squeeze pressure was used). The filter paper and porous plate used in their experiment would actually promote the dehydration of slurry to a greater extent than what would happen in a real wellbore.

Conventional wisdom suggests that a particle will flow through a fracture space or micro annuli without bridging as long as the aperture width is 2 to 5 times the maximum particle size [20, 21]. These assumptions are only valid for inert particles that do not react with each other [20]. Cement exhibits substantial interactions due to electrostatic surface charge, combined with fluid loss causing the effective particle size to be much larger [20]. Gap penetration tests showed that bridging of cement particles started when the gap size was roughly 10 times the largest particle size [20].

There have been lots of studies investigating the penetration potential of conventional cements, microfine cement, engineered microfine cements, and resin [8, 9, 10, 16, 18, 20]. Most, if not all, of these experiments have some limitations associated with them such as not replicating field conditions.

Upon reviewing the literature, it became evident that squeeze cementing tests need to be done under more realistic conditions. During remediation, the injected slurry needs to either remediate a micro annulus or a micro crack. This means that the cement needs to be squeezed in-between either a cement-cement interface or a cement-casing interface. The squeeze tests also need to be carried out at much higher injection pressures than previous experiments which used only low injection pressures or arbitrary pressures (e.g., 90 psi) [10, 16, 18, 20]. An additional gap observed in the literature was the lack of permeability testing or verification of the remediation process. All of the previous studies focused on the penetration potential of the cement, but no permeability data has been provided before and after the remediation process. The objective of a squeeze operation is to stop fluid leakage from formation to surface, which could be achieved by lowering the permeability of the entire system. Permeability of the system is actually the key metric to determine the success of a squeeze job.

This led to the design of a comprehensive testing procedure we used in this study. Cement cores made from conventional cements were cut in half, with shim stocks placed on the edges of the core to maintain a fracture width. The cement cores were then imaged using a state-of-the-art CT scanning technique. The fracture width of the cores was measured using the CT images. The fractured cement core was then remediated with three different types of slurry and the cores were imaged again to visually observe the cement slurry pathways. Finally, the remediated fracture conductivity was tested and compared to the open fracture conductivity.

The study presented here has two main objectives: 1) determine the penetration potential of three different types of cement that can be used for squeeze cementing job and determine the gap width where bridging starts and 2) to compare the fracture conductivity of the sample before and after remediation.

4.3 Methodology

4.3.1 Materials

Three types of cement blends were used for this study. The cement mixing ratios and additives for each blend are listed below in Table 4-3.

Cement blend	Water: cement mixing ratio	Additives	Slurry density (kg/m^3)
0:1:0 Class G + additives	0.434	Accelerator, Fluid Loss, Dispersant & Defoamer	1901
Portland limestone	0.558	Accelerator, Fluid Loss, Dispersant, Defoamer	1750
Microfine cement	0.696	Accelerator, Fluid Loss, Dispersant, Defoamer	1650

Table 4-3: Cement blends used in this study

The functions of different additives are explained below:

Accelerator – Aids in the development of early strength at low temperature and aids in the stability of the slurry by preventing particle settling.

Fluid Loss – Prevents fluid loss from the cement slurry.

Dispersant – Lowers the viscosity of the slurry for easier mixing and pumping and enhances the performance of the fluid loss additive.

Defoamer – Reduces the entraining of air bubbles in the cement slurry, facilitating easier field operations.

The particle size distribution of all 3 cement blends used in this study is shown in figure 4-1. The microfine cement had a mean grain size of 8 microns, with the largest particles in the 30-micron range. The Portland limestone cement had a mean grain size of 18 microns with the largest grains exceeding 100 microns. The standard class G cement had a mean grain size of 30 microns with the largest grains exceeding 100 microns.

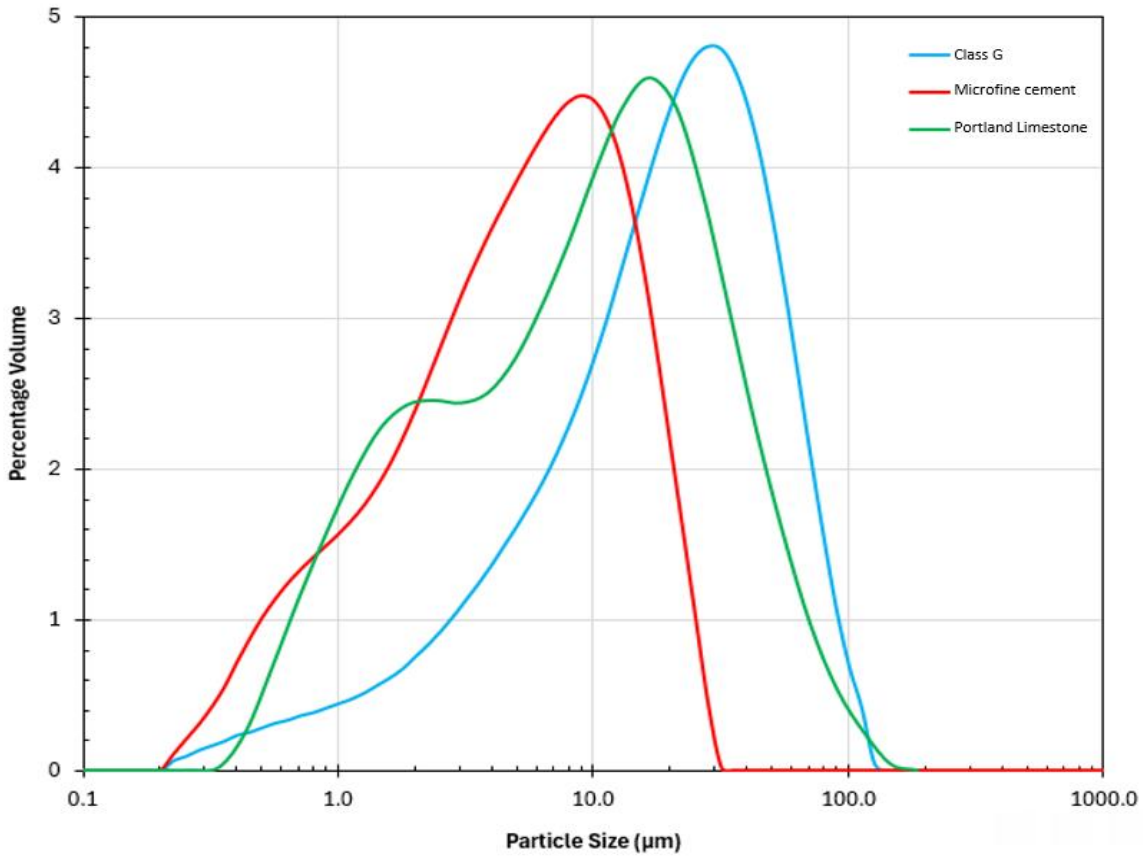

Figure 4-1: Particle size distribution of the three cement blends used for the squeeze cementing experiments

4.3.2 Cement Mixing Procedure

The cement was mixed as per the API-10B-2 standard [22] as described in Section 3 of Chapter 2. All fractured cement samples were created by using Class G cement.

4.3.3 Bulk Cement Sample Preparation

The cement mould was first assembled. The hose clamp was secured around the mould and tightened at the bottom as shown in figure 4-2. After the cement has finished conditioning, the mixed cement was poured into the mould. The top cap was placed on top of the mould to cover the cement and a second hose clap was secured to the top of the mould. The mould was then placed into a curing cell and cured at a pressure of 1000 psi and a temperature of 50 C for a period of 7 days. After curing, the cell was depressurized over four hours and the cement core was taken out of the mould. The sample length ranged from 1.1 inches to 1.4 inches and the diameter of the sample was 1 inch.

Figure 4-2: PTFE mould used to cure the bulk cement core

4.3.4 Sample Cutting

The cured sample was cut using a diamond saw as shown in figure 4-3.

Figure 4-3: Diamond saw used for cutting the cement cores

4.3.5 Fracture Generation

Shims stocks were used in this study to keep the fracture space open during cement squeezing and fluid flow conductivity measurements. The shim stocks were made from 316 stainless steel and a total of three fracture widths were investigated. The shims were placed at the edges of the half core lengthwise and an electrical tape was wrapped around the cement core to keep the shims in place. A shim thickness of 50 µm, 100 µm and 150 µm were used in this study. Figure 4-4 shows the fracture space generated after placing a 100 µm shim stock between the cement half cores.

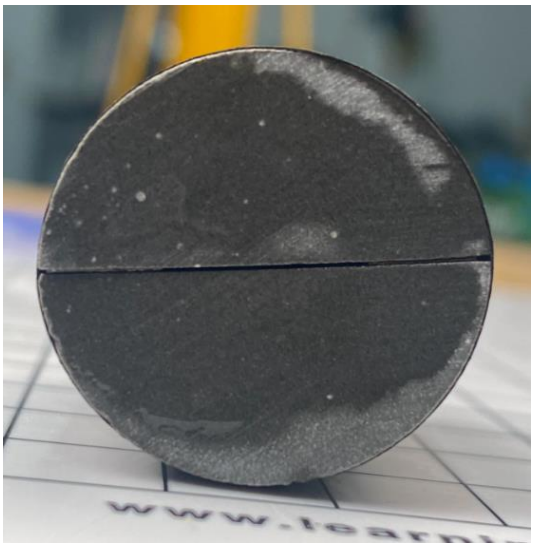

Figure 4-4: Cement core showing the inlet side of the fracture opening after placing the shims

4.3.6 Open-Fracture Conductivity Testing

Conductivity of the fractured cement samples (before and after squeeze cementing) were measured using the core flow set-up shown in Figure 4-5.

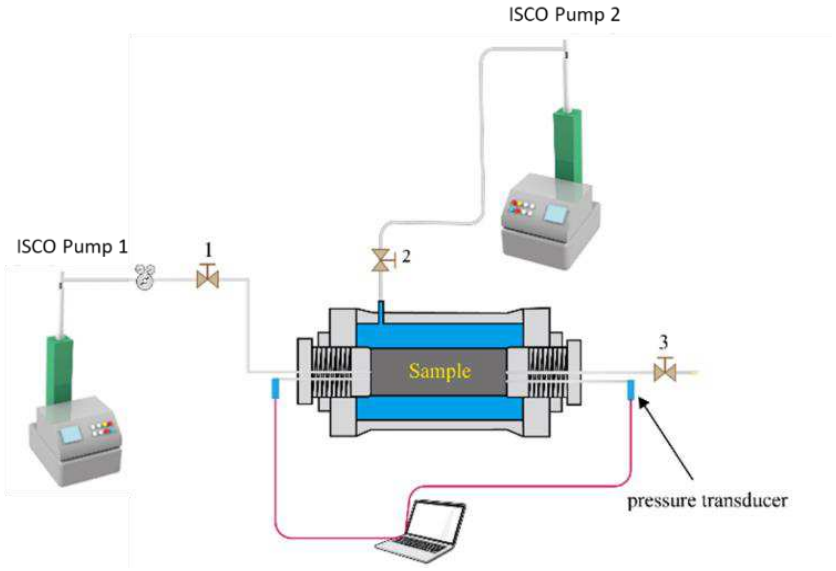

Figure 4-5: Experimental setup to test the open fracture conductivity.

Following test procedure was used to determine the conductivity of the open-fracture:

1. The confining pressure was first ramped up to 200 psi using pump 2 over a period of 5 minutes using the constant pressure gradient mode.
2. Pump 1 was set to constant flow rate mode and the delta P (pressure drop) values were recorded at 25 ml/min, 50 ml/min and 100 ml/min.
3. After recording three sets of flow rate data vs delta P data, the confining pressure was increased to 300 psi using pump 2 over a period of 2 minutes using the pressure gradient mode.
4. The permeability experiments were repeated using the same constant flow rate conditions of 25, 50 and 100 ml/min.
5. After three more sets of flow rate data vs delta P data were recorded, the confining pressure was increased to 400 psi using pump 2 over a period of 2 minutes.
6. The delta P data was once again recorded at constant flow rates of 25, 50 and 100 ml/min.
7. The confining pressure was then ramped down over a period of 60 minutes to atmospheric conditions using the constant pressure gradient mode.

8. The flow rate vs delta P data was then plotted on a graph to evaluate if the fracture space was changing.

4.3.7 CT Scanning for Fracture Width Determination

After testing the conductivity of the open fracture, the sample was CT scanned using the ZEISS Xradia 620 Versa. The resolution of the CT scans was around 35 µm. After scanning the sample, the data was imported into Dragonfly software for further processing and the fracture widths were measured at set intervals. Figure 4-6 shows an example CT-scan slice of the sample used for fracture width measurement. The fracture widths were also verified by inserting a feeler gauge strip into the open fracture. The sample was imaged twice, once after testing the conductivity of the open fracture and once after remediating the sample with the designated cement slurry.

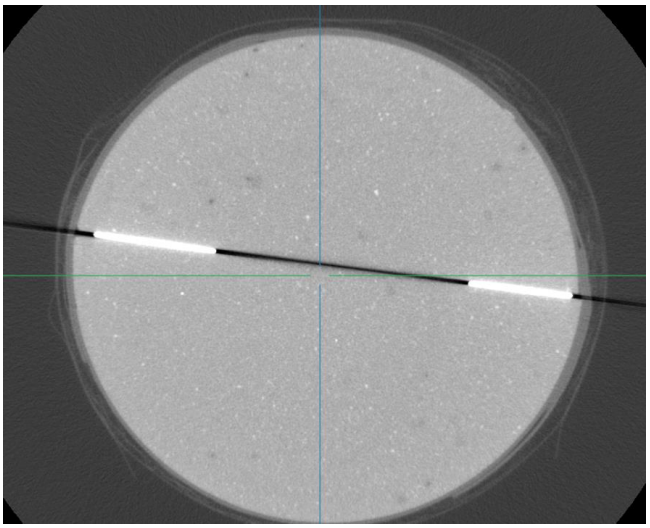

Figure 4-6: A slice taken from the radial direction of the cement core to determine fracture width.

4.3.8 Cement Squeezing Procedure

The cement slurry used for the squeeze job was mixed as per the API-10B-2 standard [22] as described in Section 3 of Chapter 2. During the last 5 minutes of cement mixing, Berea sandstone core plug and the fractured cement core were placed inside the rubber sleeve of the core holder. After cement mixing, the density of the cement slurry was measured using a 1 milliliter syringe. After measuring the density, 2-3 milliliters of cement slurry was placed in the slurry holder and the slurry holder was also placed inside the rubber sleeve as shown in figure 4-7. The slurry holder was essentially a hollow cylinder with a piston inside. The piston had an O-ring which could isolate the cement from the injected water. A cross-sectional view of the slurry holder is shown in Figure

4-8. Once the set up was assembled as shown in figure 4-7, the confining pressure was increased to 400 psi over a period of 8 minutes. The inlet pressure was increased to 300 psi over a period of 6 minutes. The experiment was allowed to run for a period of 22 hours at room temperature (20°C). After 22 hours, both the inlet and confining pressure was reduced to atmospheric pressure over a period of 60 minutes. This was done to prevent the formation of microcracks in the sample. The sample was taken out and several images of the inlet and outlet side were captured. After imaging with a camera, the sample was CT scanned once again.

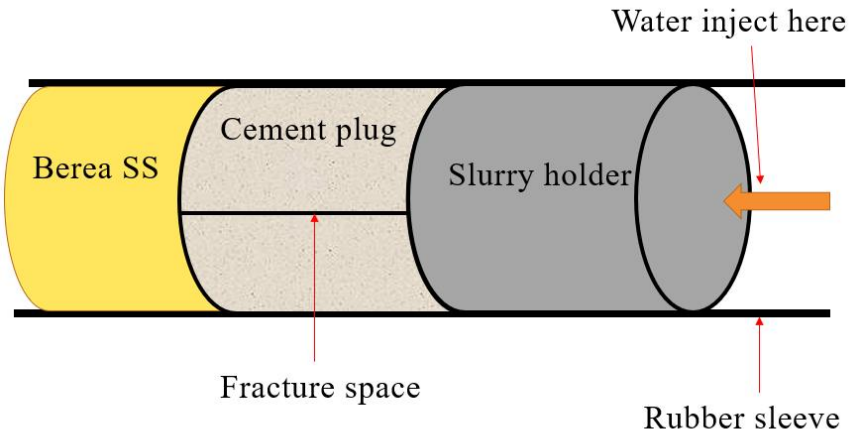

Figure 4-7: Schematic showing how the squeeze experiments were carried out

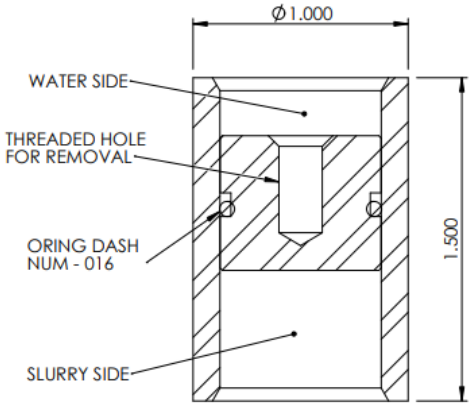

Figure 4-8: Cross section schematic of the slurry holder showing all the individual components.

4.3.9 Fracture Conductivity Measurements after Remediating the Cement Core

After CT scanning the remediated sample, the conductivity of the remediated fracture was tested by injecting water. The experimental setup shown in figure 4-5 was used to test the conductivity of the remediated fracture. The confining pressure was first ramped up to 400 psi over a period of 8 minutes. Water injection pressure was ramped up to 300 psi over a period of 6 minutes and the flow rate was recorded by the pump over a period of 15+ hours. Water flow rate readings were recorded at every 5-minute intervals. The average flow rates during the last hour of experiments were used to determine the remediated fracture conductivity. The fracture conductivity of all the samples were compared at the same confining pressure of 400 psi and an injection pressure of 300 psi. The fracture conductivity was calculated using the following equation:

$$\text{Fracture conductivity} = \frac{Water\ Flow\ rate\ (\frac{ml}{minute})}{\text{Inlet pressure (psi)}}$$

4.3.10 Opening the Cement Half-Cores

After completing the fracture conductivity experiment, the experimental setup was depressurized over a period of 60 minutes. The sample was taken out of the core holder and the electrical tape was peeled away to visually inspect the half-cores, and multiple photos of both the half-cores were captured to verify the CT data.

4.4 Results and Discussion

Results of the squeeze cement tests conducted using cement samples of varying fracture gap sizes are presented in this section. Metal shims of 150, 100 and 50 micron thickness were used to create a variable fracture gap size. Note that all fractured cement samples were prepared by using cement blend of Class G while three different cement blends (Class G, Portland Limestone, and microfine cements) were used to conduct squeeze cement jobs.

4.4.1 Squeeze Cementing Experiments using the 150 µm Shim

4.4.1.1 Open Fracture Conductivity of all the Samples

The first step of the experiments was to measure the conductivity of the open fracture. Three samples were prepared using 150 µm shims. Figure 4-9 shows the open fracture conductivity of the samples prepared by using 150 µm shims. The conductivity of all three samples were similar and the average fracture conductivity was calculated as 843 (±10) ml/min/MPa.

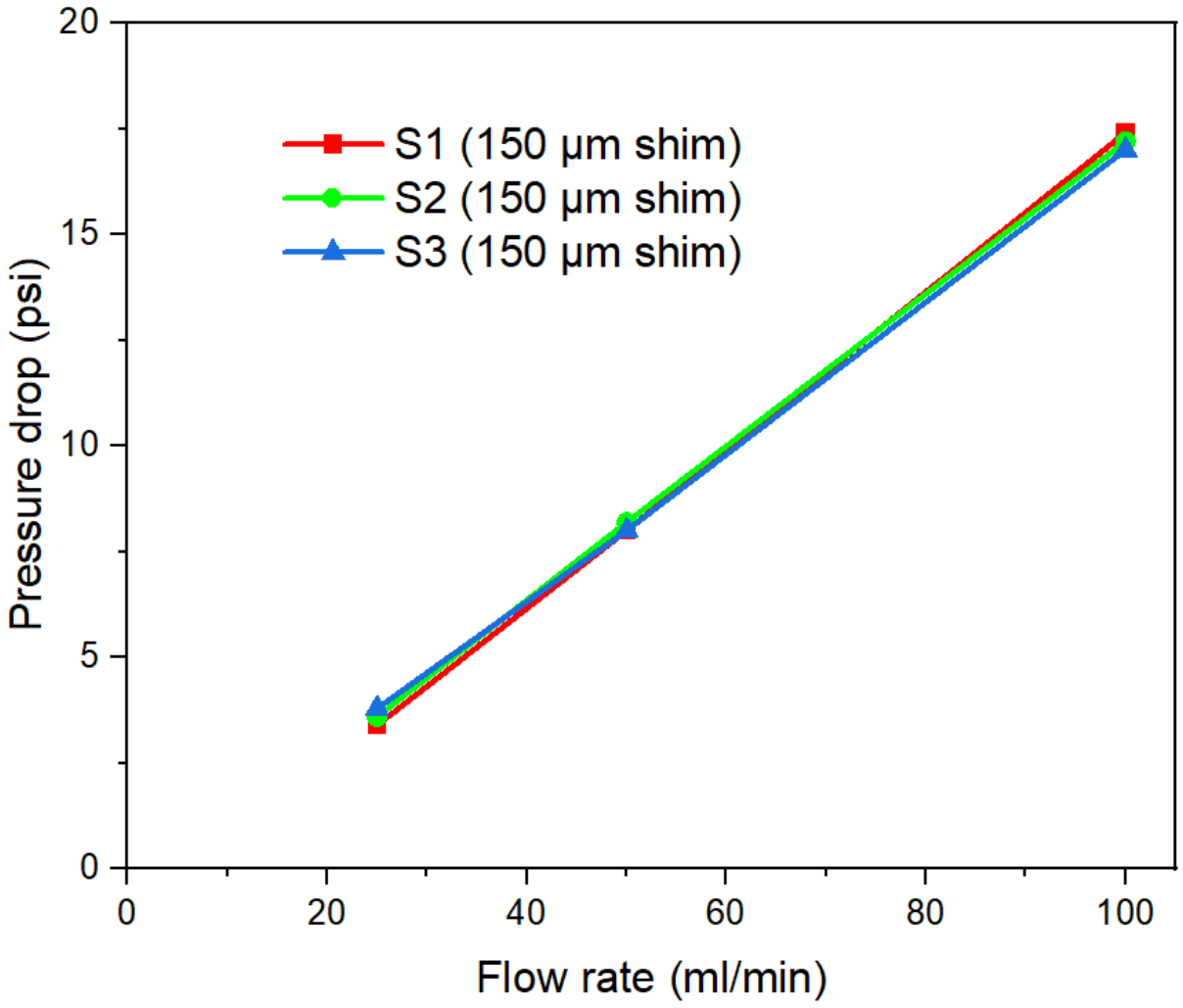

Figure 4-9: Open fracture conductivity of the samples prepared by using 150 µm shims. Conductivity was tested at variable flow rates and at a confining pressure of 400 psi.

4.4.1.2 Fracture Width Determination using CT Scan Results

After completing the fracture conductivity test, the sample was CT scanned. Figure 4-10 shows the fracture width distribution at the narrowest points through (along the longest axis of the sample) the open fracture. Due to the cutting process, a perfectly flat surface could not be achieved. Visually the half cores looked perfectly flat but the samples appeared to be narrow at the center of the core and become wider towards the inlet and outlet. Fracture width varied between. 65 micron to 180 micron, indicating the rugosity of the cement surfaces in the fracture. Fracture width distribution was very similar in all 3 samples, providing a relatively good confidence level for the suitability of the fracture generation method for the purpose of the squeeze cementing experiments.

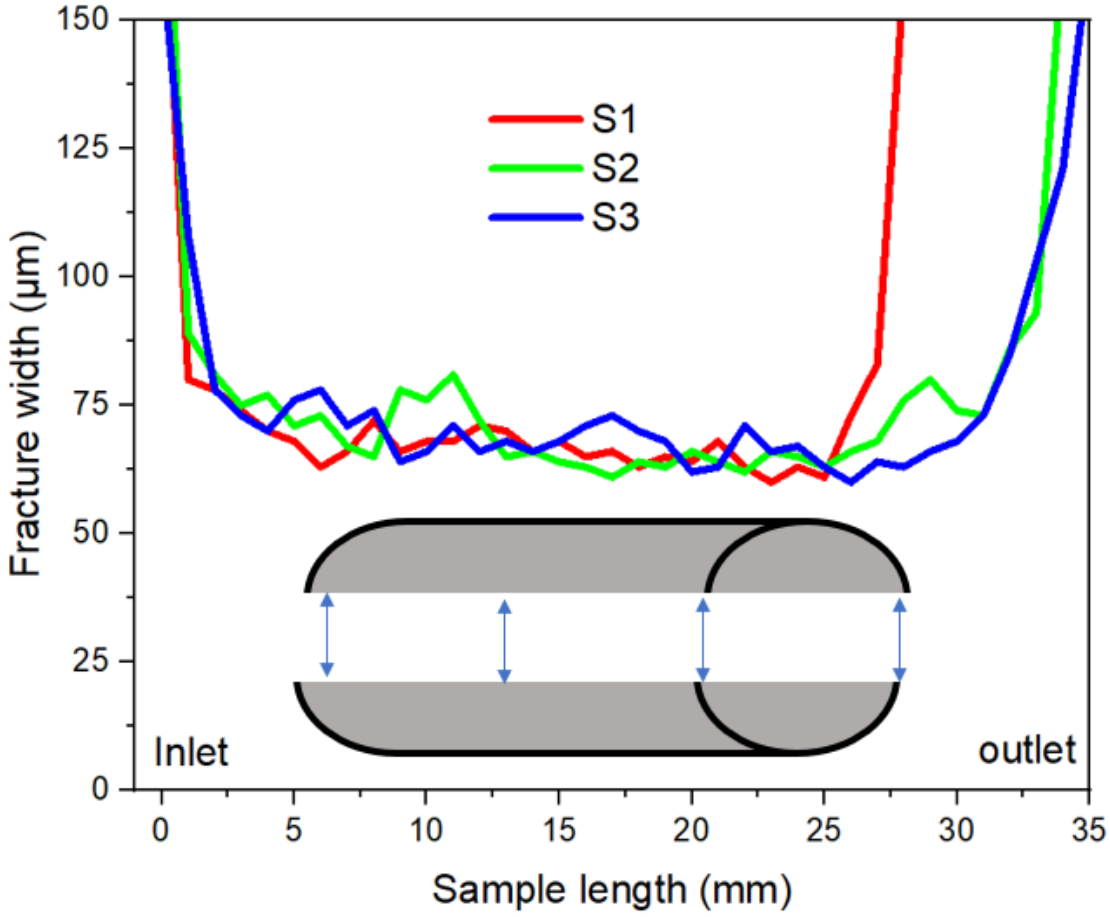

Figure 4-10: Distribution of the narrowest fracture gap size along the sample length – Fracture space was generated using 150 micron thick shims.

4.4.1.3 Sample Imaging after Conducting the Squeeze Cementing Experiments

Figure 4-11 shows pictures of both the inlet and outlet sides of the sample after the squeeze experiments. The cement slurry was squeezed into the fracture space and allowed to cure for a period of 22 hours (at a pressure of 300 psi and a temperature of 20°C). After curing the sample was taken out and imaged using CT-Scan.

For sample 1 (S1), Class G blend was used for squeezing experiment where cement bridging was observed at the inlet side and no cement slurry was observed on the outlet side, indicating that the cement could not penetrate the entire fracture space when squeezing with the class G cement (Figure 4-11-Top row). For sample 2 (S2), Portland limestone cement was used for squeezing experiment where the cement slurry had fully penetrated the sample and some excess slurry was observed at the outlet side of the sample (Figure 4-11-Middle row). For sample 3 (S3) Microfine cement was used for squeezing experiment where excess cement slurry was observed at the outlet side, indicating that the cement had penetrated the entire length of the fracture (Figure 4-11-Bottom row). On the inlet side, the microfine cement adhered to the sample surface more than any other blend. This excess cement on the inlet side formed a dome shape which was polished down into a flat surface as seen in Figure 4-11 (Bottom row).

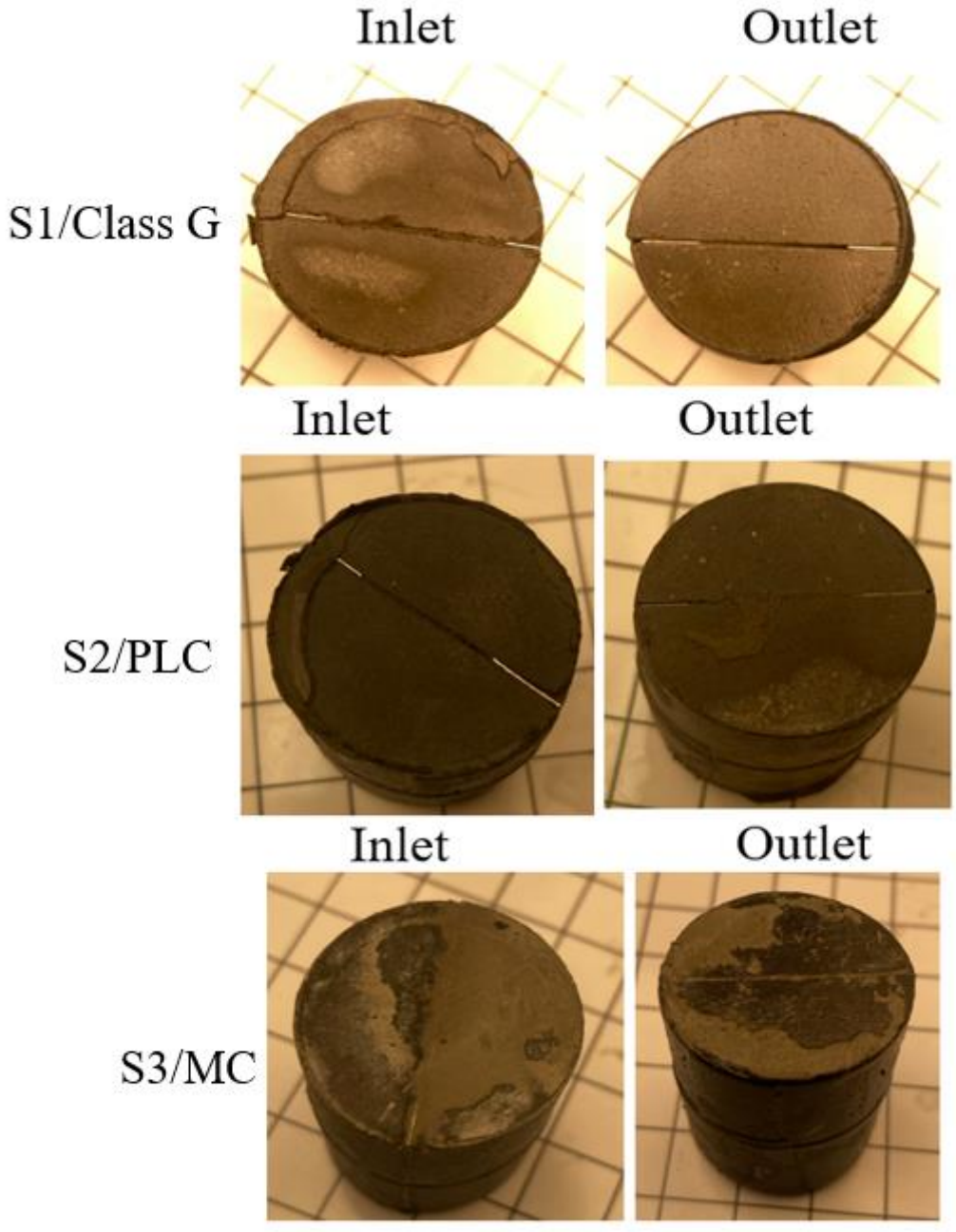

Figure 4-11: Inlet and outlet sides of all the samples after squeeze experiments (150 μm shim), Class G (top), Portland limestone (middle), microfine cement (bottom).

4.4.1.4 2D CT-Scanning Images of the Samples after Squeeze

The original two-dimensional scan is shown in Figure 4-12. The dark areas in Figure 4-12 represent the void space (i.e. fracture space), the light grey to dark grey areas represent the injected cement slurry and the white areas seen on the edge of the sample are the shim stocks. For sample 1, class G cement was injected into the fracture space and the injected slurry filled the void spaces in patches and in a fingering manner as seen in Figure 4-12-Left. The injected slurry appears to fill the fracture uniformly for the first 4 mm and then is deposited in a fingering manner and as a filtrate for the next 18mm. For sample 2, Portland limestone cement was injected into the fracture space and the sample was filled uniformly. For sample 3, microfine cement was injected into the fracture space and the sample was filled uniformly.

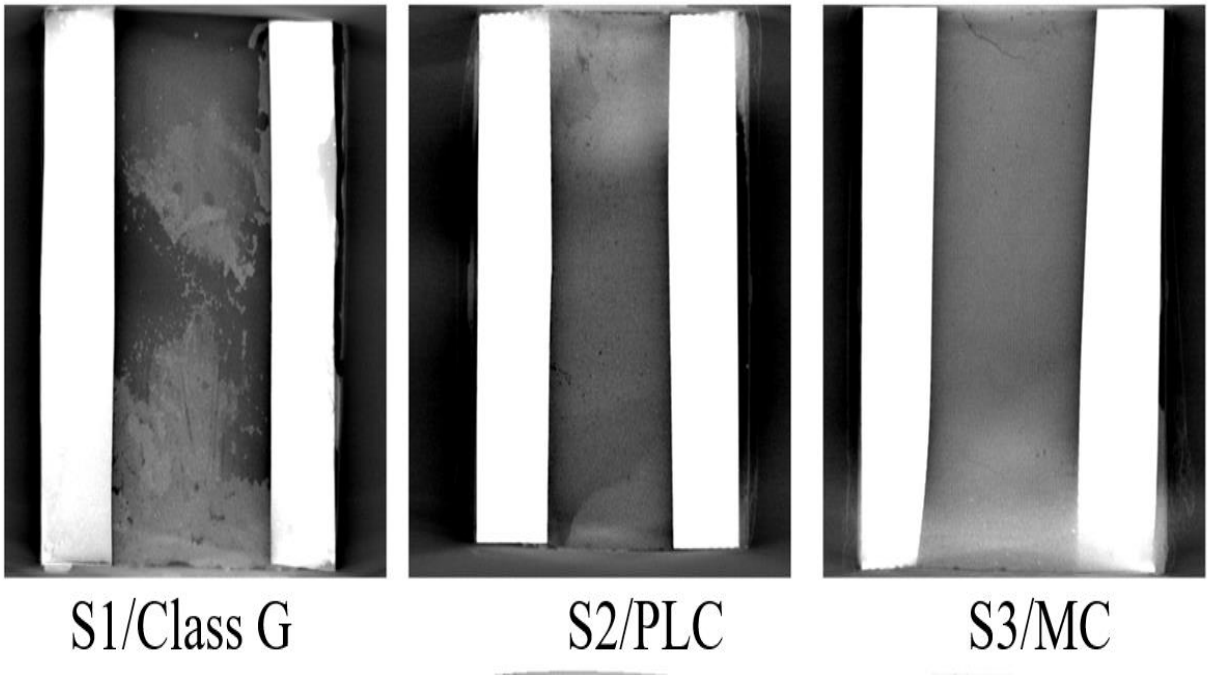

Figure 4-12: 2D slice across the fracture surface (axial direction) showing the injected slurry pathways.

4.4.1.5 3D CT-Reconstruction of the Samples after Squeeze

3D models of the samples were built to visualise the slurry penetration pathways for all three experiments. Figure 4-13 shows the CT rendering results. The red colour indicates the shim stocks, the green colour indicates void spaces (i.e. fracture) and the grey colour represents the injected slurry. From the CT rendering results, it can be seen that the PLC (Figure 4-13-Middle) and the MC (Figure 4-13-Right) filled the entire fracture space whereas the class G cement only filled about a quarter of the fracture space

Artifacts in the form of a green strip could be seen close to the shim stock (S2/PLC). These artifacts formed as a result of the high-density shim stocks absorbing most of the X-rays that were being emitted by the source. As most of the X-rays were being absorbed, a shadow was cast just behind the shim stock. This shadow was then shown as a void space (modelled in green) that was not filled during squeezing. Due to the presence of artifacts in the data, the 3D models are used just to establish a general trend and no quantitative assessments can be made.

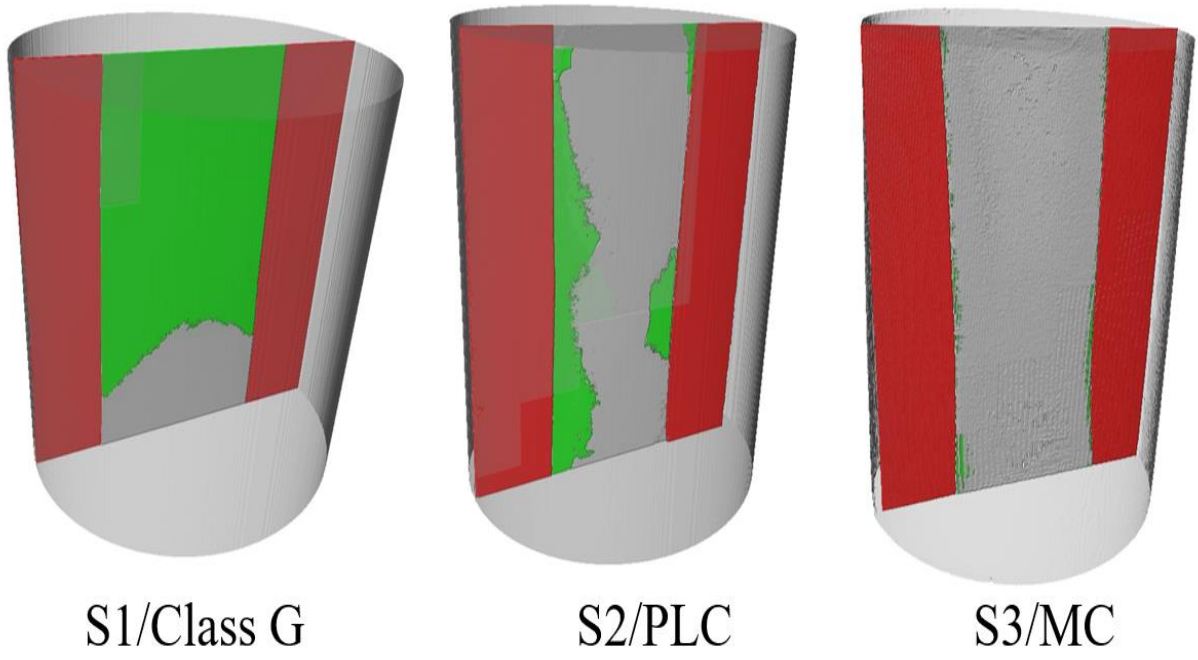

Figure 4-13: CT rendering of the cement slurry pathways

4.4.1.6 Remediated Fracture Conductivity

Figure 4-14 compares the fracture conductivity of the remediated samples. The conductivity of the fracture was initially high, but as the experiment progressed, the flow rates of all the samples declined until it stabilized. Water breakthrough was observed during the experiment for all the samples. Initially, the water flow rate (used as a measure of conductivity) was relatively high. At the start of the experiment, the cement was at a low point in terms of total volume, and with access to a continuous stream of water, the cement is expected to rehydrate and expand, counteracting the shrinkage effect of the setting cement, this caused further plugging of the fracture by squeezed cement and, as a result, the conductivity of the sample across the plug became lower over time.

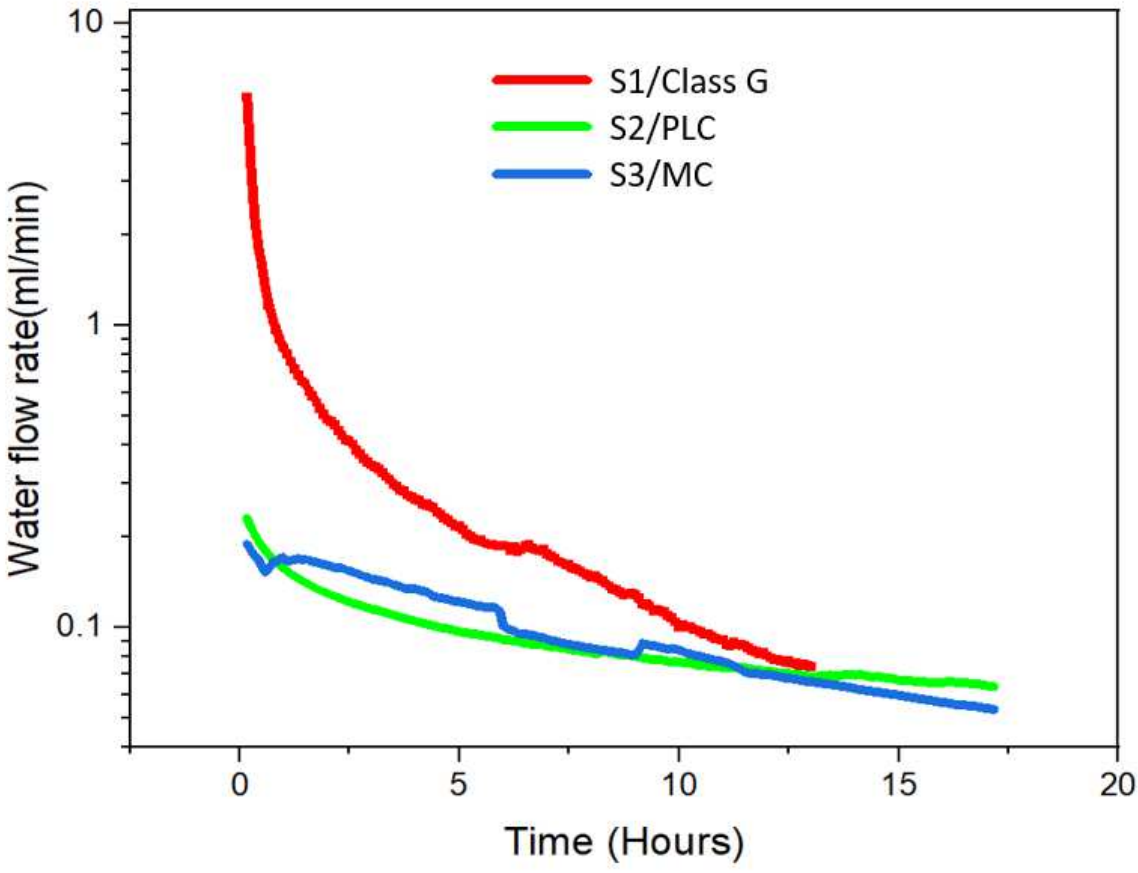

Figure 4-14: Water flow rate comparisons of the remediated samples measured at an injection pressure of 300 psi and a confining pressure of 400 psi

Table 4-4 summarizes the fracture conductivity results of the open fracture and the remediated fractures. It was observed that the microfine cement performed the best (i.e. exhibited lowest conductivity) among all the samples.

Sample	Injected slurry	Conductivity before remediation ml/min/MPa.	Conductivity after remediation ml/min/MPa.
S1	Class G	834	0.036
S2	PLC	842	0.032
S3	MC	852	0.01

Table 4-4: Fracture conductivity results

4.4.1.7 Opening the Remediated Cement Core and Comparing the Remedial Cement Penetration Performance

After testing the conductivity of the sample, the half cores were opened up to physically observe the cement slurry pathways. Figure 4-15 shows the cement slurry pathways for all three experiments carried out using the 150-micron shim stock.

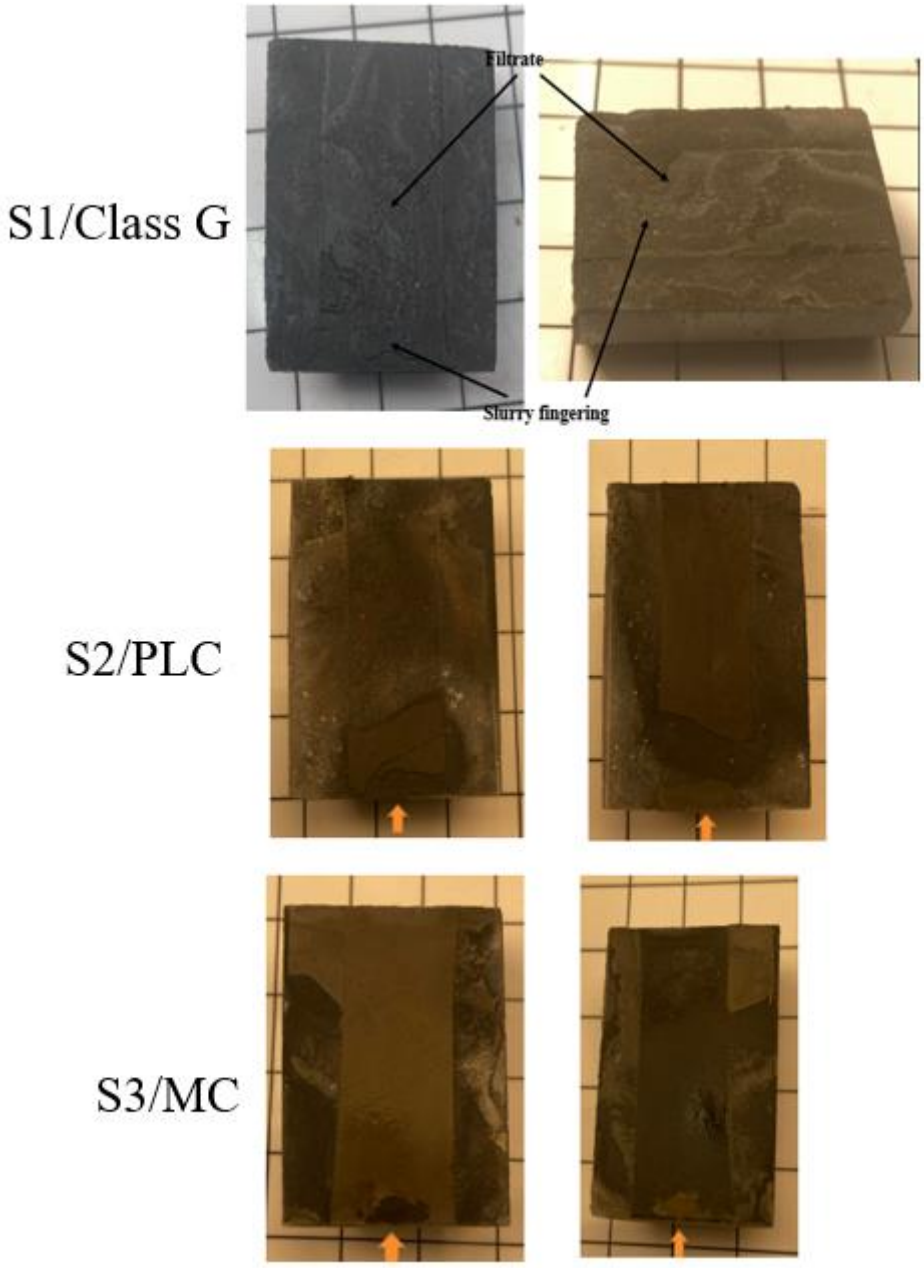

Figure 4-15: Slurry pathway for all the squeeze experiments (150 μm shim), S1 (Class G), S2 (Portland Limestone cement), S3 (Microfine cement).

Figure 4-15 shows how the fracture size varies at the inlet of the sample. The fracture width at the inlet ranged from 150 to 200 microns.

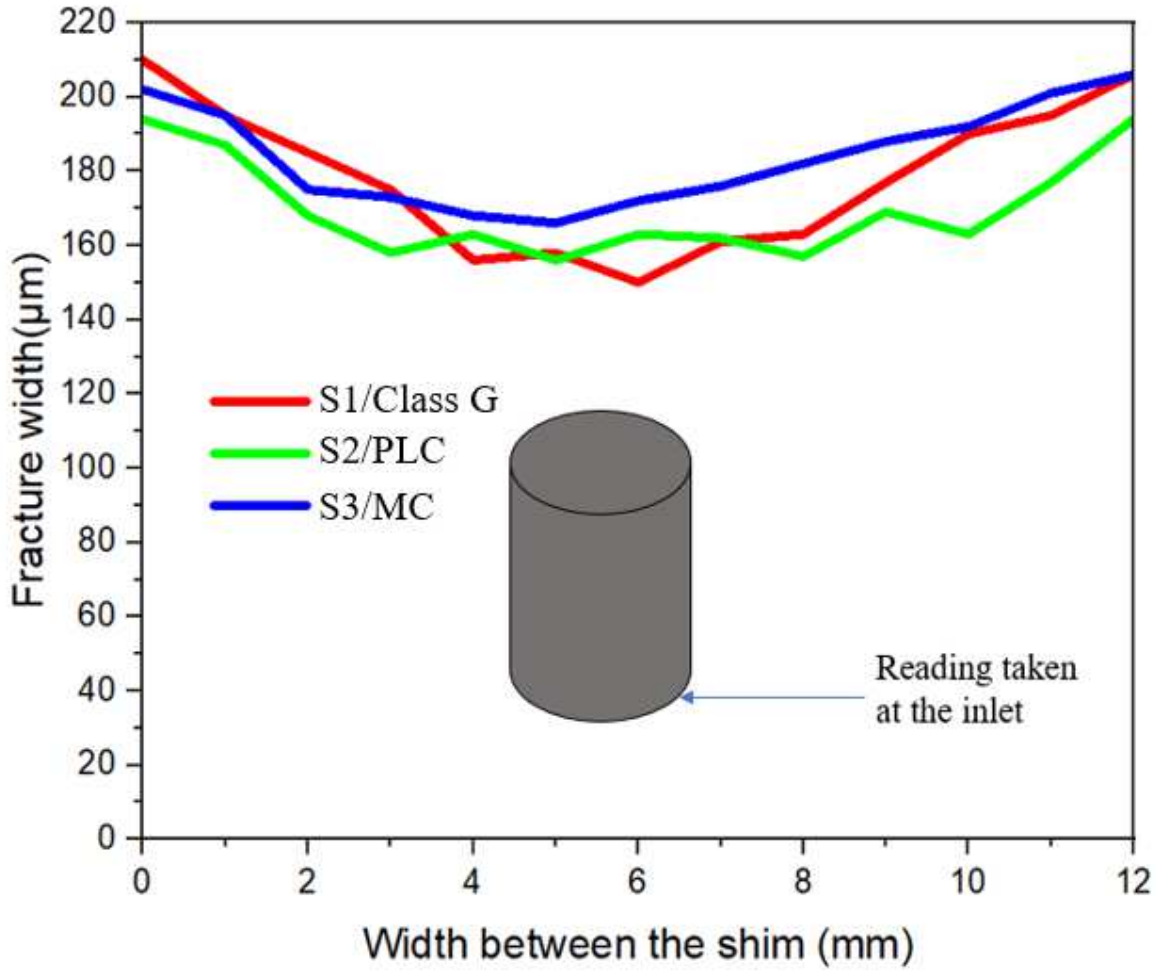

Figure 4-16: Fracture width variation at the inlet side of the cement samples. S1 (Class G), S2 (Portland limestone cement), S3 (Microfine cement).

Cement bridging was observed at the inlet of the sample when the squeeze experiments were carried out using class G cement slurry (Figure 4-15-top). The slurry pathway taken by the class G cement was non-uniform and followed a fingering pattern. It was also seen that the Portland limestone cement slurry (Figure 4-15-middle) and the Microfine cement slurry (Figure 4-15-bottom) were able to penetrate the fracture space at the inlet.

Figure 4-17 shows how the fracture width changes 8 mm from the inlet of the sample. Pictures of the opened up half cement samples indicate that Portland limestone cement slurry (Fig.4-15-middle) and the Microfine cement slurry (Figure 4-15-bottom) were able to penetrate up to the narrow points (~70 μm) without bridging (8mm from the inlet). At this point, however, the class G sample was no longer deposited in a fingering pattern, but it appeared as a filtrate. Small particles of class G cement could be seen, completely disconnected from the main body of the cement slurry, which was initially deposited in a fingering pattern.

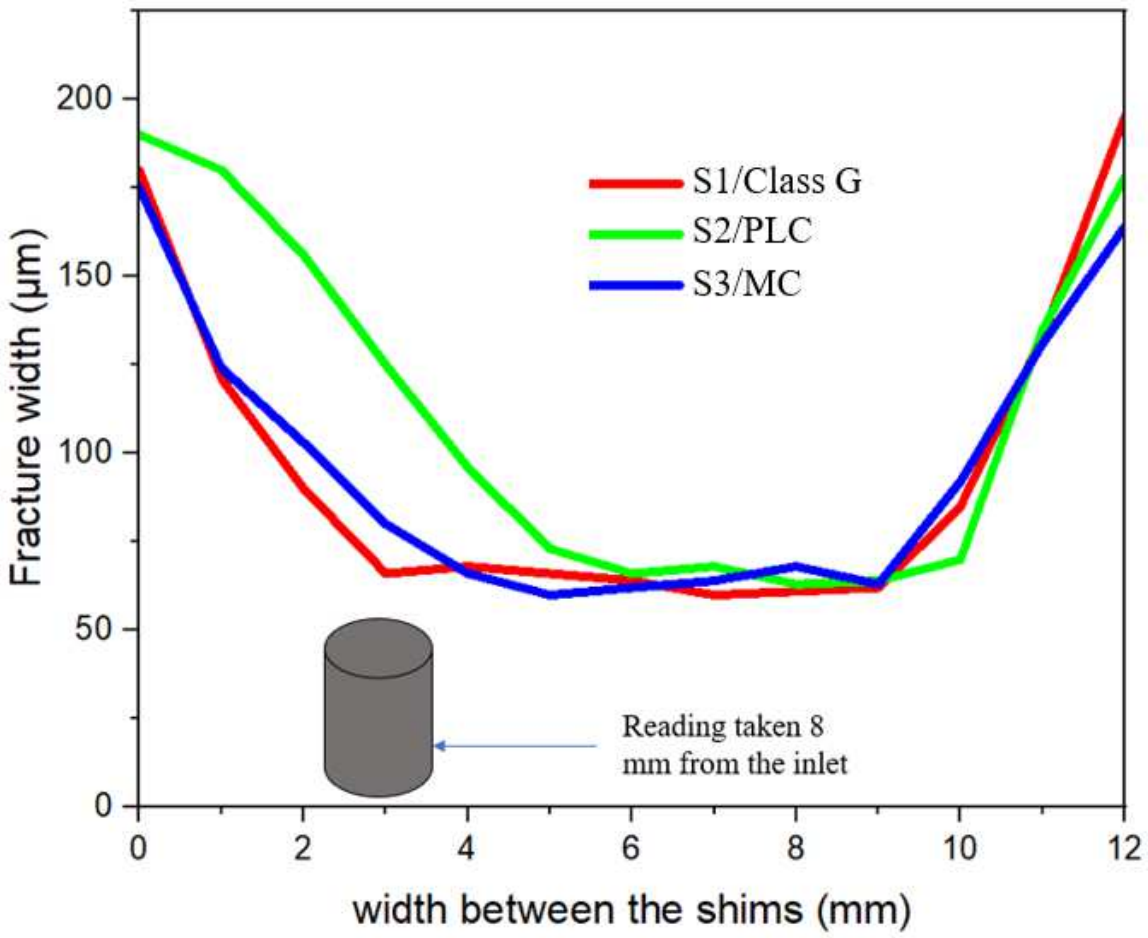

Figure 4-17: Fracture width distribution 8 mm from the inlet. S1 (Class G), S2(Portland limestone cement), S3(Microfine cement).

Figure 4-18 shows how the fracture width changes at the outlet of the samples. Cement breakthrough was observed for both the Portland limestone cement slurry and the Microfine cement slurry. However, no cement was observed at the outlet side of the sample remediated with class G cement. Overall, the results from this experiment showed that the Portland limestone cement and the Microfine cement was capable of remediating a micro annuli or micro fractures as small as 70 microns. The class G cement was unable to remediate fracture, which have a gap size as large as 200 microns. Note that although 150 micron thick shims were used in these experiments, fracture width of 200 microns were observed at the outlet of the fractured cement samples, due to the irregularity (rugosity) of the cement surface.

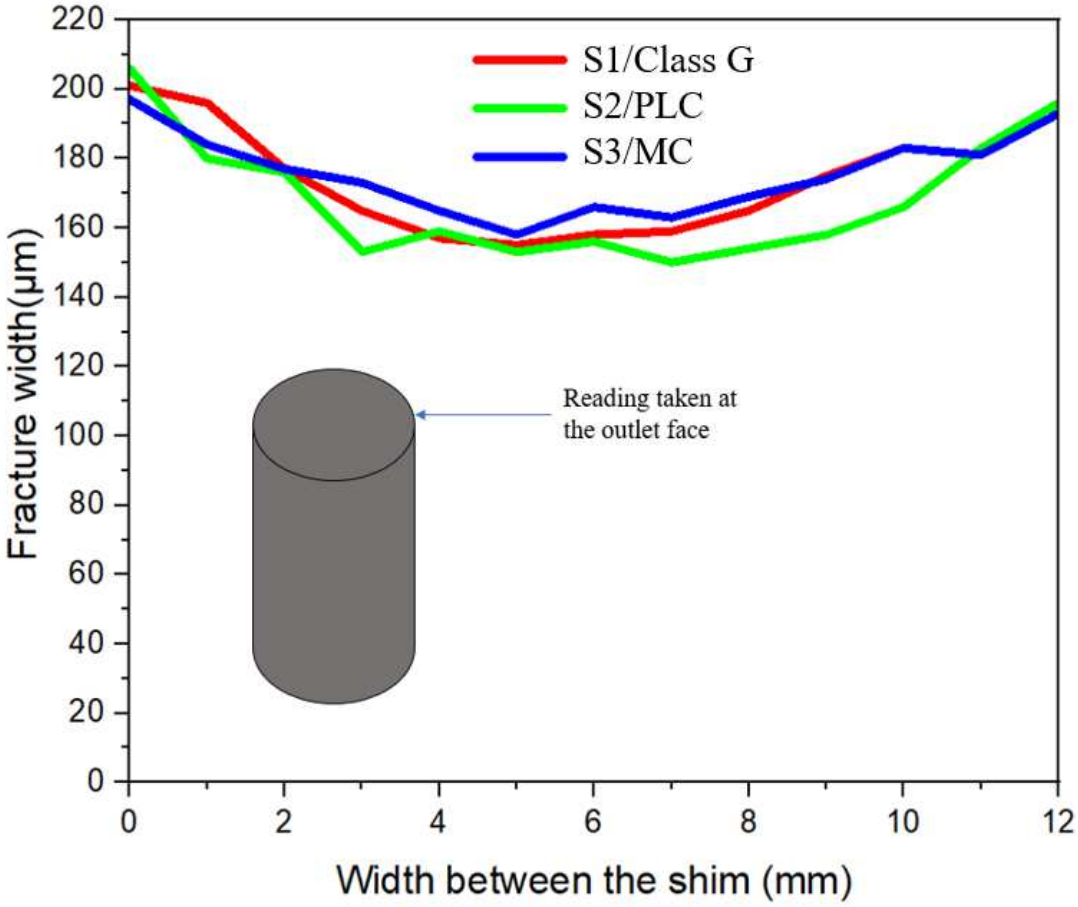

Figure 4-18: Fracture width distribution at the outlet side. S1 (Class G), S2 (Portland limestone cement), S3 (Microfine cement).

4.4.2 Squeeze Cementing Experiments using the 100 µm Shim

4.4.2.1 Open Fracture Conductivity of all the Samples

The first step of the experiments was to measure the conductivity of the open fracture. Three samples were prepared using 100 µm shims. Figure 4-19 shows the open fracture conductivity of the sample using a variable flow rate at a confining pressure of 400 psi. The conductivity of all three samples were similar and the average fracture conductivity was calculated as 610 (±20) ml/min/MPa.

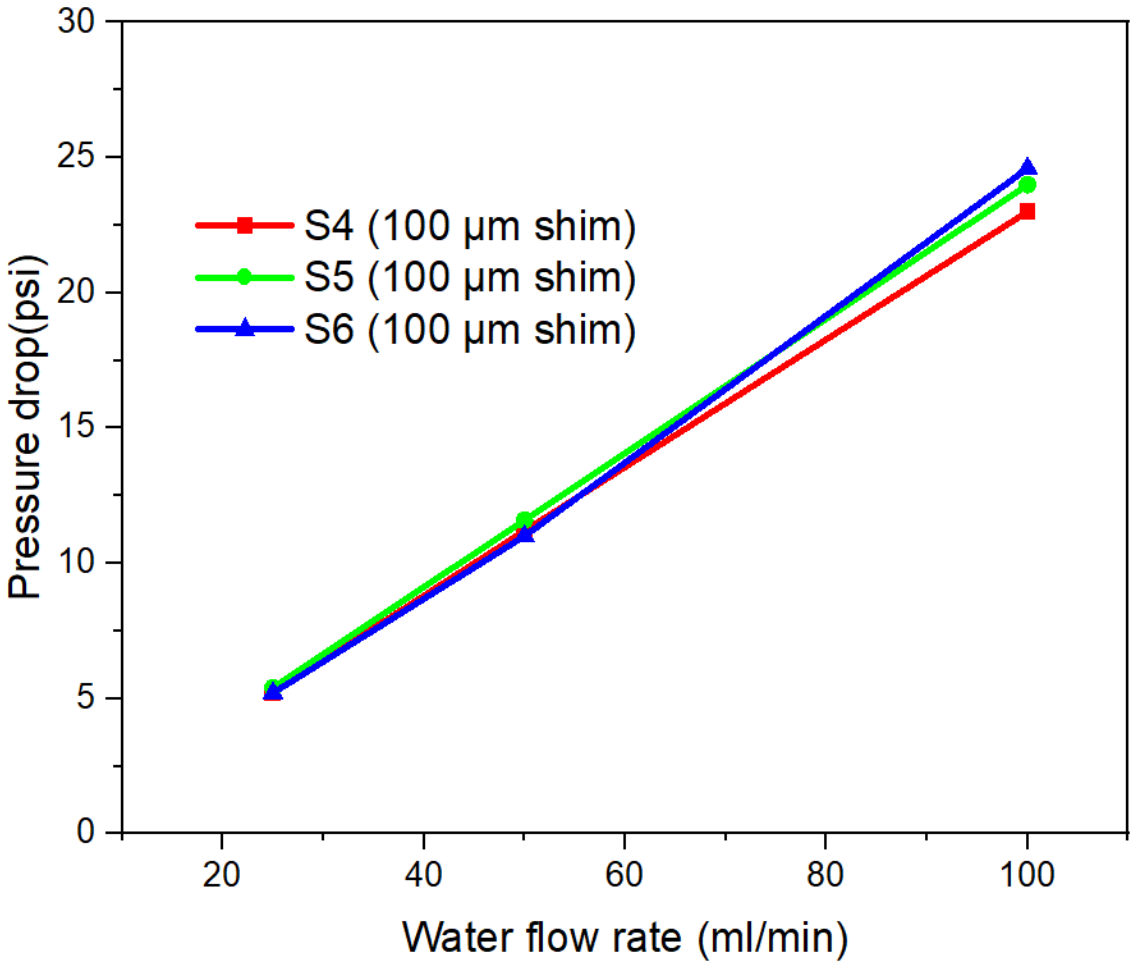

Figure 4-19: Open fracture conductivity of the samples prepared by using 100 µm shims. Conductivity was tested at variable flow rates and at a confining pressure of 400 psi.

4.4.2.2 Fracture Width Determination using the CT Scan Results

After completing the fracture conductivity test, the sample was CT scanned. The following graph (Figure 4-20) shows the fracture width distribution at the narrowest points through (along the longest axis of the sample) the open fracture. Due to the cutting process, a perfectly flat surface could not be achieved. The fracture width for S5 (8-16 mm from the inlet) and S6 (8mm-17 mm from the inlet) fell below our resolution limit of 35µm. The width along these sections were plotted as 35µm, but we could safely assume that the fracture width was below this limit. Fracture width varied between <35 micron to 140 micron, indicating the rugosity of the cement surfaces in the fracture. Fracture width distribution was very similar in all 3 samples, providing a relatively good confidence level for the suitability of the fracture generation method for the purpose of the squeeze cementing experiments.

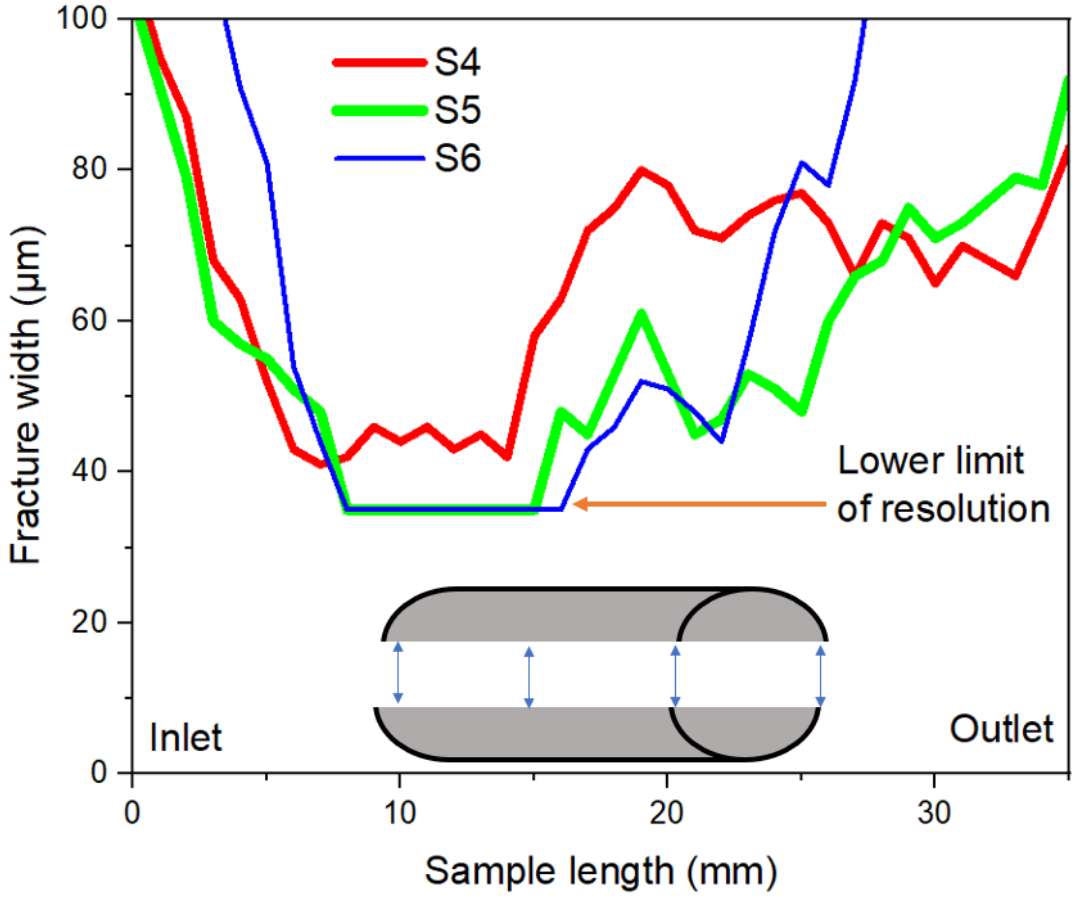

Figure 4-20: Distribution of the narrowest fracture gap size along the sample length – Fracture space was generated using 100 micron thick shims.

4.4.2.3 Sample Imaging after Conducting the Squeeze Cementing Experiments

Figure 4-21 shows pictures of both the inlet and outlet sides of the sample after the squeeze experiments. The cement slurry was squeezed into the fracture space and allowed to cure for a period of 24 hours at a pressure of 300 psi and room temperate. After curing the samples were taken out and imaged using CT-Scan.

For sample 4 (S4), Class G cement was used for squeezing experiment where, cement bridging was observed on the inlet side of the cement core and no cement slurry was observed on the outlet side, which indicated that the cement could not penetrate the entire fracture space (Figure 4-20-Top row). For sample 5 (S5), Portland Limestone cement was used for squeezing experiments where minor amount of cement bridging was observed at the inlet face of the sample. No cement slurry was observed at the outlet side, which indicated that the cement could not penetrate the entire fracture space (Figure 4-20-Middle row). For sample 6 (S6), Microfine cement was used for squeezing experiment where excess cement slurry was observed at the outlet side of the sample, which indicated that the cement had penetrated the entire length of the fracture. At the inlet side, the microfine cement adhered to the sample surface more than any other blend. This excess cement at the inlet side formed a dome shape which was polished down into a flat surface as seen in Figure 4-20 (Bottom row).

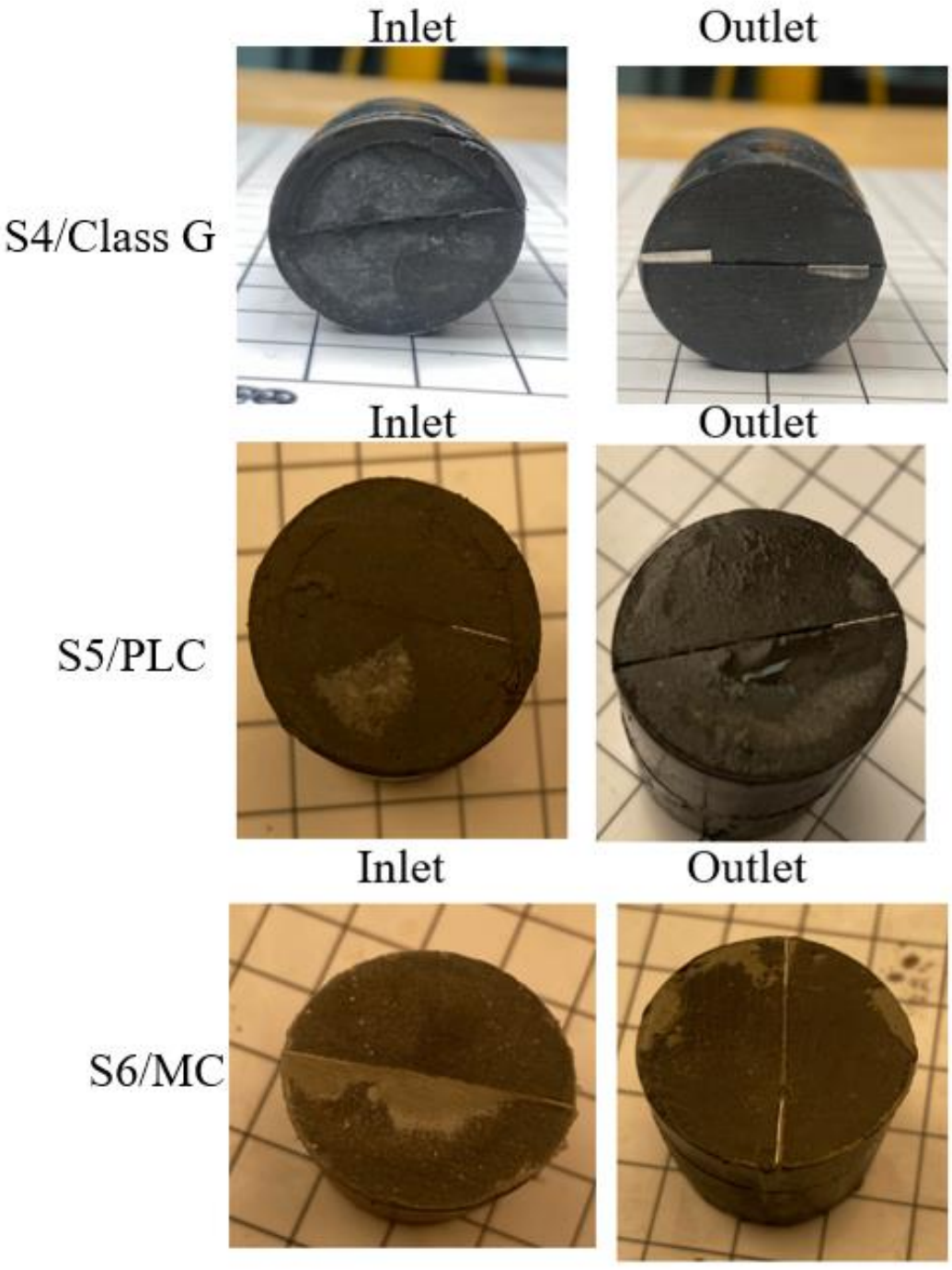

Figure 4-21: Inlet and outlet side of the samples after carrying out squeeze experiments (100 µm shims). Class G (top), Portland limestone (middle), microfine cement (bottom).

4.4.2.4 2D CT-Scanning Images of the Samples after Squeeze

The original two-dimensional scan is shown in Figure 4-22. The dark areas in Figure 4-22 represent the void space (i.e. fracture space), the light grey to dark grey areas represent the injected cement slurry and the white areas seen on the edge of the sample are the shim stocks. For sample 4, class G cement was used for squeezing experiment where bridging was observed at the inlet of the sample, the slurry travelled about 12 mm into the fracture space before coming to halt. For sample 5, Portland Limestone Cement was used for squeezing experiment where some minor bridging was observed at the inlet side of the sample. The injected slurry filled the fracture space uniformly for about 6-7 mm. After 7 mm, the injected slurry was deposited in a fingering pattern for the next 6mm. For sample 6, Microfine cement was used for squeezing experiment where the fracture was filled uniformly and excess cement slurry was observed at the outlet end of the sample.

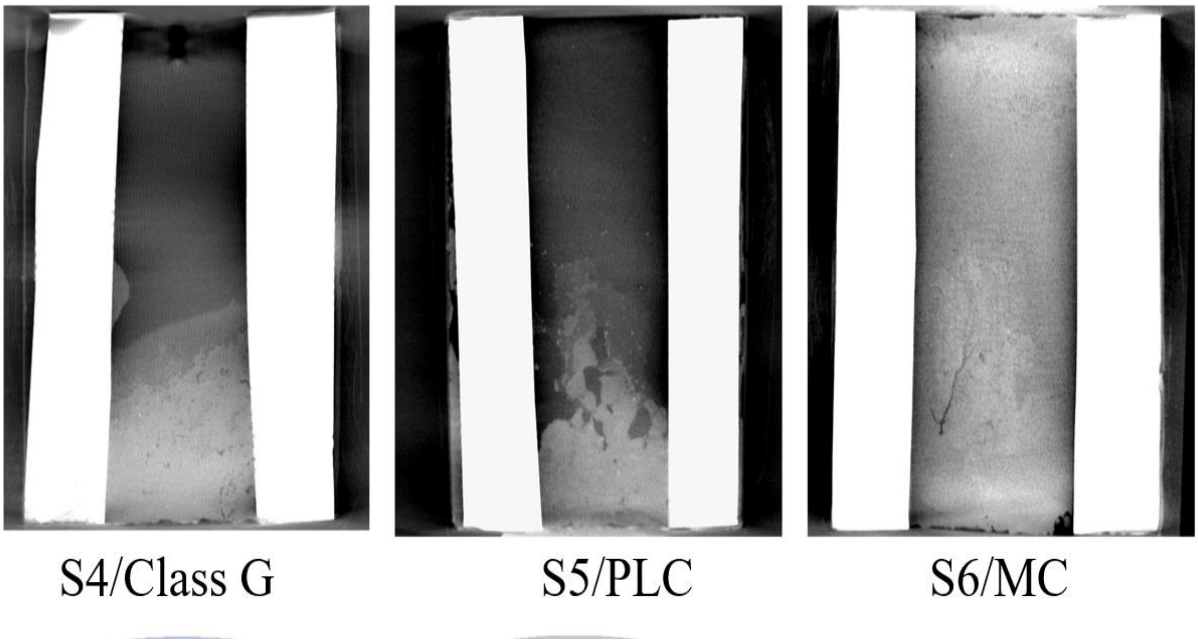

Figure 4-22: 2D slice across the fracture surface (axial direction) showing the injected slurry pathways.

4.4.2.5 3D CT-Reconstruction of the Samples after Squeeze

3D models of the samples were built to visualise the slurry penetration pathways for all three experiments. Figure 4-23 shows the CT rendering results. The red colour indicates the shim stocks, the green colour indicates void spaces (i.e. fracture) and the grey colour represents the injected slurry. From the CT rendering results, it can be seen that only the MC (Figure 4-23-Right) filled the entire fracture space. PLC cement filled about a quarter of the fracture space (Figure 4-23-Middle) whereas the class G could not penetrate into the fracture.

Artifacts in the form of a green strip could be seen close to the shim stock (S6/MC). These artifacts formed as a result of the high-density shim stocks absorbing most of the X-rays which were being emitted by the source. Due to the presence of artifacts in the data, the 3D models are used just to establish a general trend and no quantitative assessments can be made.

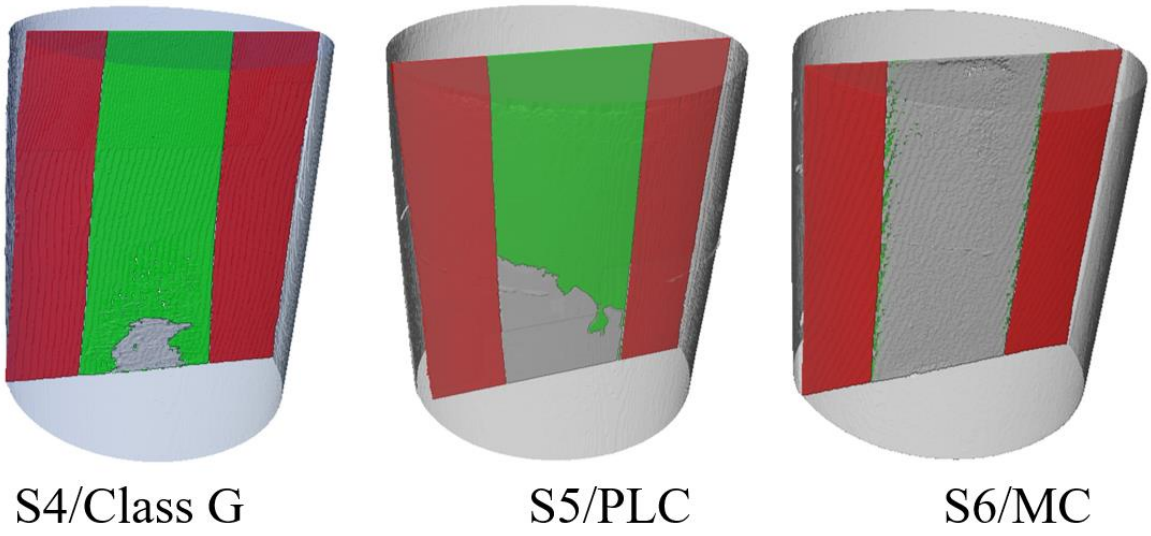

Figure 4-23: CT rendering of the cement slurry pathways.

4.4.2.5 Remediated Fracture Conductivity

From Table 4-5 it could be seen that the open fracture conductivity of all 3 samples were very similar. Figure 4-24 compares the fracture conductivity of the remediated sample. After remediation, the fracture conductivity of sample 6 was the lowest. The microfine cement was able to penetrate the entire fracture and seal off gaps as small as 35 microns. The sealing performance of the Portland limestone was the worst. Even though it was able to penetrate further into the sample, its sealing capabilities was not as good as both the class G sample and the microfine sample. The sealing performance of the class G cement was intermediate. Although it was not able to penetrate the fracture as well as the PLC cement, it was able to provide a better seal.

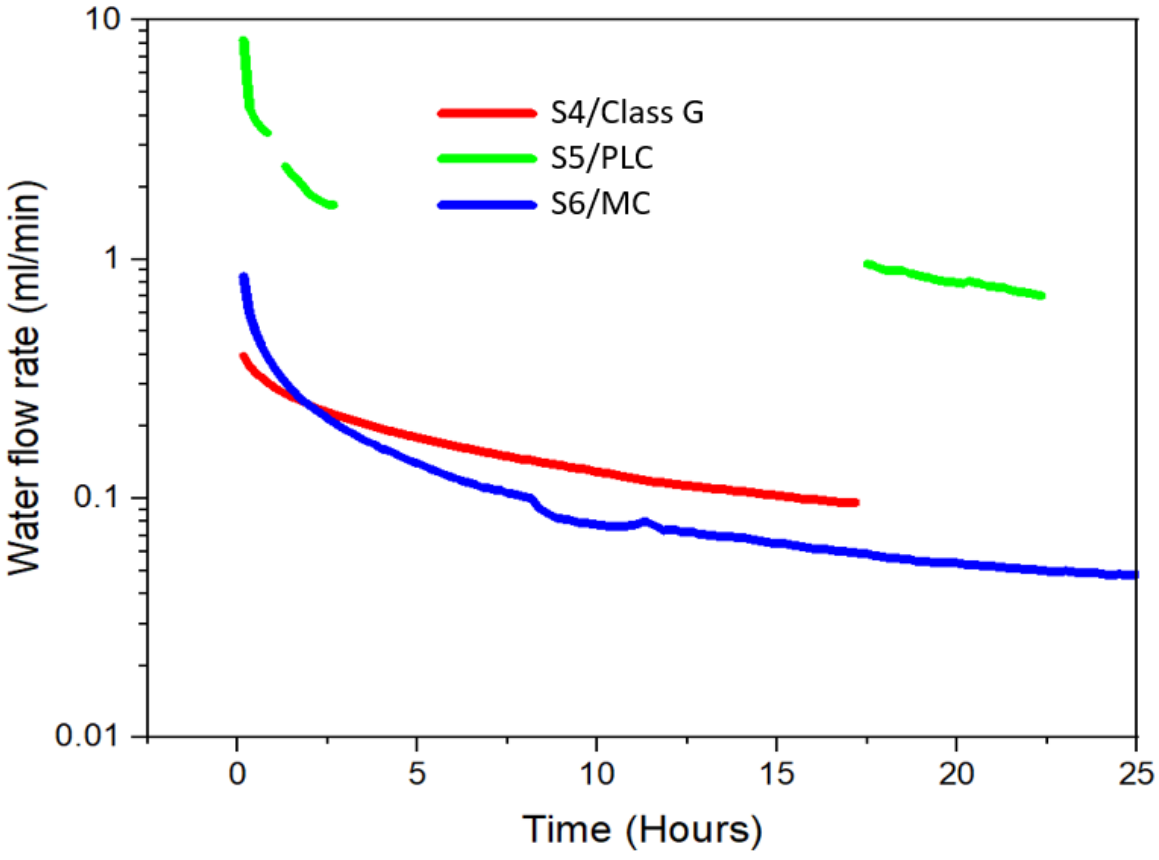

Figure 4-24: Remediated fracture flow rate comparisons measured at an injection pressure of 300 psi and a confining pressure of 400 psi

Sample	Injected slurry	Conductivity before remediation (ml/min/MPa	Conductivity after remediation (ml/min/MPa
S4	Class G	630	0.046
S5	PLC	603	0.33
S6	MC	590	0.01

Table 4-5: Conductivity comparisons of the remediated fractures

4.4.2.6 Opening the Remediated Cement Core and Comparing the Remedial Cement Penetration Performance

After testing the conductivity of the sample, the half cores were opened to physically observe the cement slurry pathways. Figure 4-25 shows the cement slurry pathways for all three experiments carried out using the 100-micron shim stock.

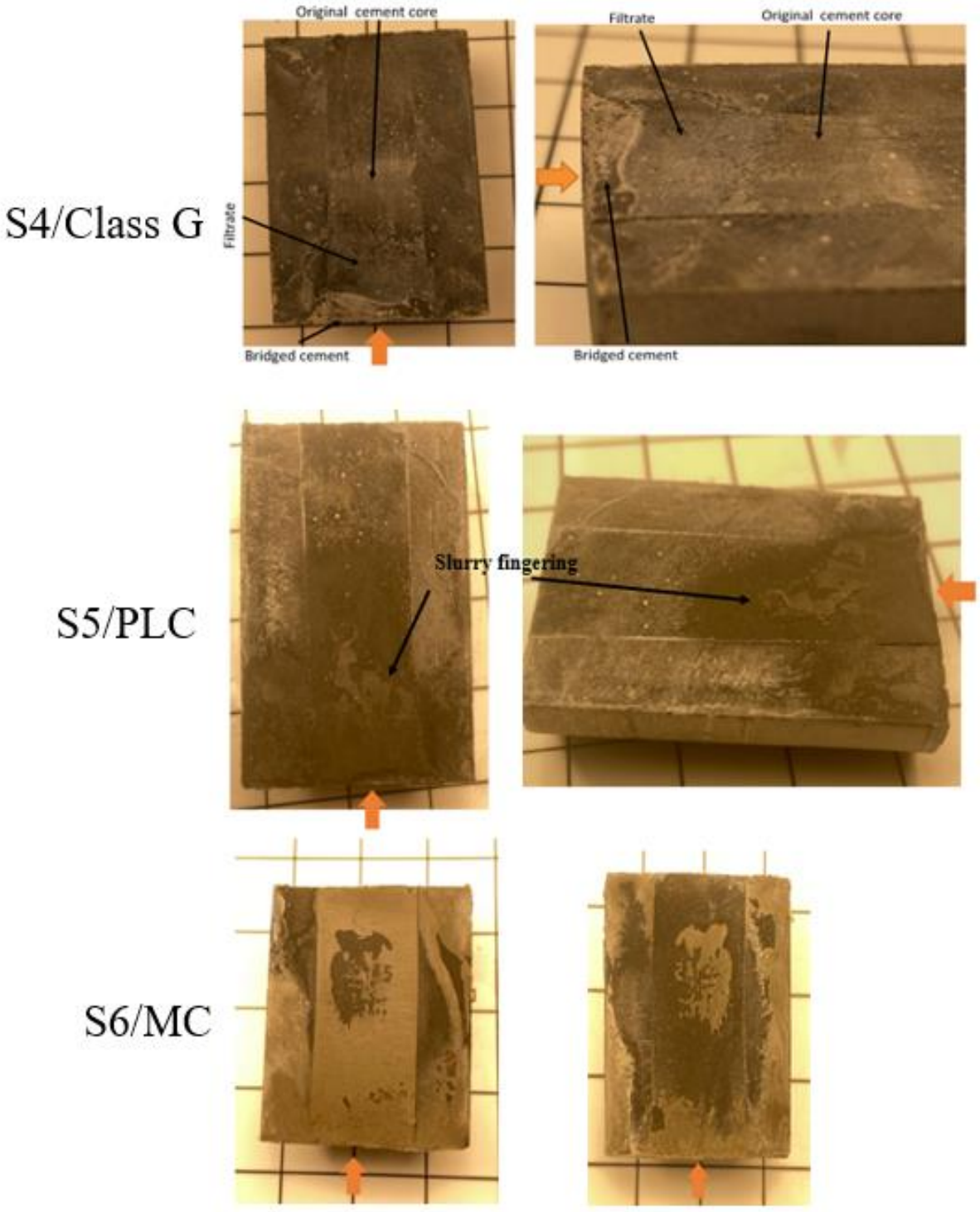

Figure 4-25: Slurry pathway for all the squeeze experiments (100 μm shim), S1 (Class G), S2 (Portland Limestone cement), S3 (Microfine cement).

Figure 4-26 shows the fracture width variation at the inlet of the samples. It could be seen that the fracture width of S6 (MC) was much higher than the fracture width of both S4 (class G) and S5 (PLC) at the inlet. Due to how the samples are cut, differences in the range of 10's of microns could not be controlled. From the squeeze experiments, it was observed that all 3 cement slurries were able to penetrate a fracture width of 120 microns. Very clear bridging was observed with S4 (Fig.4-21-Top). Slight bridging was observed with S5 (Figure 4-21-Middle).

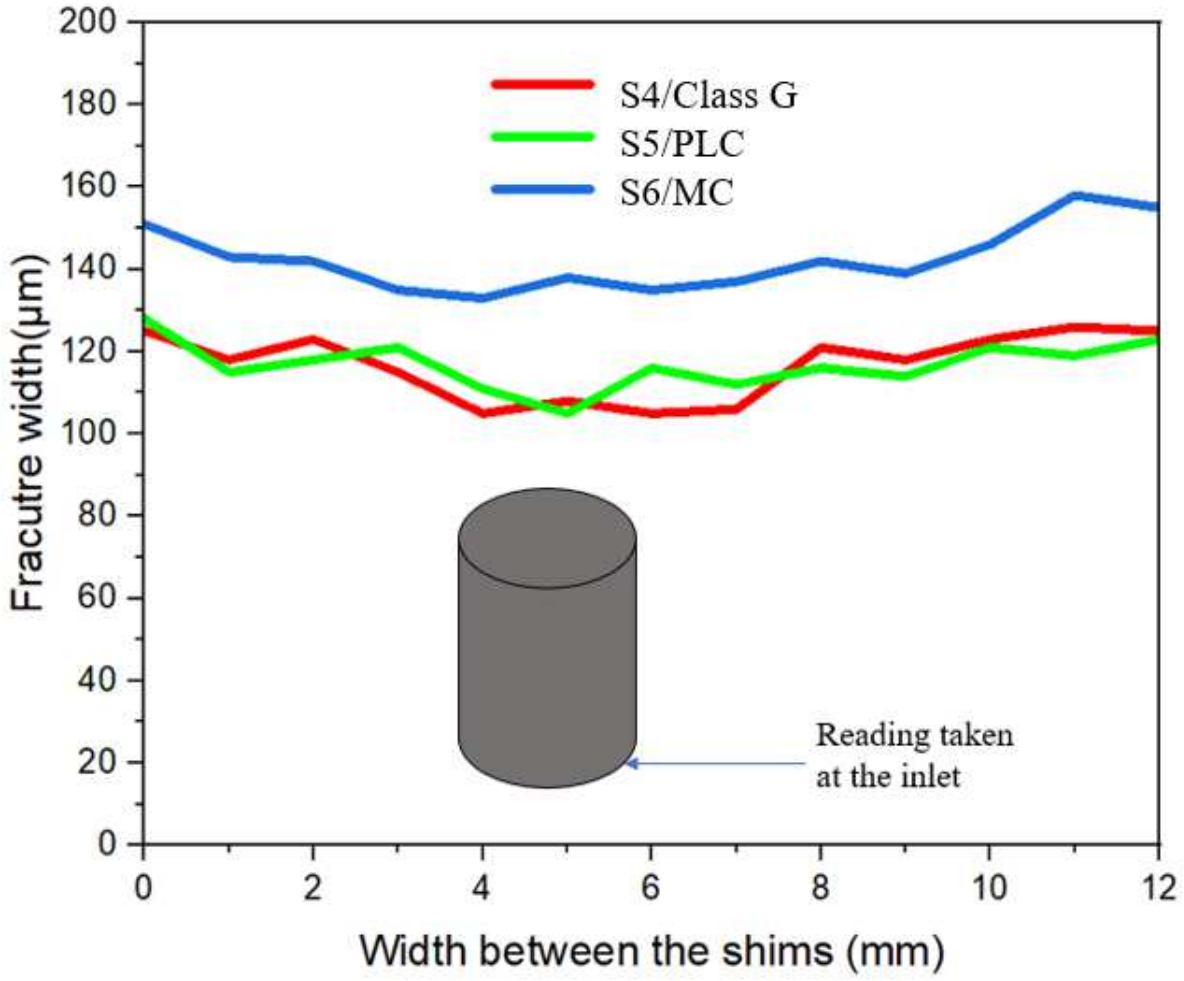

Figure 4-26: Fracture width variation at the inlet of the samples

Figure 4-27 shows the fracture width distribution 2mm from the inlet of the sample. at this location was chosen as this was the point where the Class G cement slurry (S4) stopped flowing and only filtrate particles (Figure 4-25-Top) were allowed beyond this fracture width. At fracture widths of around 90 microns, some filtrate was able to pass through the gap, but majority of the slurry stopped flowing. Portland Limestone cement (Figure 4-25-Middle) and microfine cement (Figure 4-25-Bottom) was able to flow through this gap without any issues.

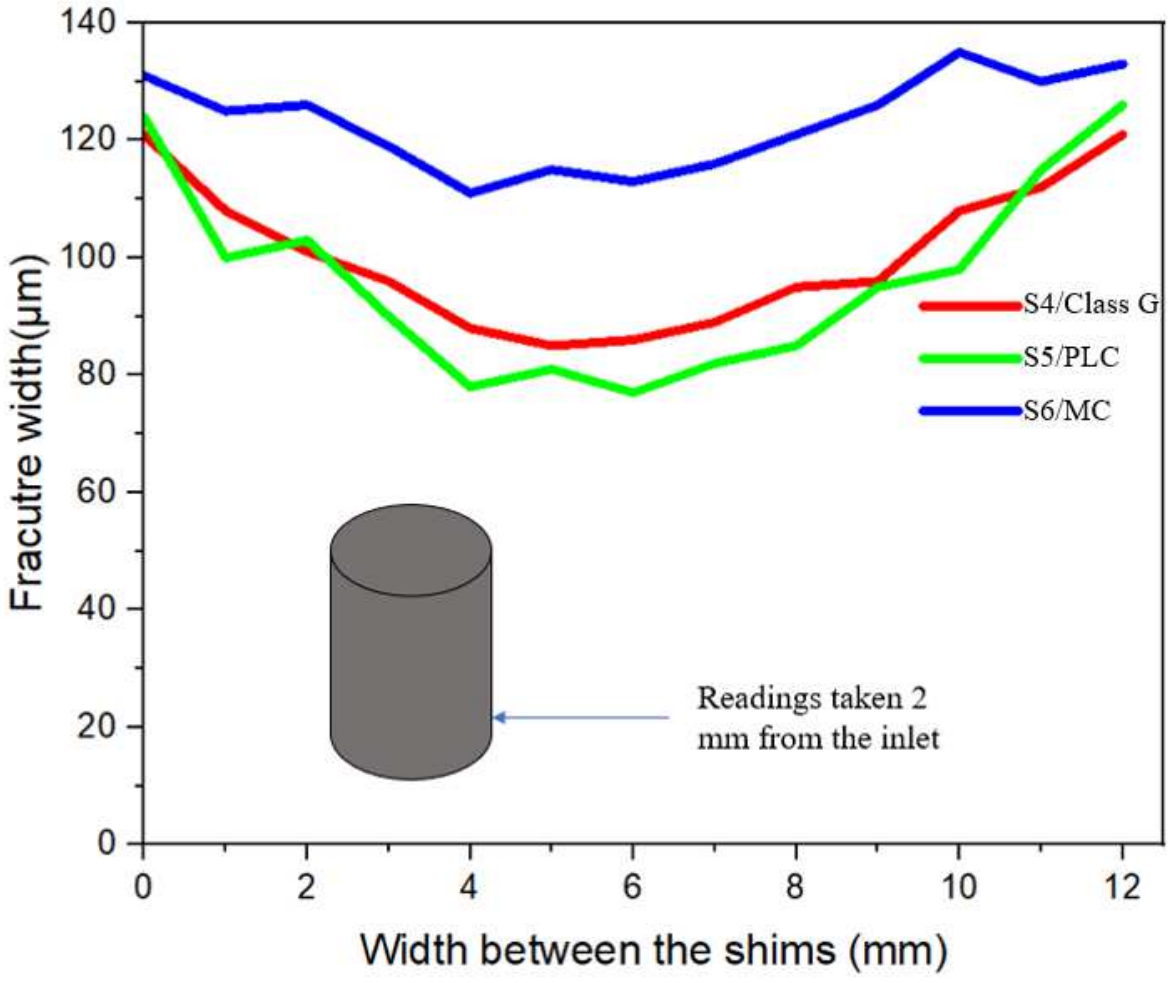

Figure 4-27: Comparison of the fracture width distribution 2mm from the inlet of the sample

Figure 4-28 shows the fracture width distribution 10 mm from the inlet of the sample. This location was chosen for two reason. This was the location at which the filtrates associated with the class G slurry stopped flowing (Figure 4-25-Top). Either the filtrate was too dehydrated to penetrate the fracture any further or the particle size of the filtrate was too large to fit into a gap size of 45 microns. At this locality in sample 5 (Figure 4-25-Middle), the Portland limestone slurry was deposited in a fingering pattern. At a fracture width below the resolution limit of 35 microns, the Portland limestone was not able to penetrate further into the sample. No obvious signs of bridging were observed in S5, but the transition from a plug flow to a fingering pattern indicated that some filtration and bridging took place. The microfine cement (Figure 4-25-Bottom), however, did not have any issues penetrating a fracture width below our resolution limit (35 microns) and was able to fill the entire fracture.

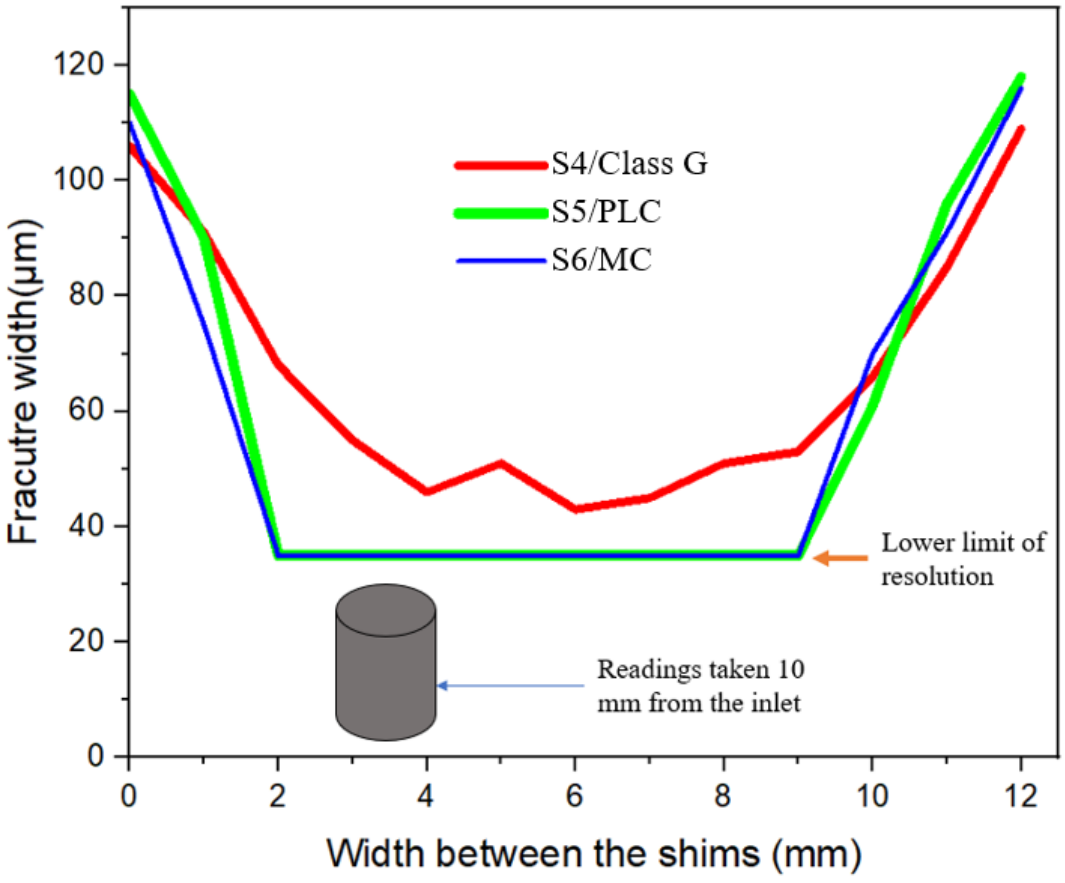

Figure 4-28: Comparison of the fracture width distribution 10 mm from the inlet of the sample.

4.4.3 Squeeze Cementing Experiments using the 50 µm Shim

4.4.3.1 Open Fracture Conductivity of all the Samples

The first step of the experiments was to measure the conductivity of the open fracture. Three samples were prepared using 50 µm shims. Figure 4-29 shows the open fracture conductivity of the sample at a confining pressure of 400 psi with varying flow rates. The conductivity of all three samples varied greatly. It seemed that as we reduced the thickness of the shim, the fracture width was controlled by the sample roughness. It is also possible that at certain sections along the fracture, the half cores may be in contact with each other. The conductivity of S7 was the highest at 207 ml/min/MPa. The conductivity of S8 was 134 ml/min/MPa and the conductivity of S9 was 115 ml/min/MPa.

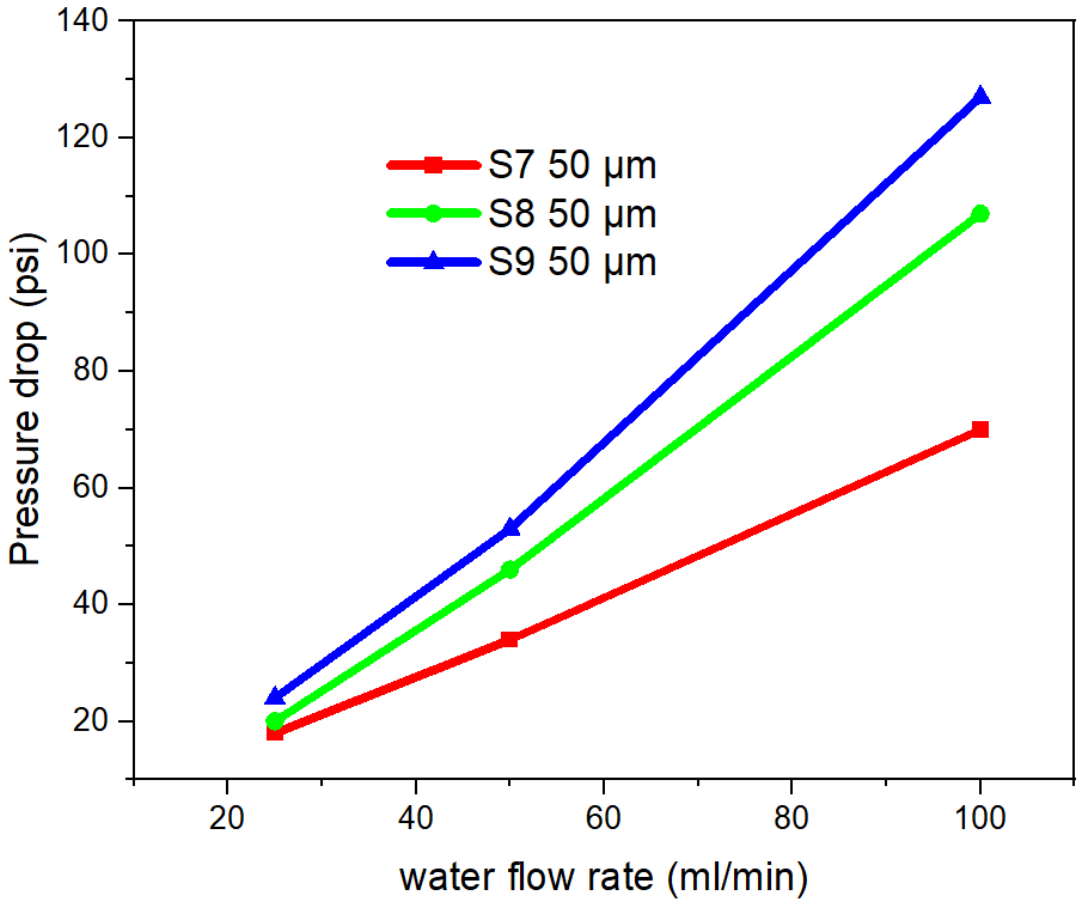

Figure 4-29: Open fracture conductivity of the sample prepared using 50 µm shims. Conductivity was determined by using varying flow rates at a confining pressure of 400 psi.

4.4.3.2 Fracture Width Measurements using the CT Scan Results

We were unable to measure the fracture width of the sample as the fracture width fell below our lower limit of resolution (<35 μm). We tried to insert a feeler gauge of 40 microns (smallest size available) into the fracture space with no success, confirming that the fracture was below our CT detection limit of 35 microns.

4.4.3.3 Sample Imaging after Conducting the Squeeze Cementing Experiments

The cement slurry was squeezed into the fracture space and was allowed to cure for a period of 24 hours at an injection pressure of 300 psi and room temperature. After curing the sample was taken out and imaged. Figure 4-30 shows both the inlet and outlet sides of the sample after squeeze experiments. For sample 7. Class G cement was used to carry out squeeze experiments where cement bridging was observed at the inlet side of the cement core (Figure 4-30-Top). For sample 8, Portland limestone cement was used to carry out squeeze experiments where cement bridging was observed at the inlet side of the cement core (Figure 4-30-Middle). No cement slurry was observed on the outlet side for both sample 7 and 8, which indicated that the cement could not penetrate the entire fracture space. For sample 9, Microfine cement was used to carry out squeeze experiments where the cement slurry was adhering to the inlet side and formed a domed shape. This was polished down to a flat surface as seen in Figure 4-30-Bottom. Due to the adhering nature of the microfine cement, we were unable to determine if bridging had occurred. Some slurry was seen just at the opening of the fracture at the outlet side but unlike other experiments with microfine cement, no excess slurry flowed out of the fracture space.

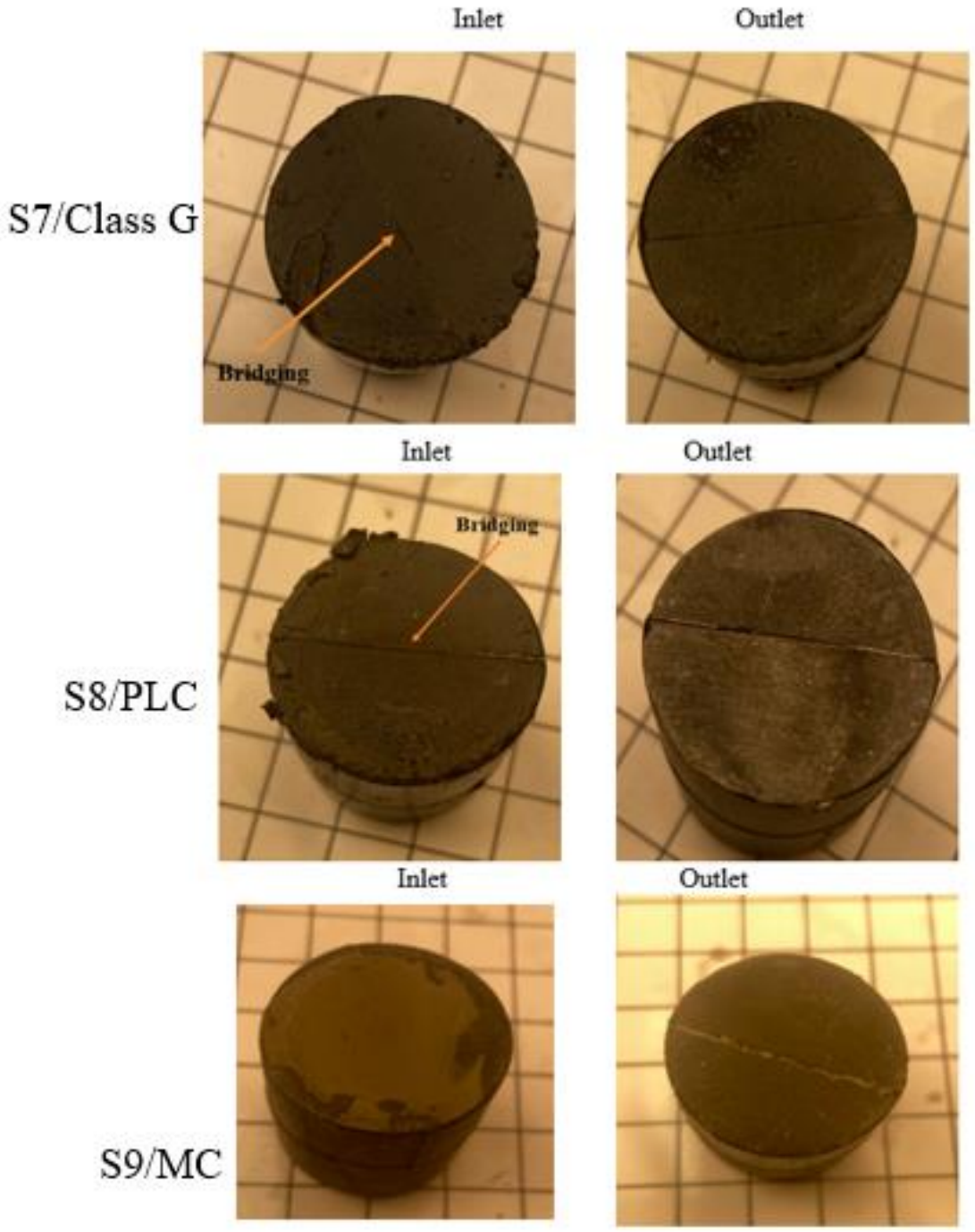

Figure 4-30: Inlet and outlet sides of the samples after carrying out squeeze experiments 50 µm shim

4.4.3.4 2D CT-Scanning Images of the Samples after Squeeze

The original two-dimensional scan is shown in Figure 4-31. The dark areas in Figure 4-31 represent the void space (i.e. fracture space), the light grey to dark grey areas represent the injected cement slurry and the white areas seen on the edge of the sample are the shim stocks

For sample 7, (class G) the slurry was deposited in a fingering manner for about 9 mm before coming to a stop. For sample 8, (PLC) the injected slurry appears to fill the fracture space uniformly for about 8 mm. After 8 mm, the injected slurry was deposited in a fingering pattern and as filtrate for the next 10mm. For sample 6 (MC), the slurry filled the fracture uniformly for about 4mm before coming to an abrupt halt.

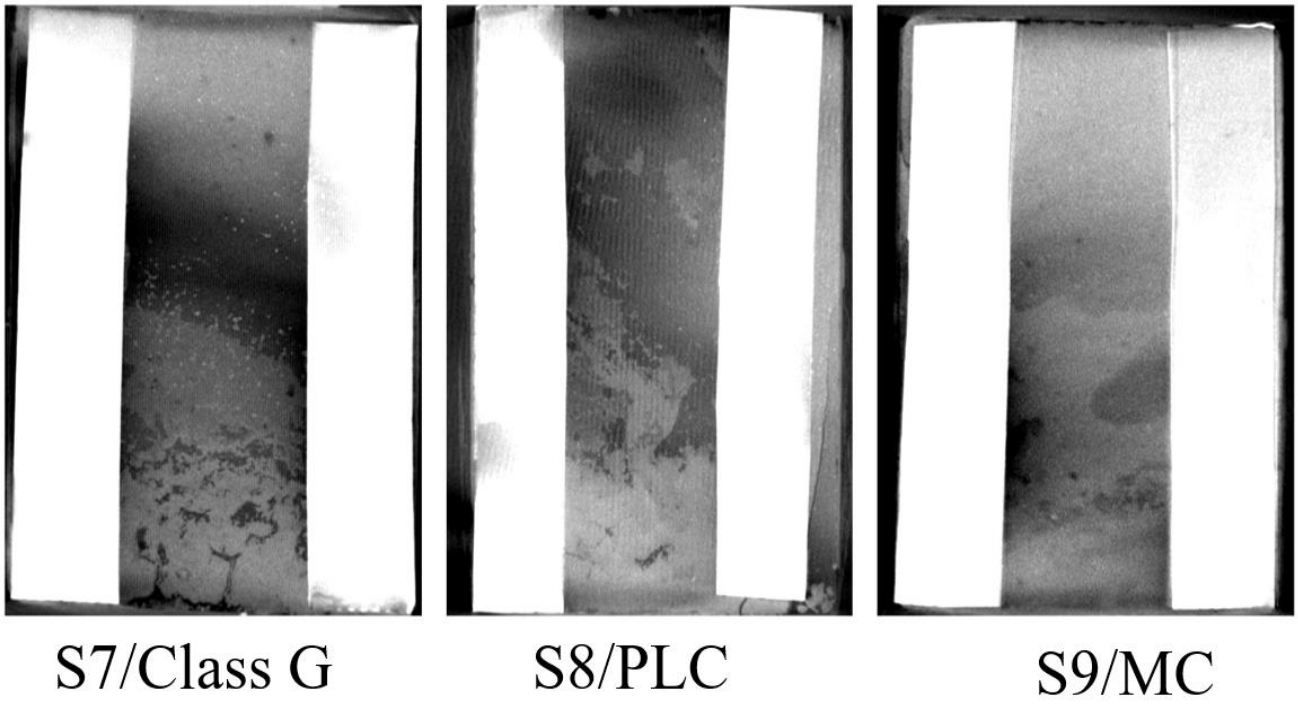

Figure 4-31: 2D slice across the fracture surface (axial direction) showing the injected slurry pathways.

4.4.3.5 3D CT-Reconstruction of the Samples after Squeeze

3D models of the samples were built to visualise the slurry penetration pathways for all three experiments. Figure 4-32 shows the CT rendering results. The red colour indicates the shim stocks, the green colour indicates void spaces (i.e. fracture) and the grey colour represents the injected slurry. From the CT rendering results, it can be seen that none of the slurries were able to penetrate the narrow fracture.

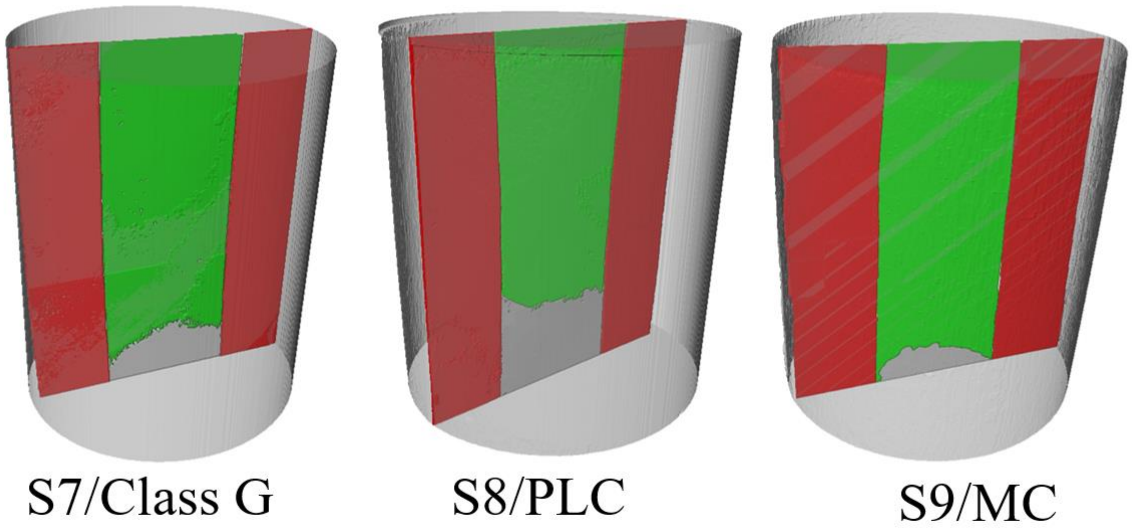

Figure 4-32: CT rendering of the cement slurry pathways

4.4.3.6 Remediated Fracture Conductivity

Figure 4-33 compares the fracture conductivity of the remediated samples. The water flow rates of the Class G cement and the microfine cement were very similar. The conductivity of sample 7 (class G) and 9 (MC) was reduced by four to five orders of magnitude. The water flow rates for the sample 8 remediated with the Portland limestone cement was very high. The gaps in the data represent periods where the pump was empty and no water flooding was taking place. The flow rate did stabilize after 20 hours (experiment time) and the conductivity of the sample was reduced by two orders of magnitude. The water flow rate for the sample remediated with Portland limestone sample was much higher than samples remediated with both the class G and microfine cement. Table 4-6 compares the fracture conductivity of the open fractures versus the remediated fractures.

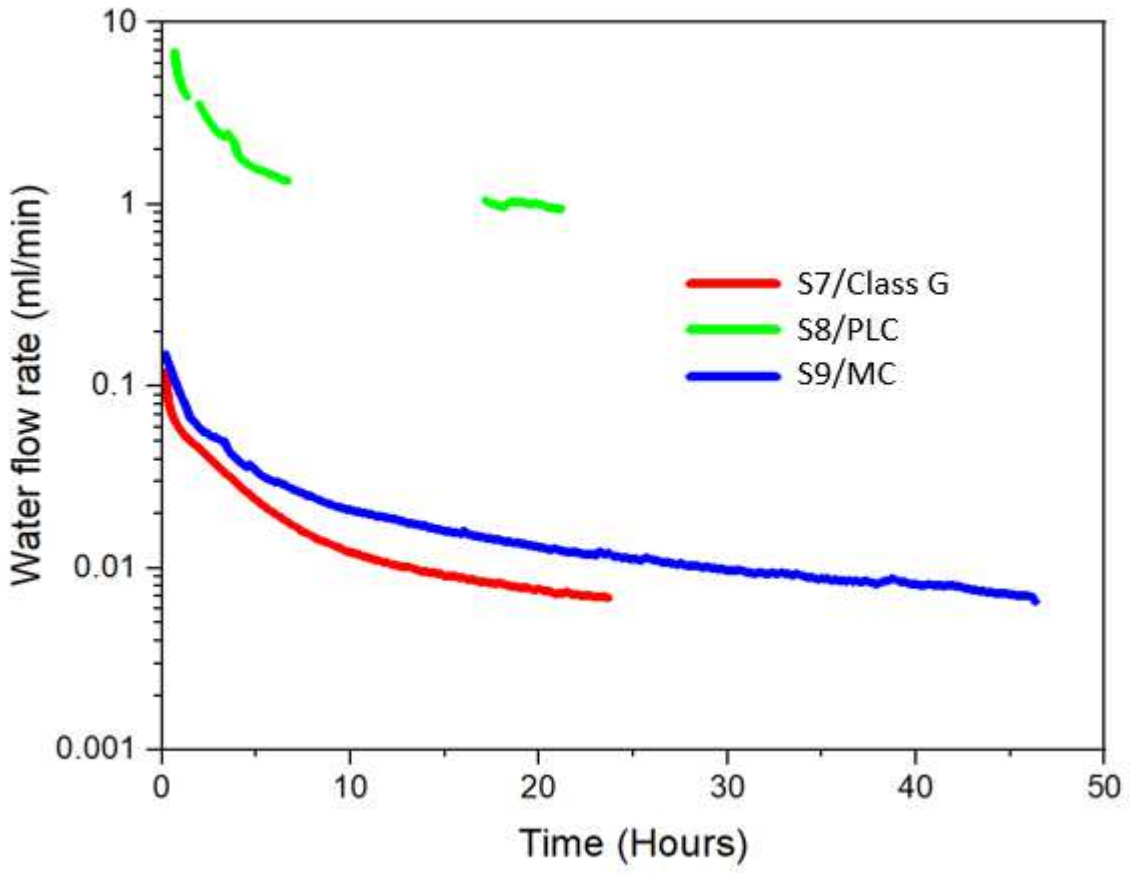

Figure 4-33: Water flow rate of the remediated fractures (50-micron shim) measured at an injection pressure of 300 psi and a confining pressure of 400 psi

Sample name	Injected slurry	Open fracture conductivity ml/min/MPa	Remediated fracture conductivity ml/min/MPa
S7	Class G	207	0.0033
S8	PLC	135	0.30
S9	MC	115	0.0030

Table 4-6: Summary of the fracture conductivity measured for the open fractures and the remediated fractures.

4.4.3.7 Opening the Remediated Cement Core and Comparing the Remedial Cement Penetration Performance

The fractures space was only partially filled for all experiments carried out using the 50-micron shim. For sample 7 (class G) and sample 8 (Portland limestone cement), bridging was observed at the inlet, and the cement was deposited in a fingering pattern at the entrance of the fracture. Some filtrates from S7 and S8 were able to travel further into the fracture. These filtrates were disconnected from the main body of cement (slurry deposited in a fingering pattern). S9 (microfine) appeared to be filled uniformly and came to an abrupt halt. No particle filtrates were observed in S9 suggested that the slurry could have stopped at a point where both cement cores were touch each other as opposed to fracture narrowing as S9 had the lowest fracture conductivity before remediation experiments.

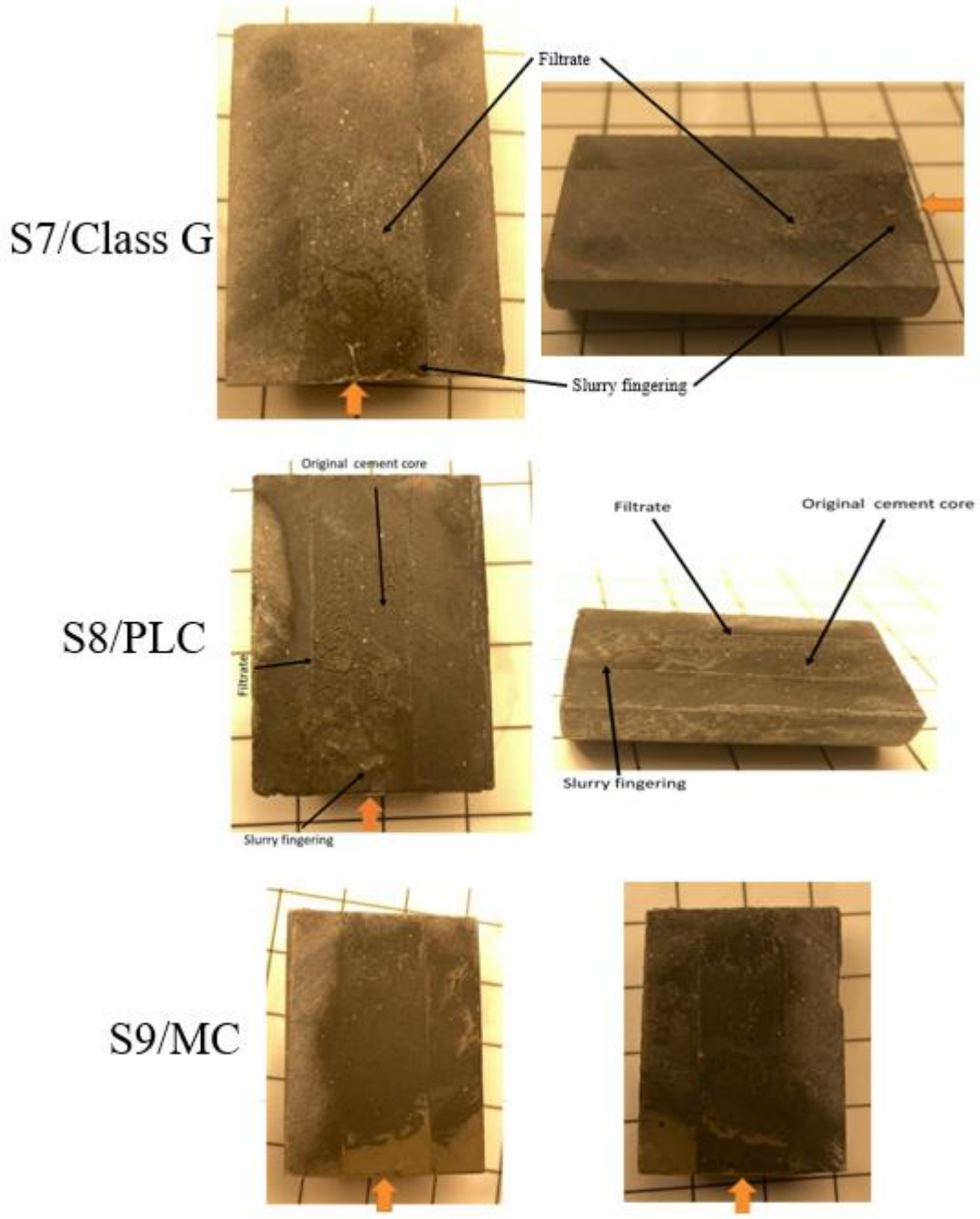

Figure 4-34: Slurry pathway for all the squeeze experiments (50μm shim)

4.5 Conclusions

Three types of cement systems were tested for their penetration potential into narrow fracture spaces. The fracture widths were controlled by varying the thickness of the shim stocks. From the experiments carried out with the 150 microns shims (thickness), we were able to determine that the standard class G cement sample bridged at a fracture space of around 200 microns (this was the largest width observed in our experiment). Although bridging took place, the class G slurry filled the fracture space in a fingering manner. The narrowest fracture widths observed during these experiments were about 70 microns. The Portland limestone cement and the microfine cement had filled the fracture space uniformly and no bridging or fingering of the slurry was observed. If the fracture space or micro annuli was larger than 70 microns, these cement systems performed very well.

From the experiments carried out with the 100 microns shims (thickness), we were able to determine that the class G cement could not penetrate a fracture space of 90 microns and only filtrate from the slurry was allowed below this fracture width. The filtrates of the class G cement travelled a further 8 mm and stopped after the fracture width was reduced to 45 microns. At a fracture width of 35 microns, the Portland limestone cement could not fill the fracture space uniformly and the slurry was deposited in a fingering manner. The microfine cement performed very well even when the fracture space was below 35 microns. The fracture was filled uniformly and no fingering was observed.

From the experiments carried out with the 50 microns shims (thickness), we verified that only filtrates could flow through a fracture space of 50 microns for the class G cement. Bridging was observed at a fracture width of 50 microns for the Portland limestone cement. The PLC cement slurry was deposited in a fingering pattern beyond the initial bridging. Some filtrate was observed further up the fracture indicating a further narrowing of the fracture up the sample. Bridging could not be identified with the samples that were remediated with microfine cement due to its adhesive nature.

From the fracture conductivity experiments, we observed that the fracture conductivity of the remediated sample was anywhere between two and five orders of magnitude lower than the open fracture sample, indicating good success with all the remediation experiments. The microfine cement had the best performance when it came to reducing the conductivity of the fracture. The Portland limestone sample was able to reduce the fracture conductivity of the sample by 4 orders of magnitude if the fracture space was completely filled. When the Portland limestone cement bridged or fingered, the sealing performance of the sample was reduced by two orders of magnitude. The class G sample was able to reduce the fracture conductivity to a similar level when compared to the microfine cement; however, it did not penetrate deeply into the fracture. It seems that the class G cement acted as a band aid solution to remediate the fracture by just covering up the opening of the fracture and not remediating the entire fracture.

From an industrial standpoint, the microfine cement would be the best choice to remediate a micro annulus or a micro fracture. Results have shown that the microfine cements could penetrate fracture widths as narrow as 35 microns without bridging. When a well needs to be remediated, the cement is first perforated. After perforation, microchannels are formed around that perforation. If class G was injected into this space, the class G cement would only close up the fracture space around perforations (acting like a band aid). The microfine cement would penetrate further into the fracture space and close up any associated micro fractures.

4.6 References

[1] AER, June 2024. Number of licensed wells in each stage of the life cycle, https://www.aer.ca/providing-information/data-and-reports/data-hub/well-status

[2] Watson, T.L. and Bachu, S., 2009. Evaluation of the potential for gas and CO2 leakage along wellbores. SPE Drilling & Completion, 24(01), pp.115-126

[3] Barclay, I., Pellenbarg, J., Tettero, F., Pfeiffer, J., Slater, H. and Staal, T., 2001. The beginning of the end: a review of abandonment and decommissioning practices. Oilfield Review, 13(4), pp.28-41.

[4] Yousuf, N., Olayiwola, O., Guo, B. and Liu, N., 2021. A comprehensive review on the loss of wellbore integrity due to cement failure and available remedial methods. Journal of Petroleum Science and Engineering, 207, p.109123.

[5] Forster, P., Storelvmo, T., Armour, K., Collins, W., Dufresne, J.L., Frame, D., Lunt, D., Mauritsen, T., Palmer, M., Watanabe, M. and Wild, M., 2021. The Earth's energy budget, climate feedbacks, and climate sensitivity. Chapter 7 of IPCC Sixth Assessment Report.

[6] Yang, X., Kuru, E., Gingras, M., Iremonger, S., Chase, P. and Lin, Z., 2021. Characterization of the microstructure of the cement/casing interface using esem and micro-CT scan techniques. SPE Journal, 26(03), pp.1131-1143.

[7] Nelson, E.B. and Guillot, D., 2006. Well cementing, 2006. Schlumberger, Sugar Land, Texas, USA.

[8] Todorovic, J., Raphaug, M., Lindeberg, E., Vrålstad, T. and Buddensiek, M.L., 2016. Remediation of leakage through annular cement using a polymer resin: a laboratory study. Energy procedia, 86, pp.442-449.

[9] Manceau, J.C., Hatzignatiou, D.G., De Lary, L., Jensen, N.B. and Réveillère, A., 2014. Mitigation and remediation technologies and practices in case of undesired migration of CO2 from a geological storage unit—Current status. International Journal of Greenhouse Gas Control, 22, pp.272-290.

[10] Meek, J.W. and Harris, K., 1993. Repairing casing leaks using small-particle-size cement. SPE Production & Facilities, 8(01), pp.45-50.

[11] Rike, J.L. and Pledger, T.M., 1981, March. Clean Fluids Improve Completion Results. In SPE Oklahoma City Oil and Gas Symposium/Production and Operations Symposium SPE-9752. SPE.

[12] Bradford, B. and Reiners, B., 1985. Analysis gives successful cement squeeze. Oil & Gas Journal, 83(13), pp.71-74.

[13] Goodwin, K.J. and Phipps, K., 1984. Salt-free cement an alternative to collapsed casing in, plastic salts (includes associated papers 12952 and 13012). Journal of Petroleum Technology, 36(02), pp.320-324.

[14] Nasional, B.S., 2002. SNI 13-6910-2002 Drilling Operation for Safe Conduct of Onshore and Offshore in Indonesia-Implementation.

[15] Normann, A.S., 2018. The most common causes for leaks in oil wells and 8 questions to consider before you select solution.

[16] Ewert, D.P., Almond, S.W. and Bierhaus, W.M., 1991. Small-particle-size cement. SPE Production Engineering, 6(02), pp.213-216.

[17] Dusseault, M.B., Gray, M.N. and Nawrocki, P.A., 2000, November. Why oilwells leak: cement behavior and long-term consequences. In SPE International Oil and Gas Conference and Exhibition in China, SPE-64733. SPE.

[18] Slater, H.J., Stiles, D.A. and Chmilowski, W., 2001, February. Successful sealing of vent flows with ultra-low-rate cement squeeze technique. In SPE/IADC Drilling Conference and Exhibition, Amsterdam, Netherlands, SPE-67775. SPE.

[19] Wu, B., Arjomand, E., Tian, W., Dan, B. and Yan, S., 2020. Sealant technologies for remediating cement-related oil and gas well leakage. CSIRO.

[20] Farkas, R.F., England, K.W., Roy, M.L., Dickinson, M., Samuel, M. and Robert, E.H., 1999, October. New cementing technology cures 40-year-old squeeze problems. In SPE Annual Technical Conference and Exhibition, Houston, Texas, USA, SPE-56537-MS. SPE.

[21] Gong, F., Babadagli, T., Huang, H. and Li, H., 2024. Resolved CFD-DEM simulation of proppant aggregating and bridging mechanisms in a narrowing fracture. Powder Technology, 437, p.119548.

[22] The American Petroleum Institute, 2013. Recommended practice for testing well cement, API recommended practice 10-B2, Second edition.

Chapter 5 Conclusions and Recommendations

5.1 Conclusions

The interest in well abandoned has been increasing especially in the use of alternative materials to cement. Cement has been demonized in the literature and the leakage issues in petroleum wells have been predominantly blamed on cement shrinkage. Although alternative materials to cementing might sound appealing, it will be very difficult to get industry personnel to adopt these alternative materials as they cost anywhere between 10 and 100 times more than what conventional (Portland cement based) cementing would cost. The motivation of academia is to find the best solutions to the problem; however, the motivation of industry is to adopt the best solution only if the price is right.

In this thesis, we attempt to bridge that gap by determining what actually causes well leakage, and how we can better prevent well leakage issues seen in petroleum wells.

The main contributions of this research are summarized into 4 groups: 1) determining flow pathways in small scale abandonment plugs (Chapter two); 2) upscaling and testing abandonment plugs using the wellbore simulator (Chapter two); 3) investigating the effect of contamination on the integrity of cement plugs (Chapter three) and; 4) investigating the squeeze cementing remediation techniques by replicating downhole conditions (Chapter four).

In Chapter 2, we wanted to understand the basic behaviour of cement. To do this we first cured two small scale samples (neat G cement), a bulk cement plug and a cement plug inside a metal pipe. The objectives of the small-scale experiments were to determine the effect of adding an interface around a cement plug and if it would affect the sealing capabilities of cement. From our water permeability experiments, we found that the flow rate of the cement sample inside a metal pipe was two orders of magnitude higher than the bulk sample, though the actual permeability numbers are still in the order of nano-Darcies. When we carried out nitrogen permeability experiments, we observed that the shear bond between the cement and metal pipe failed during the experiment, causing high flow of gas while no breakthrough was observed with the bulk cement sample. The experiment was then upscaled using a wellbore simulator and two cement systems were studied: Class G neat cement and Class G cement with additives. From our experiments, we observed that the cement blend with additives outperformed the neat G cement in every testing

scenario and by carefully engineering the cement blend to well conditions, the sealing performance of the cement was improved. Based on the results observed from chapter 2, the following conclusions can be offered:

- Cement on its own has very low permeability, but the addition of an interface can increase the permeability of the sealing system.
- By carefully engineering a cement system with a careful selection of additives, the sealing performance of the cement can be vastly improved.
- Well-designed cement plugs can withstand extreme testing conditions if placed optimally.

In Chapter 3, we investigated the effect of contamination on cement integrity. The cement slurry was contaminated with both oil and water. From our experiments, we observed that the sealing potential of cement was reduced as the cement was diluted with water. As the water content in the slurry increased, the heavier cement particles settled to the bottom and the excess free water moved up in the cement column. This excess water was trapped in the pore space, forming flow pathways in the cement column. We also observed that fluid loss additives might have worsened this effect, causing the permeability of the cement plug to be increased significantly. For the oil contaminated experiments, we observed that minor amounts of residual oil did not affect the sealability of the cement as long as the cement plug remains under the same pressure conditions it was cured under. Any changes to the effective stresses acting of the cement caused the cement to lose its isolation capabilities far more than the uncontaminated sample. The sensitivity to the formation of a micro annulus was increased in the presence of contamination. Based on the results the following conclusions can be offered:

- Fluid intermixing in the wellbore can cause the cement system to drastically lose its isolation capabilities.
- The additives used in the cement blends need to account for the types of contaminations found in the wellbore.
- Improper well cleaning before abandonment can pose a risk to cement integrity.
- Minor amounts of residual oil do not immediately affect the integrity of the abandonment plug, but over time can cause well integrity issues.

In Chapter 4, we investigated the remediation capabilities of three types of cements. The most common technique to remediate micro fracture or micro annuli is squeeze cementing. From our previous experiments, we observed that the dominant fluid pathway was through the cement casing interface. The penetration performance of Class G cement, Portland limestone cement with smaller grain size than class G cement and a microfine cement with smaller grain size than Portland limestone cement were investigated. For class G cements, we observed that the cement bridged at a fracture width of 200 microns. Below 200 microns, cement was deposited in a fingering pattern. Fingering stops and only particle filtrates could penetrate a fracture space below 90 microns (class G cement) and the filtrates could not pass a fracture space of 45 microns. For Portland limestone cement, we observed bridging at 50 microns gap size and slurry was deposited in a fingering manner at around 35 microns. Portland limestone cement cannot penetrate a fracture space below 35 microns. The microfine cement was capable of penetrating a fracture space of 35 microns and no bridging was observed at this gap size suggesting that the micro fine cement was the best cement slurry to use for remediation. Based on the results the following conclusions can be offered:

- Class G cement cannot penetrate a fracture width less than 200 microns efficiently.
- By reducing the mean grain size of the cement particles, the slurry can penetrate further into the fracture.
- The Portland limestone cement can remediate larger micro annuli or fractures in the range of 80 microns.
- The microfine cement can remediate smaller fractures in the range of 40 microns.

5.2 Recommendations for Future Work

Many experiments in this thesis have been carried out to investigate cement integrity under the influence of realistic wellbore conditions and how to remediate cement samples with cement squeeze operations. Additional avenues to explore with these experiments are given below. For the small-scale tests, we suggest the following future work:

- Carry out oil and water contamination experiments using the small-scale samples.
- CT image the contaminated samples to see how the contaminants alter the pore space and the cement casing interface of cement sample.
- Contaminate the cement with brine solution.

- Carry out permeability experiments using hydrocarbons instead of water and nitrogen to replicate field conditions.

For the wellbore-simulator-based tests, we suggest the following future work:

- Contaminate the cement sample with higher dosages of oil to determine a trend.
- Contaminate the cement with brine solution.
- Carry out compressive strength tests on the wellbore simulator samples, especially the samples which have been contaminated with water.

For the remediation experiments, we suggest the following future work:

- Try to replace the metal shim with a less dense material to get more accurate CT scans.
- Try to carry out the squeeze operations using the wellbore simulator. The apparatus used for the remediation experiments can be upscaled and used inside the wellbore simulator to replicate field conditions.

Bibliography

Achang, M., Yanyao, L. and Radonjic, M., 2020. A review of past, present, and future technologies for permanent plugging and abandonment of wellbores and restoration of subsurface geologic barriers. Environmental Engineering Science, 37(6), pp.395-408.

AER, June 2024. Number of licensed wells in each stage of the life cycle, https://www.aer.ca/providing-information/data-and-reports/data-hub/well-status

Agbasimalo, N. and Radonjic, M., 2014. Experimental study of the impact of drilling fluid contamination on the integrity of cement–formation interface. Journal of Energy Resources Technology, 136(4), p.042908.

Aughenbaugh, K., Nair, S., Cowan, M. and van Oort, E., 2014, September. Contamination of deepwater well cementations by synthetic-based drilling fluids. In SPE Deepwater Drilling and Completions Conference, Galveston, Texas, USA, SPE-170325-MS. SPE.

Barclay, I., Pellenbarg, J., Tettero, F., Pfeiffer, J., Slater, H. and Staal, T., 2001. The beginning of the end: a review of abandonment and decommissioning practices. Oilfield Review, 13(4), pp.28-41.

Bonett, A. and Pafitis, D., 1996. Getting to the root of gas migration. Oilfield Review, 8.

Boukhelifa, L., Moroni, N., James, S.G., Le Roy–Delage, S., Thiercelin, M.J. and Lemaire, G., 2004, March. Evaluation of cement systems for oil and gas well zonal isolation in a full-scale annular geometry. In SPE/IADC Drilling Conference and Exhibition, Dallas, Texas, USA, SPE-87195-MS. SPE.

Bourgoyne, A.T., Scott, S.L, and Manowski, W., 2000. A review of sustained casing pressure occurring on the OCS, Bureau of safety and environmental enforcement.

Bradford, B. and Reiners, B., 1985. Analysis gives successful cement squeeze. Oil & Gas Journal, 83(13), pp.71-74.

Celia, M.A., Bachu, S., Nordbotten, J.M., Gasda, S.E. and Dahle, H.K., 2005. Quantitative estimation of CO2 leakage from geological storage: Analytical models, numerical models, and data needs, In Greenhouse Gas Control Technologies 7, pp. 663-671, Elsevier Science Ltd.

Clark, C.R. and Carter, G.L., 1973. Fluid displacement with cement slurries. Journal of Petroleum Technology, 25(07), pp.775-783.

Coleman, J.R. and Corrigan, G.L., 1941. Fineness and water-cement ratio in relation to volume and permeability of cement. Transactions of the AIME, 142(01), pp.205-215.

Corina, A.N., Opedal, N.V.D.T., Vrålstad, T. and Sangesland, S., 2019, June. Cement plug sealing studies of silica cement systems. In International Conference on Offshore Mechanics and Arctic Engineering, Glasgow, Scotland, UK, OMAE2019-95928. American Society of Mechanical Engineers.

Dusseault, M.B., Gray, M.N. and Nawrocki, P.A., 2000, November. Why oilwells leak: cement behavior and long-term consequences. In SPE International Oil and Gas Conference and Exhibition in China, SPE-64733. SPE.

Ewert, D.P., Almond, S.W. and Bierhaus, W.M., 1991. Small-particle-size cement. SPE Production Engineering, 6(02), pp.213-216.

Farkas, R.F., England, K.W., Roy, M.L., Dickinson, M., Samuel, M. and Robert, E.H., 1999, October. New cementing technology cures 40-year-old squeeze problems. In SPE Annual Technical Conference and Exhibition, Houston, Texas, USA, SPE-56537-MS. SPE.

Forster, P., Storelvmo, T., Armour, K., Collins, W., Dufresne, J.L., Frame, D., Lunt, D., Mauritsen, T., Palmer, M., Watanabe, M. and Wild, M., 2021. The Earth's energy budget, climate feedbacks, and climate sensitivity. Chapter 7 of IPCC Sixth Assessment Report.

Garnier, A., Saint-Marc, J., Bois, A.P., and Kermanac'h, Y., 2008. A singular methodology to design cement sheath integrity exposed to steam stimulation, In SPE International Thermal Operations and Heavy Oil Symposium, pp. SPE-117709. SPE.

Gong, F., Babadagli, T., Huang, H. and Li, H., 2024. Resolved CFD-DEM simulation of proppant aggregating and bridging mechanisms in a narrowing fracture. Powder Technology, 437, p.119548.

Goodday, V. and Larson, B., 2021. The Surface Owner's Burden: Landowner Rights and Alberta's Oil and Gas Well Liabilities Crisis. The School of Public Policy Publications, 14.

Goode, J.M., 1962. Gas and water permeability data for some common oilwell cements. Journal of Petroleum Technology, 14(08), pp.851-854.

Goodwin, K.J. and Phipps, K., 1984. Salt-Free Cement An Alternative to Collapsed Casing in, Plastic Salts (includes associated papers 12952 and 13012). Journal of Petroleum Technology, 36(02), pp.320-324.

Kamali, M., Khalifeh, M., Eid, E. and Saasen, A., 2022. Experimental study of hydraulic sealability and shear bond strength of cementitious barrier materials. Journal of Energy Resources Technology, 144(2), p.023007.

Kang, M., Kanno, C.M., Reid, M.C., Zhang, X., Mauzerall, D.L., Celia, M.A., Chen, Y. and Onstott, T.C., 2014. Direct measurements of methane emissions from abandoned oil and gas wells in Pennsylvania. Proceedings of the National Academy of Sciences, 111(51), pp.18173-18177.

Khalifeh, M. and Saasen, A., 2020. Introduction to permanent plug and abandonment of wells (p. 273). Springer Nature.

Li, M., Ou, H., Li, Z., Gu, T., Liu, H. and Guo, X., 2015. Contamination of cement slurries with diesel-based drilling fluids in a shale gas well. Journal of Natural Gas Science and Engineering, 27, pp.1312-1320.

Li, Z., Liu, H., Guo, X., Ou, H. and Gu, T., 2016. Contamination of cement slurries with oil based fluid and its components in cementing operations. Journal of Natural Gas Science and Engineering, 29, pp.160-168.

Lin, Z., Kuru, E., Iremonger, S., Yang, X., Fisher, B. and Spence, J., 2022. Design and Development of a High Pressure-High Temperature Wellbore Simulator for Investigation of the Impact of Cyclic Stresses on the Integrity of Wellbore Sections with Cement/Casing Interfaces, In SPE Annual Technical Conference and Exhibition, Houston, Texas, USA, SPE-210223-MS, SPE.

Mabeyo, P.E., Ibrahim, Y.S. and Gu, J., 2020. Effect of high metakaolin content on compressive and shear-bond strengths of oil well cement at 80 C. Construction and Building Materials, 240, p.117962.

Mainguy, M., Longuemare, P., Audibert, A. and Lécolier, E., 2007. Analyzing the risk of well plug failure after abandonment. Oil & Gas Science and Technology-Revue de l'IFP, 62(3), pp.311-324.

Manceau, J.C., Hatzignatiou, D.G., De Lary, L., Jensen, N.B. and Réveillère, A., 2014. Mitigation and remediation technologies and practices in case of undesired migration of CO2 from a geological storage unit—Current status. International Journal of Greenhouse Gas Control, 22, pp.272-290.

Meek, J.W. and Harris, K., 1993. Repairing casing leaks using small-particle-size cement. SPE Production & Facilities, 8(01), pp.45-50.

Meng, M., Frash, L.P., Carey, J.W., Li, W., Welch, N.J. and Zhang, W., 2021. Cement stress and microstructure evolution during curing in semi-rigid high-pressure environments. Cement and Concrete Research, 149, p.106555.

Nasional, B.S., 2002. SNI 13-6910-2002 Drilling Operation for Safe Conduct of Onshore and Offshore in Indonesia-Implementation.

Nelson, E.B. and Guillot, D., 2006. Well cementing, 2006. Schlumberger, Sugar Land, Texas, USA.

Normann, A.S., 2018. The most common causes for leaks in oil wells and 8 questions to consider before you select solution.

Ogienagbon, A.A. and Khalifeh, M., 2023. Investigation of the hydraulic integrity of cement plug: Oilwell cementitious materials. Geoenergy Science and Engineering, 231, p.212261.

Opedal, N., Corina, A.N. and Vrålstad, T., 2018, June. Laboratory test on cement plug integrity. In International Conference on Offshore Mechanics and Arctic Engineering, Madrid, Spain OMAE2018-78347. American Society of Mechanical Engineers.

Ozyurtkan, M.H., Altun, G., Mihcakan, I.M. and Serpen, U. An experimental study on mitigation of oil well cement gas permeability, In IPTC 2013: International Petroleum Technology Conference, pp. cp-350, European Association of Geoscientists & Engineers.

Patel, A.D., Wilson, J.M. and Loughridge, B.W., 1999, February. Impact of synthetic-based drilling fluids on oilwell cementing operations. In SPE International Conference on Oilfield Chemistry, Houston, Texas, USA, SPE-50726-MS. SPE.

Poon, C.S., Wong, Y.L. and Lam, L., 1997. The influence of different curing conditions onthe pore structure and related properties of fly-ash cement pastes and mortars. Construction and Building Materials, 11(7-8), pp.383-393.

Rike, J.L. and Pledger, T.M., 1981, March. Clean Fluids Improve Completion Results. In SPE Oklahoma City Oil and Gas Symposium/Production and Operations Symposium, SPE-9752. SPE.

Schiffner, D., Kecinski, M. and Mohapatra, S., 2021. An updated look at petroleum well leaks, ineffective policies and the social cost of methane in Canada's largest oil-producing province. Climatic Change, 164(3), pp.60.

Scrivener, K.L., Crumbie, A.K. and Laugesen, P., 2004. The interfacial transition zone (ITZ) between cement paste and aggregate in concrete. Interface Science, 12, pp.411-421.

Slater, H.J., Stiles, D.A. and Chmilowski, W., 2001, February. Successful sealing of vent flows with ultra-low-rate cement squeeze technique. In SPE/IADC Drilling Conference and Exhibition, Amsterdam, Netherlands, SPE-67775. SPE.

Thaika, MA., Hu, K., Kuru, E., Li, H., Iremonger, S., Lin, Z., & DeBruijn, G., 2024. Experimental investigation of well cement integrity in abandoned oil and gas, In International Conference on Offshore Mechanics and Arctic Engineering, Singapore, OMAE2024-130296. American Society of Mechanical Engineers.

The American Petroleum Institute., 2013. Recommended practice for testing well cement, API recommended practice 10-B2, Second edition.

Thiercelin, M.J., Dargaud, B., Baret, J.F. and Rodriquez, W.J., 1998. Cement design based on cement mechanical response. SPE Drilling & Completion, 13(04), pp.266-273.

Todorovic, J., Raphaug, M., Lindeberg, E., Vrålstad, T. and Buddensiek, M.L., 2016. Remediation of leakage through annular cement using a polymer resin: a laboratory study. Energy Procedia, 86, pp.442-449.

Van Eijden, J., Cornelissen, E., Ruckert, F. and Wolterbeek, T., 2017. Development of experimental equipment and procedures to evaluate zonal isolation and well abandonment materials, In SPE/IADC drilling conference and exhibition, The Hague, The Netherlands, SPE-184640-MS. OnePetro.

Vrålstad, T., Saasen, A., Fjær, E., Øia, T., Ytrehus, J.D. and Khalifeh, M., 2019. Plug & abandonment of offshore wells: Ensuring long-term well integrity and cost-efficiency. Journal of Petroleum Science and Engineering, 173, pp.478-491.

Watson, T.L., and Bachu, S. Evaluation of the potential for gas and CO2 leakage along wellbores." SPE Drilling & Completion 24, no. 01 (2009): 115-126.

Wu, B., Arjomand, E., Tian, W., Dan, B. and Yan, S., 2020. Sealant technologies for remediating cement-related oil and gas well leakage. CSIRO.

Xu, R. and Wojtanowicz, A.K., 2017. Pressure buildup test analysis in wells with sustained casing pressure. Journal of Natural Gas Science and Engineering, 38, pp.608-620.

Yang, X., Kuru, E., Gingras, M., Iremonger, S., Chase, P. and Lin, Z., 2021. Characterization of the microstructure of the cement/casing interface using esem and micro-CT scan techniques. SPE Journal, 26(03), pp.1131-1143.

Yousuf, N., Olayiwola, O., Guo, B. and Liu, N., 2021. A comprehensive review on the loss of wellbore integrity due to cement failure and available remedial methods. Journal of Petroleum Science and Engineering, 207, p.109123.

Zuiderwijk, J.J.M., 1974, May. Mud displacement in primary cementation. In SPE Europec featured at EAGE Conference and Exhibition, Amsterdam, Netherlands, SPE-4830-MS. SPE.